Design and Optimization of Tunnel Guidance Systems for Tunneling subject to Constrained Space and Limited Visibility

by

Sheng Mao

A thesis submitted in partial fulfillment of the requirements for the degree of

Doctor of Philosophy

in

Construction Engineering and Management

Department of Civil and Environmental Engineering
University of Alberta

ABSTRACT

Modern construction, which is part of the whole industrialization process, evolves to be more both cost-efficient and time-efficient, meanwhile still preserving high quality. The core of the process is to extract and migrate precious body of knowledge and practical experience of the craftsmen (engineers, workers, etc.) to well-defined systems. Comparing to the scarceness of skillful craftsmen, the established systems will be able to replicate and distribute the knowledge and skills more quickly to new situations where related expertise is hard to obtain and scientific decision support is much desired in coping with real world challenges.

The rapid expansion of cities worldwide demands fast construction of municipal infrastructures. The service tunnels, e.g. drainage tunnels and sanitary tunnels are very crucial to the life quality of the residents. However, the traditional tunnel construction is not efficient in either cost or time terms. Sufficient tunnels cannot serve these problems cause residents in reasonable time. The underground construction undertakings are never easy: from engineering aspect, besides the unpredictable changes of geotechnical conditions during the construction, the modern survey technologies like GPS cannot be applied to underground construction; the difficulties in underground construction are very high. From management aspect, the tunnels have less concurrency of different tasks due to the space constraints, and these results in less contingency for the management: even a small event may invalidate a thorough plan.

Thanks to the modern construction techniques, for example, the guidance system of tunnel-boring machine, the tunnel construction has become much easier. The guidance system embeds survey as part of the construction, and feeds the construction with real-time guidance and checks. The technology results in

productivity improvement and lower cost, and fast-feedback and without the help of the survey-based guidance system, the cost and difficulty of TBM construction are unimaginable. The guidance systems, especially those equipped with robotic survey tools, not only change the process of tunnel construction, but also can change the process of designing for construction implementation, which are currently solely comprehended by engineers and their experienced colleagues in the field relying on “gut” feeling.

The research focuses on designing temporary facilities for tunnel construction. The engineering design of the tunnels concerns about functionality and geotechnical conditions, and in comparison, the design of temporary facilities cares more about practical implementation of the construction process. This research proposes a new framework to help with designing and optimizing temporary facilities by eliminating expensive and efficiency-killing full survey while preserving high quality. The survey-error based design framework utilizes the state-of-the-art guidance system as part of core design: the automation of the guidance system is the key to simplify the traditional construction, and make the new design possible. Therefore, the research will be illustrated in three steps: first the thesis introduces a state-of-the-art automation TBM guidance system and the mechanism of the latest guidance method; then the thesis discusses how to adapt the automatic guidance system into extreme cases of tunnel construction; and eventually, the thesis reveals why and how the automatic system becomes part of a design framework to facilitate tunneling under practical field constraints.

PREFACE

Chapter 3 of this thesis has been published as S., Mao, X. Shen, and M. Lu. 2014. “Virtual Laser Target Board for Alignment Control and Machine Guidance in Tunnel-Boring Operations.” Journal of Intelligent & Robotic Systems, September, 1–16. doi:10.1007/s10846-014-0113-y. I was responsible for the design and implementation of the automatic system. Dr. Shen was the author of the three-point positioning algorithm for tunnel-boring machine and the leader of the project. Dr. Lu was the supervisory author and in charge of the direction of the research.

ACKNOWLEDGEMENTS

First of all, I would like to thank Dr. Ming Lu. As my supervisor, he supports me for my entire Ph.D. life, and turns me into a better researcher. He is an excellent teacher, an insightful researcher, and a caring friend.

I would also like to thank Dr. Xuesong Shen, Mr. Xiaodong Wu and Mr. Duanshun Li. They are reliable and dedicated teammates, and I am so lucky to work with them on tunnel researches.

Thank you, Dr. AbouRizk, for teaching me so much about construction, and providing me such a good opportunity with The City of Edmonton. In addition, thank you, Mr. Fernando, Mr. Schneider, Mr. Pratt, Mr. Milton, and everyone from The City of Edmonton, you are the best supporters. Without you, I will not find the interesting problem for my research and I will never have the excellent test beds for my research. Thank you, Dr. Vineet R. Kamat, Dr. Alireza Bayat, and Dr. Zhigang Tian for helping me through my defense!

I want to thank Miss Xiaolin Hu, Mr. Xianrong Mao, and Mrs. Jiaqi Sheng. You are my most lovely family, and you are the whole world to me.

Thank you, my friends, every one of you. You enlighten my life.

TABLE OF CONTENTS

LIST OF TABLES

LIST OF FIGURES

Chapter 1. INTRODUCTION

1.1 INDUSTRIALIZATION

The philosophies of craftsmanship and industrialization are fundamentally different. Craftsmanship descends from the ancient human history, and passes down the generations. It is the original form of human making tools. The knowledge of craftsmanship are learnt, improved and taught as legacy between mentor and protégé. A craftsman polishes his/her skills during the lifetime of the career, and always after maturity of the expertise, the craftsman can amaze the customers with unbelievable, fabulous pieces of arts. However, the craftsmanship is very hard to train, and thus learning is slow, and when human society expands themselves at an exponential rate, the production rates of both well-trained craftsmen and high-quality products hardly meet the need of the society. Another side-effect of craftsmanship is that the costs are too high for middle-class.

Everything changed after the invention of machine, and it came the rise of industrialization. Industrialization solves the dilemma between supply and demand by replacing made-by-craftsman with made-by-machine. A machine is designed to replicate craftsmanship and produce the same products. It is always less flexible (one machine, one purpose), less accurate (the experience of the craftsmen are not always exactly structured into machine design), and less customized (every product is built in the same way). However, the machine is easy to be reproduced, the production rate is much higher, and the design of machine can be improved during the life cycle.

The philosophy of industrialization fundamentally changes the landscape of the human society. Humans are freed from boring routine tasks, and only assigned to take over when the machines are incapable. More important, the production of machines can meet the demand of the expansion of society, and the quantity-limited, precious craftsmen are only utilized in high-value work, achieving an optimum resource utilization of the society. Thus the production can eventually be affordable by the majority people of the society.

A fraction of researchers of applied disciplines should steer their research focus to how to replicate human expertise and experience in the machines, and moreover, how to create processes to achieve optimum production and quality to match the abilities of underneath machines.

As more and more construction projects are built for everyone in the society, not for the top-tier elite, modern construction demands both higher productivity and lower cost. However, unlike manufacturing, construction always starts out on an uncontrolled ground: no control over weather, no control over geotechnical conditions, and expensive to make temporary facilities. What's more, the construction facilities are all temporary, and will be removed after completion; it is not considered viable to build expensive permanent structures only to be abandoned after a few months or a couple of years. When engineers start to design a construction project, the details will more or less differ from the previous ones, and they should adapt to the new environments and conditions. Their work partially resembles the craftsmanship: heavily relying on the experiences, while the solutions being case specific, not one for all. This situation hinders the fast replication of knowledge and experience.

1.2 INTEGRATION OF CONSTRUCTION AND SURVEY

The scope and complexity of modern construction projects have increased significantly, placing great pressure to the project management team responsible for maintaining the quality and progress of construction. Engineers always define several checkpoints, as such; construction crews can get feedback on the correctness and quality of their work. Fast feedback on position and quality of work being laid out in the field is one of the answers that can boost construction in efficiency and cost-saving. The feedback assures field crews on the quality of their work; meanwhile, such feedback also provides project managers with timely information for progress measurement and project control.

Although feedback is an effective helper, feedback itself may not always be feasible. One of the most critical factors is the cost of the feedback. For example, in earth moving projects, the management can calculate amount of work accomplished, either by observing changes of the level of the ground, or payload of each hauling truck. But it is not easy to quantify the payload of each truck or measure the level of ground. The feedback systems are always intrusive, and may interrupt current processes. The management has to lower the frequency of the feedback, or change from real-time to post-process feedback.

Survey is one of the feedback methods, and traditionally, survey was treated as outsourced tasks, carried out only before and after the related construction works are done in the field. This detachment between construction and survey postpones the feedback, leaving much desirable quality assurance and project control during construction processes in shadows. However, in additional to requiring different expertise and equipment, field survey is treated as separated work from construction for a reason: survey work generally occupies

the work space for construction and interrupts the regular working process by construction crews. Municipal service tunnel is a typical example for illustrating this detachment. As construction proceeds underground, tunnel projects are prone to position errors. Operators of the drilling machines, e.g. Tunnel-boring Machine (TBM), demand real-time positioning aid from surveyors. However, as the service tunnels are usually limited in size, therefore construction work and survey process have conflicts in the confined space such that performing one process demands the temporary shutdown of the other. The operators, foremen and surveyors face a classic dilemma: allocating more time for construction, the project would have higher probability of deviating from design, thus causing quality defects; on the other hand, allocating more time for survey, the construction crew needs to shut down the tunnel, waiting for an extended period until surveyors complete their work. The ability to make the decision as of when to shut down construction turns into an art. Often, stakeholders need to balance the trade-off by "guessing" the solution. The tunnel-boring guidance technologies, which have emerged in the past decades, successfully bridge the gap between construction and survey to a certain degree. The guidance systems are integrated with the tunnel construction practice in order to deliver timely position feedbacks to TBM operator.

The detachment originates from the intrusive nature of alignment control survey, and the reason is that survey is not integrated into the construction process and survey is not considered as the part of the construction. Without integration, the need for survey is mostly ignored during construction by contractor's crews; only as construction is done, the crew turns over their work to surveyors to find out whether the product conforms to design/standard or not. Once significant deviation from the design is identified, it would become too late

for construction crews to take corrective measures but entail expensive rework, causing project delay and cost overrun.

The detached survey does not contribute to the construction process itself, and construction in turn treats survey as a verification of the completion of the project, the approval of which leads to payment (as-built survey to check the as-built and as-designed conformity and standard abiding). This situation calls for change and improvement as survey technology is very capable to add more value to construction, with the key to the added value being "integration". Survey should be integrated into construction, and survey results should be up-to-date, and ready for interpretation by construction professionals. Construction crews can proceed their work with the guidance of technology-enabled survey processes on a real-time basis. Tunnel is an excellent case to materialize such integration. Due to the confined, "invisible" underground workspace at the workface, tunnel projects rely on the survey to provide guidance for better quality and assurance. Tunnel construction crews have been applying the survey-based guidance systems for decades, and operators are provided with real-time position and pose information in an intuitive way.

This thesis will experiment on the tunnel-boring machine guidance problem for industrialization of knowledge and construction integration. In this research, the first process to be defined is the "integration" of survey into construction. There are two levels of integration: construction level and design level. In construction level, the surveyor and survey equipment should be included as part of the construction crew. For example, the earth-moving crew will be able to measure the payload (Caterpillar Inc. 2012) and level of the ground as the construction proceeding (Caterpillar 2014). Survey is considered as necessary and essential as other parts of the crew, and what's more important,

survey itself should place no extra effort to slow down the current construction practice.

In the design level, the integration makes engineers to plan the survey as part of the construction project. Survey is part of the temporary facilities that engineers can design and schedule. At this stage, survey is no longer an out-sourced package, but a toolbox with refined tools. Engineers can pick the right tool for the right purpose, balancing on cost, schedule and outcome as designing other parts of the project.

1.3 OBJECTIVES

This thesis is built upon the ideas of industrialization and integration. The author intends to formalize the knowledge and experience of construction engineers and surveyors, and to further materialize the knowledge into analytical frameworks. The frameworks can automatically guide the design of tunnel guidance systems, including both guidance method and supporting facilities, based on the engineering designs. This enables the engineers to accurately plan the setup and maintenance of the guidance system as part of the whole project. Moreover, the frameworks are practical and realistic: the as-designed guidance system is fully integrated into the planning and construction process, and feasible to be implemented in the field.

To serve this purpose, it emphasizes on three factors of integration: (1) automatic system enables seamless construction-level integration; (2) adaptiveness to extreme scenario reduces the necessity of intrusive practice; (3) automatic design algorithms enhance the design-level integration, and embed survey as part of design from the very beginning. The final scope of the research can be found in Figure 1.

To fulfill the objectives, the thesis examines the most important three aspects of tunnel-boring guidance systems. It is more than just proposing a guidance method, but a thorough design of a guidance system. It first introduces the design of automatic system, which performs routine survey and guidance work for the construction crew in real-time, without introducing extra operational difficulties or surveyor on-site. Then it discusses a one-point algorithm to cope with extreme guidance scenarios. This algorithm ensures that the guidance system can work in the most adversary environment, and thus the non-intrusive automatic guidance system needs less intrusive attendance by surveyors. And eventually, the design algorithm is proposed, which optimizes the temporary facility design for tunnel guidance, and especially works for the automatic guidance system. Engineers can design guidance-related facilities during design phase, and schedule the survey so as to best serve the needs of tunnel construction.

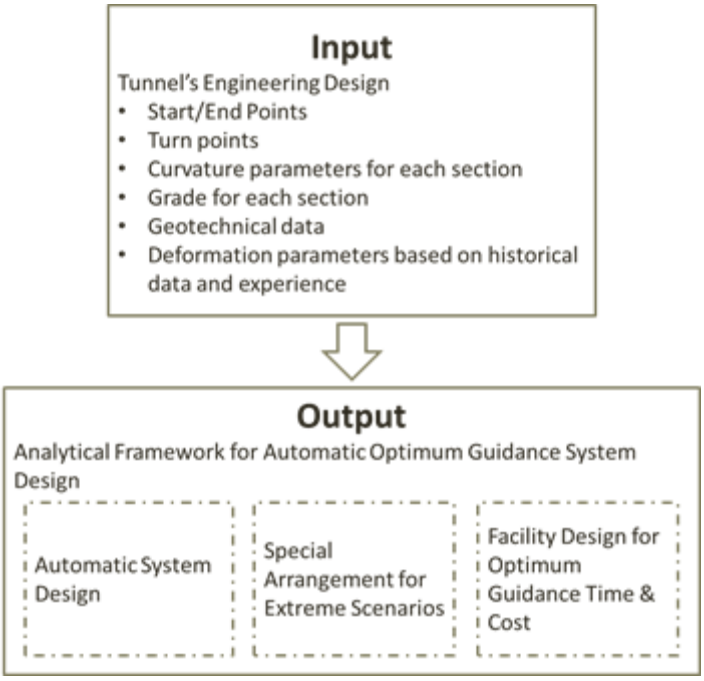

Figure 1. Body of knowledge of the thesis

Chapter 2. BACKGROUND

2.1 TUNNEL-BORING CONSTRUCTION

Tunnel-boring machines are very complex and sophisticated, and the author recommends "Mechanised Shield Tunnelling" (Maidl et al. 2013) to all readers seeking for a thorough understanding of tunnel-boring machine. In this thesis, a brief introduction of tunnel-boring machine construction will cover the interesting topics for construction-background readers, and this gives a clear overview of how TBM works and how the guidance system helps steering the machine. As shown in Figure 2, there are four main parts in a tunnel: TBM, concrete liners, gantry facilities, and rail system.

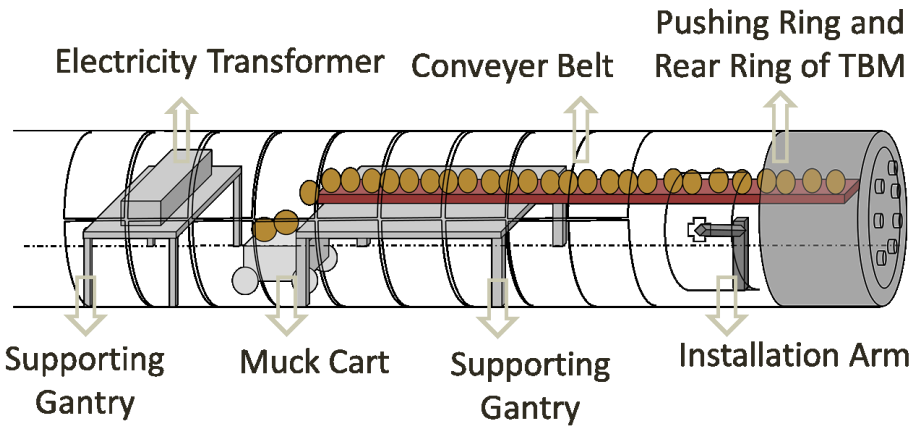

Figure 2. Tunnel boring machine and supporting facilities.

2.1.1 Tunnel-boring Machine

In guidance, TBM is treated abstractly as a cylinder: its cutter head (as shown in Figure 3) faces the earth, and rear end (as shown in Figure 4) connects the tunnel liners. The cutter head is equipped with spinning blades, cutting the earth off the front surface in the advancing direction. While the cutter head is boring, the hydraulic cylinders at the rear end (in Figure 4, pushing cylinders are

the six shining metal poles visible; in Figure 5, one cylinder is zoomed in) will push back the pushing ring (the outer most red ring in Figure 4), and the ring will press on the concrete liners. The TBM is propelled by the forces of excavation at front and pushing at back.

Figure 3. Cutter head of TBM

Figure 4. Rear end of TBM

Figure 5. Hydraulic cylinder and pushing ring

2.1.2 Concrete Liners

The concrete liners are the outer boundary of the tunnel, and separate everything inside the tunnel from the earth of outside. In a typical eight-foot drainage tunnel, one section is one-meter long and consists of four pieces. The liners are lifted down to the tunnel by cranes, and loaded on liner cars. The heights of gantry sections are adjusted to let liners to pass through, and it is one of the reasons why gantry system takes up all the space in the center of the tunnel. When the liners are hauled to the front right behind the pushing ring, the mechanical arm as shown in the middle of Figure 4 will pick up the liners piece by piece, and assemble a whole section (as shown in Figure 7). The liners endure a lot of pressure when the pushing ring is being pushed back, this can lead to deformation of the liner.

Figure 6. Four pieces of one eight-foot liner section.

Figure 7. How mechanical arm assembles concrete liners

2.1.3 Gantry Facilities

Gantry facilities are the most complex system next to the TBM itself. The three most important equipment mounted on the gantry system are transformers for electricity supply, conveyor belt for muck dumping, and mechanical arms for liner assembly. As shown in Figure 8, transformers sits in the center of the upper part of tunnel, and it is the first obstacle that shapes the survey window. The conveyor belt is a long transporting system from the cutter head to the rear end of TBM. The spinning blades for the cutter head produce tons of muck and the conveyor transports the muck to the muck cars. Conveyor belt is categorized as dry transport (Maidl et al. 2013), and thus the muck will not be too moisturized.

The belt is one of the main reasons of mechanical shutdown of the project, the worn-out speed of the belt depends on the geotechnical conditions and types of fluid to assist digging.

Figure 8. Transformer on the first section of gantry.

Figure 9. Conveyor belt (picture taken in the operator's chamber)

2.1.4 Rail System

Rail system is built all along the tunnel, from the entrance shaft to the segment of liner near the pushing ring. The rail system is responsible to haul the concrete liners to the front (front means the area closest to the TBM), and transport the muck out to the back (back means the entrance shaft). As shown in Figure 10, muck cars are yellow cars on the left, and concrete cars are on the

other track. After muck is hauled out, concrete liners can be sent up front for installation; and after assembly, the muck cars will swap with liner cars.

Figure 10. Two tracks in the hand-dug section

The transportation system is designed to maximize the payload of both muck cars and liners cars, for example, as show in Figure 11, the size of muck car is almost as wide as the tunnel. This leaves very narrow safe space on the two sides for guidance system. If the muck car is piled up, the safe space will be even smaller.

Figure 11. Size of an empty muck car

2.2 TUNNEL-BORING MACHINE GUIDANCE

2.2.1 Steering Tunnel-boring Machine

Operator steers the machine by controlling the length of pushing cylinders, for a typical eight-foot TBM, there are eight cylinders (as in Figure 4). Normally the pushing cylinders have two statuses: fully extended and contracted (not pushing at all). When the TBM is right on track, the operator stretches out all cylinders and the TBM will advance straightly. If, for example, the TBM deviates to the left, operator will shut down the hydraulic cylinder on the opposite direction (right in the middle cylinder in this case), and when other cylinders push, the TBM heads to the right direction besides advancing forward. Eight cylinders empower the operator to finely steer the TBM, and a qualified guidance system should provide accurate and intuitive guidance information for operator to make proper decisions.

Figure 12. Contracted hydraulic cylinder

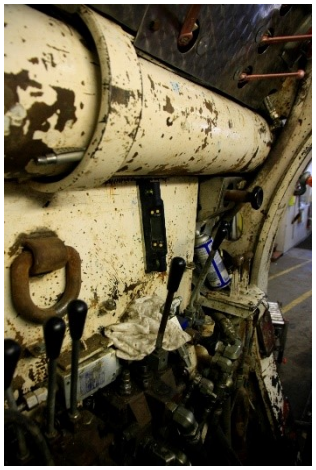

Figure 13. Control panel of TBM Steering

2.2.2 Overview of Guidance Systems

The guidance systems provide real-time and high accuracy positioning data for steering tunnel-boring machine. The guidance systems rely on the geospatial reference network for setup, calibration, error detection, and relocation purposes. Currently, the reference network is set up by surveyors based on national spatial reference system and Global Positioning System (GPS); however, all of these reference systems can only be functional above ground, and surveyors need to set up a temporary reference network for the underground tunnel guidance purpose.

Since the beginning of civil projects from ancient days, survey and measurements are one of the most critical processes. Ancient people utilized footsteps, measurement tapes, and spinning wheels to stake the site layout, and to verify the as-built objects are constructed as-designed. However, modern construction involves more than traditional houses or high-rise buildings, and it keeps encountering more and more challenging problems from industrial and infrastructure projects. The new challenges are either impossible to be built or extremely difficult and expensive to be built in the old ways. For example,

prefabricated pipe spool modules are tremendously heavy and oversize, and huge crane and lifting frame are needed to handle these projects. The same happens in Bird Nest stadium in Beijing, which consists of twisted steel pieces, and the construction workers should rely on heavy equipment to install them. Similarly, drainage tunnels in municipal infrastructure are cost-sensitive projects, tunnel-boring machine (TBM) drills tunnel from shaft to shaft. It is expected that TBM can keep advancing without deviation or interrupted, and it is needed to provide reliable and low-maintenance methods for these kinds of projects. Based on the examples, modern construction needs real-time, precise, reliable, integrated survey and measurement methods to enable tightly-constrained engineering designs, to reduce time and costs, and to liberate construction workers from low-efficiency tasks.

Generally, a reliable and real-time survey system depends on two conditions: the ability to measure the targets, and the ability to self-calibrate. However, the two main characters of the temporary reference network, one is that the network expands with the progress of the tunnel construction, and the other is that the network is instable. Both of these two characters result in recurring surveying in the tunnel for network expansion and error detection. However, surveying process will take non-trivial space in the tunnel, and for small diameter tunnels, the whole site should be shut down solely for surveying purpose. The long-time shutdown results in “fear” of the tunnel surveying, and people intend to notify surveyors only when they are totally lost in the underground darkness. However, when the tunnel is totally off the alignment, it will take more time for surveyors to make necessary amendment (they need to overcome unintentionally made curvature, or redesign tunnel alignment to steer the tunnel back on track). Moreover, surveying process in current practice

generally occurs after tunnel sections built, thus, it is impossible for the operators to notice any displacement or disorientation of the tunnel due to the settlement of installation sections.

The unnecessary high price of the tunnel surveying and guidance is a major factor undermining productivity. In construction, a golden rule is the earlier a problem is found, the cheaper and easier it can be fixed. The same philosophy applies to tunnel surveying, too. Traditionally, surveying is treated as a signature for certifying the owner payment of completed work, not as part of the construction. The connection between surveyors and construction workers forms an interface; for tunnel-boring machine operators, the interface is the laser spot, and as long as the operator can see the spot, they don't feel they need help from surveyors. However, the interface is much more fragile than everyone expects, and dozens of interior and exterior factors can invalidate this interface. Still taking tunnel guidance as an example, the gantry sections and the hoses of the machine can block the laser, the settlement of the installation segment can cause displacement and disorientation, and overloaded muck cars may hit and move the laser, etc. Some of the changes are negligible, some causes noticeable indications and alert the operators, and some stealthily alter the interface without leaving any trace. Operators may be misguided into a wrong path and eventually hit into a neighbor tunnel or produce a tunnel where the stream can never flow. In short, surveying is not an add-on signature, but the guardian of the conformity between design and construction implementation.

2.2.3 Laser-based Solution

To provide fast-feedback without harming the practices of the construction, construction industry invests heavily to seek for promising technologies. In TBM construction field, laser guidance methods have dominated

the market for decades. A laser beam, which advances straight in the air, provides an excellent visual indicator for operators. As shown in the Figure 14, the laser beam represents the as-designed path of the tunnel (referred to as the *alignment* in tunnel design). If the center point of the rear ring of TBM does not fall on the laser beam, this indicates TBM has deviated away from the alignment. The offsets between the alignment and the center of rear ring are called *line deviation* (horizontal offset, perpendicular to the advancing direction) and *grade deviation* (vertical offset), respectively. The laser guidance is set up and maintained by surveyors. In other words, surveyors deliver the design information to the TBM operator in an elegant way in the field. The decision on when to calibrate the laser projection requires experiences of the operator and the foreman of the tunnel crew: surveyors will only be called in to help when the laser beam is not reliable or visible. This method is straightforward and becomes the mainstream solution in tunnel construction.

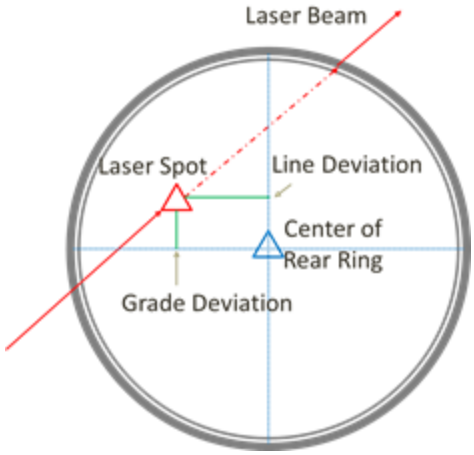

Figure 14. Deviations of TBM

However, the conventional laser solution has many disadvantages. For example, the setup process of laser is manual and only experienced survey specialists can complete the task within the time period of construction shutdown.

Another disadvantage is that due to the manual setup, laser is unsupervised between two consecutive calibrations by the surveyors. However, the laser is not guaranteed to stay in the same position and orientation during the unsupervised "dark time". For example, the pressure from TBM's hydraulic cylinders during advancement can lead to settlement of the installed tunnel liner section on which the laser theodolite is mounted, possibly causing unexpected and unnoticeable displacement and disorientation of the laser projection.

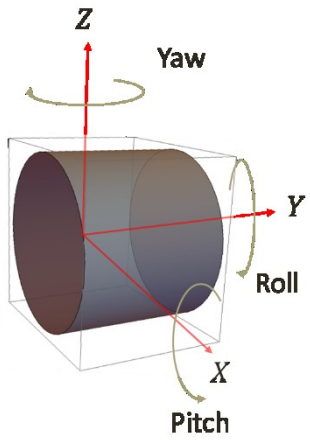

Figure 15. Pose of TBM

Due to these constraints, the industry puts many efforts to improve and enhance the laser method, and the innovations in motorized laser, programmable survey robot and gyroscope enable automation for the laser system. The enhancements include three aspects: pose measurement, position measurement, and display improvement. Every new system attempts to improve at least one aspect, and some will combine all three. Pose measurement is the most popular enhancement, and widely included. An early enhancement for pose calculation is as shown in Figure 16, in this setup there are two transparent target boards, laser beam will leave one spot on each board (totally two spots). Ideally, the two spots should be at the center of each target board, and when TBM is not in the right

pose, as shown in Figure 17, the front part of the TBM is higher than as-designed position. Operators can easily decide the next steering strategy based on the current unaligned direction.

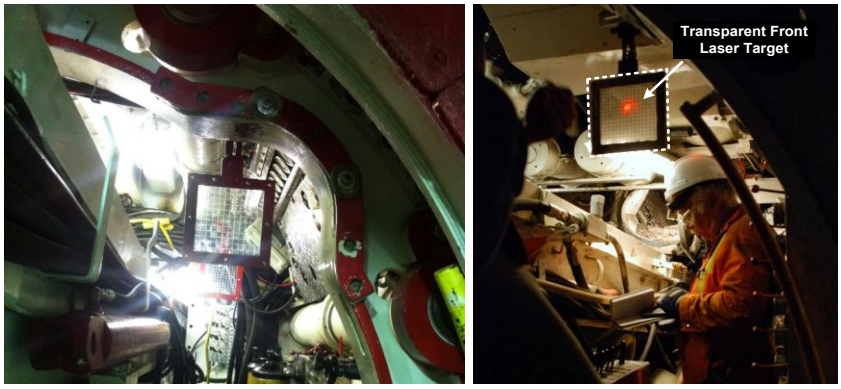

Figure 16. Two target boards system for pose measurement.

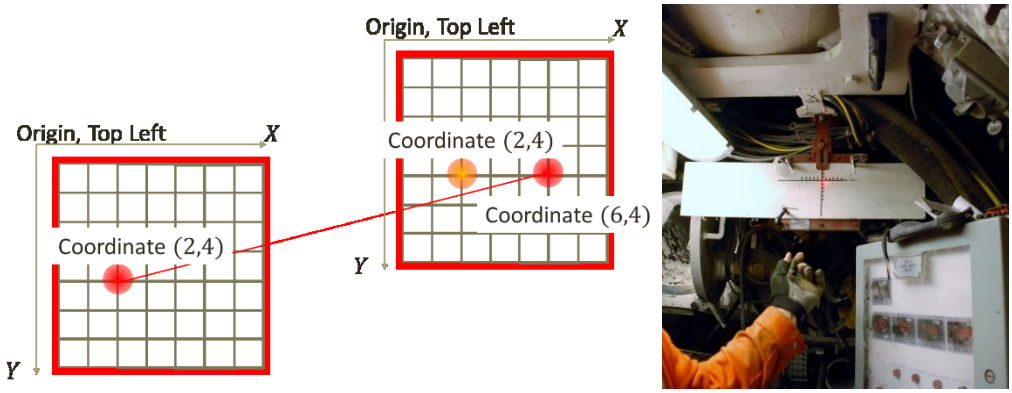

Figure 17. Laser spots on target boards.

This design of pose measuring system is still in use today. However, this method is solely for visual decision, operators still need experience to steer the machine. Moreover, the laser has no self-check during the unsupervised “dark time” and it takes long time to setup (ten to twelve hours are not rare, especially for small diameter tunnels). To address these two issues, almost all modern guidance systems accept the total station with “receiving unit method”.

The receiving units are not much different from the two transparent target boards, and a general shape is a cubic box with the two target boards as front/end faces. The receiving units are created to calculate the position of the laser dots by machine, not by operators. Some systems (Jardón et al. 2014; VMT GmbH 2003; tacs GmbH 2004; GEODATA group 2014; ZED Tunnel Guidance Ltd 2005; Herrenknecht AG 2015) utilize digital cameras with photogrammetry algorithms to retrieve the positions of the laser dots, while others use photosensitive circuits in the target boards to enable automatic measurements. It is noteworthy that all these modern laser modifications apply both motorized laser emitter and survey robot in order to simplify laser tuning and automate survey tasks by developing user-defined programs. Robotic total station, which builds a motorized laser emitter into a survey robot, can further relieve the survey crew from time-consuming laser maintenance by automating the routine self-check during the "dark time", thus eliminating the need for manual laser calibration.

It is noteworthy that all these modern laser modifications apply motorized total station, a survey equipment that can perform automated survey tasks by user-defined programs. Total station can rotate precisely to any horizontal/vertical angles, and emit a laser beam parallel to the tunnel alignment. With total station, guidance systems can automatically perform self-check during the "dark time", and eliminate the needs for manual laser setup. Different products have different strategies to utilize the motorized total station. For example, *tacs* system utilizes one back-sight prism to check the direction (tacs GmbH 2004), VMT utilizes reference prisms to check the position (VMT GmbH 2003).

2.2.4 Virtual Laser Target Board

Apart from the laser-based pose measurement improvements, there are two other types of guidance strategies. One is to utilize gyroscope to measure the pose (Maidl et al. 2013), and it is very suitable for tunnels with sharp curves. However, the commodity-level gyroscope cannot preserve the accuracy for relatively long time, and calibrations are needed to keep the accuracy at satisfactory levels. Another strategy is to apply laser and prisms to calculate the pose (S. Mao, Shen, and Lu 2014; PPS-GmbH 2015). Virtual Laser Target Board (VLTB) System is a laser-prism based pose measurement system (Shen, Lu, and Chen 2011). It is based on the theory of three-dimensional transformation of rigid body and three-point positioning algorithm. The system surveys three points on the rear ring of TBM, through the survey window, and computes positions of the cutter head of TBM as well as the pose in the three dimensional space. VLTB system also utilizes ZigBee network to work wirelessly and automatically.

Although the original VLTB design provides the guidance mode when only one or two prisms are visible (S. Mao, Shen, and Lu 2014), they are temporary solutions based on assumptions to cope with short-time invisibility. For instance, when there are only one point available, the system assumes that the cutter head and the rear of TBM deviate from the alignment with the same level and line deviations; when there are two points available, the system assumes the rotation angle of roll is zero, and calculates pitch and yaw approximately; as such, the position and pose of the TBM can be fixed (S. Mao, Shen, and Lu 2014) (Mao et al. 2014), they are temporary solutions based on assumptions so as to cope with short-time limited visibility constraints during construction (when only two or one prisms are visible to the survey robot). It is reemphasized the core of VLTB system still relies on the visibility of three prisms which are installed on the TBM

with a certain geometric layout that allows for position and pose calculation in acceptable accuracies. The one-point and two-point ad-hoc methods are temporary solutions to guide the TBM through a short period of invisibility of the target. The achievable accuracies for one-point and two-point solutions are not sufficient compared with the original VLTB solution based on three-point algorithms.

2.3 SELECTING GUIDANCE SYSTEMS

Construction engineers choose one guidance system over the other; they first make decisions based on features. Features include positioning, pose measurement, computer-aided display, and other features provided by guidance systems. Engineers choose candidate systems from the market to meet the entrance requirements. For example, if the extension of hydraulic cylinders on TBM must be measured, especially in hard-rock TBM, TAUROS system can be a good choice over the others (GEODATA group 2014).

But this is not the whole picture, there are other criteria. For example, the size of the tunnel is a huge factor. Many guidance systems are designed for large diameter tunnels, and the visibility windows are spacious for many candidate systems. But for small diameter tunnels, the constraints are totally different. We should not regard the small diameter tunnels as a special case, they stand for a lot of similar problems, which can be defined as *tunnels with confined space and limited visibility*. In this section, the constraints in these tunnels will be elaborated. For convenience, the thesis refers these tunnels as “small diameter tunnels”, but really means “tunnels with confined space and limited visibility”.

2.3.1 Space-constraint

For municipal infrastructure projects, including drainage and sanitary tunnels, unlike traffic tunnels, the TBMs for infrastructure construction are generally smaller in size, for example, most recently built tunnels in Edmonton Canada are with a diameter of either eight-foot or ten-foot. The decision for the size of the tunnel is based on both functionality and cost: tunnels should be bigger enough to handle severe storms, but not too big as they will cost more tunnel liners, produce more muck, and maybe longer construction time. However, the small diameter (in this paper, we call tunnels with eight-foot or ten-foot diameter as small diameter tunnel) causes problems in tunnel guidance systems, which work smoothly in larger tunnels, especially the lasers with receiving units. The reduction in diameter causes shrinkage of operators' chamber, survey window (especially in curved tunnels), and operational space. For example, in a typical small diameter tunnel, as shown in Figure 19, there is only one rail for muck cars, and the muck car will take up almost all the available space of the lower half of the tunnel. However, the survey work also occupies the whole passage, and the rails and wood board for walking do not allow any vibration during survey.

Figure 18. Survey in eight-foot diameter tunnel

Figure 19. Muck car on the rail (right).

Moreover, as shown in Figure 21, the author can barely stand straight in the chamber of eight-foot TBM, and the survey window is almost blocked by hoses and other obstacles, the receiving units cannot fit into this environment.

Figure 20. Author stands in the operator's chamber with Virtual Laser Target Board System

Figure 21. The survey window for laser to pass through.

2.3.2 Time-cost Model of Guidance Errors

As discussed in space-constraint subsections, we can conclude that it is impossible to allocate time to satisfy both survey and construction. However, foreman must decide the level of cautiousness, and determine the threshold to balance alignment checking against construction. Depending on the severity of the accuracy problem, the project can choose either shutdown or not. The threshold for this decision is set based on time duration. For checks that take less than one hour, it can be done during lunch break, and foreman are more than

happy to call surveyors to perform a fast validation; however, if the checks take several hours, the foreman has to shut down the project. Lu etc. (Lu, Shen, and Mao 2014) studied the time and cost saving over an eight-foot one-kilometer drainage tunnel guided by the VLTB guidance system with Monto-Carlo simulation. In that study, the interval of quick check and full check are experience-based. In this thesis, the interval is modelled on accuracy loss model (error propagation model). Therefore, accuracy is part of the construction, and guidance systems can be analytically assessed from time-cost aspect.

2.4 REFERENCE NETWORK FOR TUNNEL GUIDANCE

2.4.1 Conventional Laser Setup

Conventional laser system has many ways to calibrate the emitted laser beam to be parallel to the tunnel alignment. In this paper, the author will illustrate one manual calibration method that he observed and practiced in the field study. This method is called the three-string method.

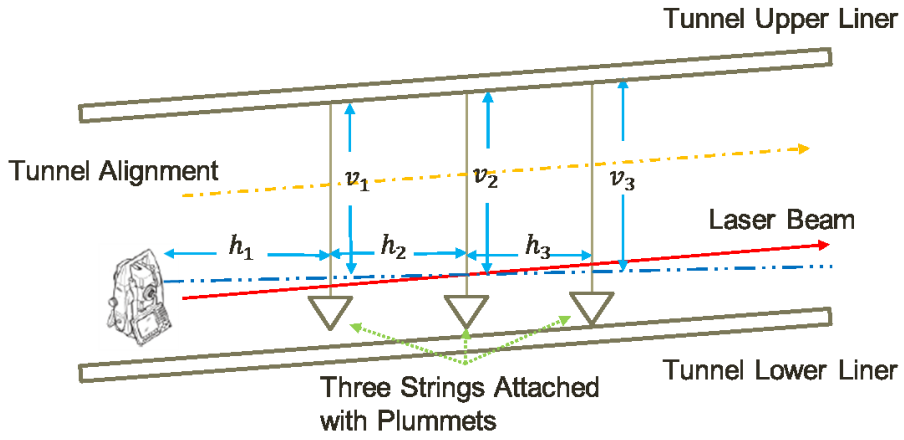

Figure 22. The three-string calibration method for conventional laser.

Two points in the space can determine one and only one line, according to Euclidean geometry, and this applies in space where the laser is set up. Surveyors

utilize at least two strings, and let laser beam passing through two marked points on the strings (one on each). Then the laser is supposed to be parallel to the alignment of tunnel. As shown in Figure 23, a total station or theodolite will be placed in the center of the tunnel, and when surveyors see through the total station, the two hanging strings of plummets must fully overlap each other. And then when total station turns 180° back, the direction total station aims is the alignment of the tunnel.

Figure 23. Set up alignment for the tunnel.

However, in real world, the laser is not a line, but a cylinder of light. As shown in Figure 24, the size of the laser spot can be larger than the diameter of hanging string. Moreover, even with a plummet, the hanging string sways constantly; it is very hard to observe the static location of the string. These two factors will introduce uncertainty and error into the calibration, and even a bit disorientation will cause dramatic displacement for the TBM. Therefore, the surveyors introduce a third line as redundancy for calibration.

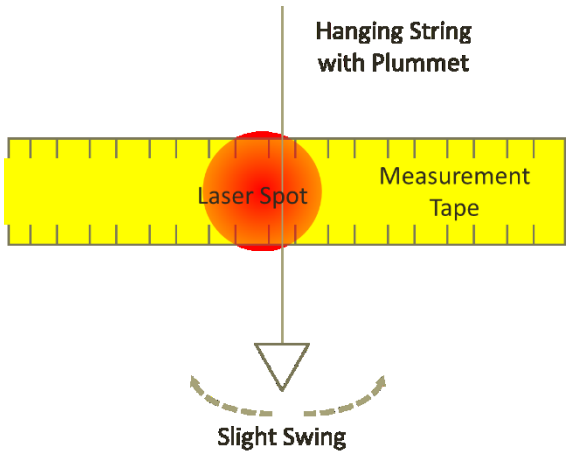

Figure 24. Adjust laser direction on yaw angle.

The calibration process includes adjustment on pitch angle and yaw angle, as shown in Figure 22 and Figure 24. Generally, surveyors will fix yaw angle first and then fix pitch angle, as yaw angle is harder to adjust. A typical yaw angle adjustment includes the following steps:

1. Setup hooks for hanging strings along the alignment on the roof. This setup is done by most experienced surveyor in the team, through several hours of calibration.
2. Find the hooks for hanging strings offset from alignment with a fixed distance along X_a axis direction.
3. Put three strings on three hooks, seven meters away from one another.
4. Adjust laser orientation with yaw angle, and emit laser beam onto three strings.
5. Use a measurement tape as shown in Figure 24, the center of the laser spot should deviate from the string with a fixed distance. The measurement tape must parallel to the X_a axis during the observation, and the string position is taken as the center of the swaying path.
6. Check the error on three strings, if any error exceeds the limit, redo step 4.
7. Check obstacles on the laser path, if any part is blocked, redo step 4.
8. Adjust laser orientation with pitch angle. Most laser-mounting base is not a sophisticated system, but a simple platform with several screws. Surveyors can move the laser on the platform and fix the laser with the screws. Minor adjustments are done by loosening or tightening the screws. Therefore, when adjusting the pitch angle, surveyors should be careful not to affect the yaw angle.
9. The center of the laser spots should pass given heights on the string, usually three different heights. Surveyors should also check step 5 with step 8, make sure no yaw angle disorientation.

10. Check the error on three strings, if error exceeds the limit, redo step 4.
11. Check obstacles on the laser path, if any part is blocked, redo step 4.

As we can see, the calibration is so error-prone and therefore time-consuming and experience demanding. It is not unusual for experts to spend ten to twelve hours just to handle this calibration. This method requires nothing but expertise of surveyors, and has been widely utilized in TBM guidance for past decades. An example in Figure 25 can demonstrate how surveyors adjust the laser. The laser theodolite shoots a laser spot on a measurement tape, which is held horizontally by the surveyor. The hanging string, which is set up by the surveyor, has a known offset from the central alignment. Assuming in the example, the string is $1m$ on the right of the alignment. When the laser spot falls on the tape, we can roughly read the central vertical line of the laser is $1cm$ on the left of the string (one dash on the tape is $1cm$ in the example), which suggests the center of the laser is $99cm$ on the right of alignment. However, surveyors must ensure current offset to be $1m$, so the laser must be moved $1cm$ to the right.

When surveyors want to move $1cm$, it is generally very easy. They can loosen and tighten the screws of the mounting bracket of the laser, and move the laser left and right. However, when they want to move $1mm$, the process is a nightmare: Even a slight movement, like loosening the screw, can tilt the laser. The laser is so sensitive, and even a small adjustment will cause a big change at the end of the laser. Surveyors need to repeat this process for three strings every time after moving the laser, and many times of moving before perfectly aiming through the string.

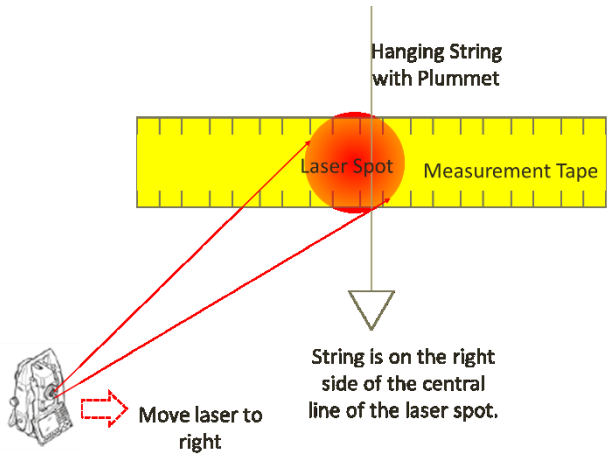

Figure 25. An example of adjusting laser horizontally

However, nightmare is still here. After laser is horizontally adjusted, the laser must be also calibrated vertically. The goal of the vertical adjustment is to ensure correct grade.

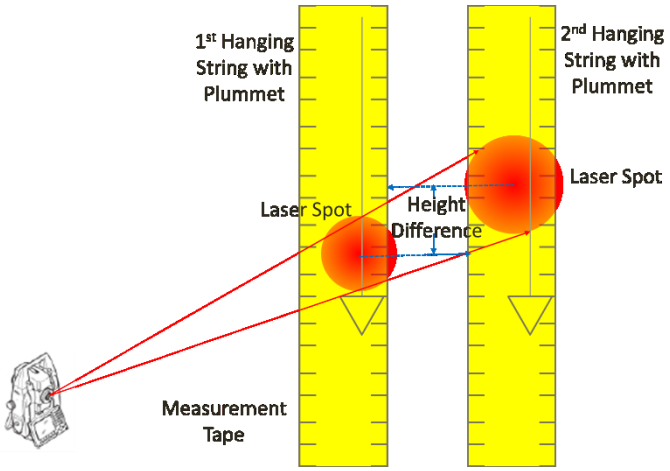

Figure 26. Adjust laser vertically

The laser will leave three laser spots on all three tapes, and for each tape, one end is touching the roof during the calibration. The center of each laser spot is measured against the tape. For example, if the grade is 0.2%, and if two strings are $7m$ apart, the height difference should be $1.4cm$. If the height difference is $1.5cm$, the grade of the laser beam is too big. The height difference must be compared among all three strings.

After horizontal and vertical calibration, surveyors will eventually check whether laser spot can fall on the target board. If the laser is blocked by any hose or other obstacles, all the calibration processes must be repeated, till the laser beam can reach the target board.

The offset between laser center and hanging string is a fixed value v_{cc} (center compensation), which is decided by the center of target board. Assume the offset between the center of target board and the center of rear ring is V_{tc}, and hanging string offsets from alignment is v_{str}, then v_{cc} can be calculated as:

$$v_{cc} \leftarrow v_{str} - X(V_tc) \tag{1}$$

The reason for this center compensation is sometimes due to curvature or unexpected obstacle, the center of target board will be temporarily redefined. As shown in Figure 27, sometimes in order to let laser pass through survey window and hit on target board, the surveyors choose temporary center with offset v_{cc} (horizontal compensation) and v_{hc} (vertical compensation).

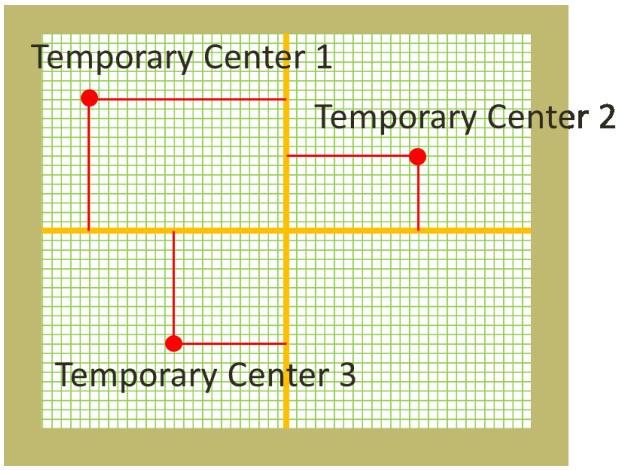

Figure 27. Target board and temporary centers.

2.4.2 Traditional Tunnel Survey

The temporary reference network for tunnel-boring guidance is a typical case for integrated surveying. Traditional tunnel-boring guidance setup consists

two processes: (1) alignment setup and (2) laser adjustment. And the alignment setup consists of two steps: (1) establishing references in the shaft, and (2) propagating references to the tunnel. As shown in Figure 29, at the beginning of the project, surveyors utilizes GPS stations to pinpoint the start/end points of the tunnel in the horizontal plane. Later, they need to measure the actual height of the start/end points by performing leveling survey, from a known height control point, which is set up by the government. Henceforth, the surveyors know about the three-dimensional coordinates of start/end points, and they will inform the workers about the depth of the shaft, and they use two plummets, which immerse in oil buckets for stabilization (as shown in Figure 28, downward the bottom of the shaft. By measuring the lengths of the strings of plummets, they eventually calculate the three-dimensional coordinates for two starting points at the bottom of the shaft.

Figure 28. Plummets immersed in oil

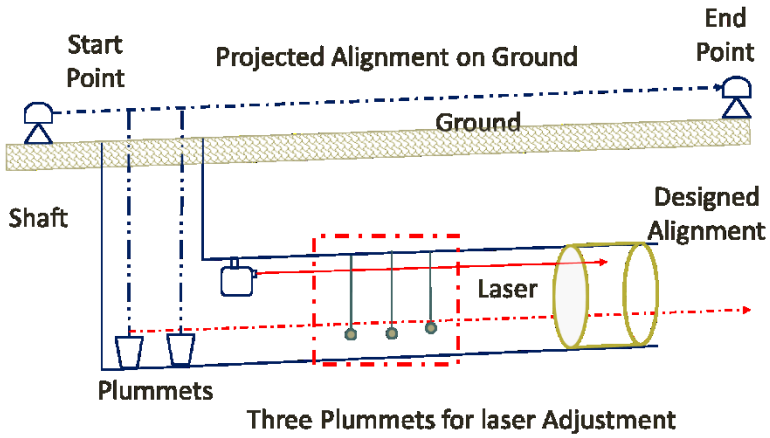

Figure 29. Tunnel-boring Guidance Setup

By far, the surveyors have set up the reference in the shaft, and the propagation of reference system into the tunnel is a repeated process, and it is both setup and calibration procedure. The reasons for the repeated survey are (1) tunnels advance with time, (2) settlement of tunnel sections with reference points installed causes displacement and disorientation, and (3) independent survey of the position of the current laser spot must be compared with the current reading periodically. The main product of the propagation is a collection of hanging points on the roof of the tunnel, with known vertical and horizontal offsets from alignment. These are the reference control points for traditional tunnel-boring guidance method. Every time when surveyors redo the propagation, they will check all these hanging points and make necessary adjustment. The final stage of reference propagation is to set up three plummets along a line, with about seven meters interval (a practical constant from surveyor' experience), as shown in Figure 29.

Figure 30. Hanging Point for Alignment and Inverse Propagation

This line is the parallel line of the tunnel alignment, and it controls the adjustment of laser. Then surveyors need to adjust the laser to coincide with the parallel line and leave a laser spot on the target board. This process consists of repeated trials and tests, which may last for several hours. There are three constraints for the adjustment: (1) the center of the laser must pass all three strings; (2) the centers of the laser spots on the three strings should be some specific heights based on tunnel grade; (3) after all, the adjusted laser should still hit on the target board in the operator's chamber. If any constraint is violated, surveyors need to move the laser, redo the calculation and recheck all three constraints again.

Laser adjustment alone is a black hole that undermines construction productivity, and because the duration is so unpredictable, tunnel foreman needs to allocate a whole shift for surveyors to calibrate the laser. However, this setup is inevitable, as a small displacement and disorientation will result in a parallel laser, and the guidance will be unpredictable till next adjustment. The requirement for high accuracy is a burden for stakeholders: surveyors pours enormous time and effort to ensure the accuracy; operators and foremen are too

cautious to call in the surveyors to make examinations, as examination itself at least includes re-calibration.

In this thesis, we name the survey work in tunnel as two parts: full survey and guidance setup. In the full survey, surveyors set up new reference benchmarks and re-check errors in existing reference benchmarks. In the guidance setup, the surveyors adjust the laser or other guidance methodologies according to the established benchmarks (a typical adjustment is like Figure 29). In full survey, there are two parts: ground control and alignment control. The ground control always utilizes Global Positioning System (GPS) and local georeferenced benchmark set by the government. A solid ground control is especially important for tunnels of several kilometers long, in which the tunnel cannot be assumed in a local Cartesian coordinate, and elevation and curvature of the earth must also be considered (Calvert 1989; W. J. T. Greening 1988; Zheng-Lu Zhang and Song-Lin Zhang 2004). The ground control is purely survey problem and will not be discussed in this paper.

In alignment control, surveyors focus on comparing the as-built path and as-designed alignment underground. They drills hooks in the middle of the tunnel on the roof of the liner, and the hooks shows the central line of the tunnel. Then surveyors perform traverse (horizontal location measurements) and leveling (vertical level measurements) to survey the alignment of tunnel (Chrzanowski 1981; S. C. Stiros 2009). In an ideal scenario, survey starts from a known location, setups a few unknown locations, and later stops at another known location. This is a closed loop, and the start and end known locations can help eliminate random errors accumulated during the survey process (Anderson and Mikhail 1998). However, the tunnel is a typical example of an open loop: it starts from one shaft and stops in front of gantry, and there is no closed loop for

error detection and adjustment. One way to solve the problem is to traverse back to the start point and form a closed loop with the same start and end point. The other is to introduce gyroscopes to provide extra information for one of the unknown points (Chrzanowski 1981).

In a survey shutdown, surveyors start with full survey, finding errors in existing benchmarks and establishing necessary new ones. Later, they calibrate the laser beam (or other methods) to match the survey results. After the shutdown, the guidance equipment is left in the tunnel and will not have another calibration till the next shutdown. However, due to the pressure of the earth and the pushing force of the TBM, the concrete liners of tunnels will be very probable to suffer different levels of deformation (V. A. Kontogianni and Stiros 2005), the guidance equipment has no resistance to these deformation, and especially the laser based solutions, a small displacement at the beginning will cause a large offset at the end.

Some solutions provide reference benchmarks (reference prisms, as shown in Figure 31) for the automatic system to perform self-check (S. Mao, Shen, and Lu 2014; tacs GmbH 2004; VMT GmbH 2003). The surveyors can set up several to dozens of prisms for the guidance system to perform self-calibration. These prisms work together as a network, and we call it reference network. In this thesis, the last and most important mission is to optimize the reference network, determining the optimum locations and timing to set up these prisms.

Open traverse in full survey seems similar to the reference design. However, there are several differences between open traverse in the full survey and reference network design: (1) the reference prisms are mounted for long time in the tunnel; (2) the locations of prisms and total stations are not interchangeable. Therefore there is no established guidelines for assessing the

effectiveness of the reference network for automatic guidance for on-going tunnel construction or designing a reference network suitable for this task.

Figure 31. Reference prism in the tunnel

Another issue is the misalignment of goals between survey and construction crews. All the answers to a reference network are developed by survey crew, to achieve higher accuracy. However, the process may be very long and cause long shutdown for construction crew and the benefit earned by dedicated survey may easily be invalidated by construction cost increase (Lu, Shen, and Mao 2014). Especially for drainage and sanitary tunnels, they are not long and very narrow, which the intrusive survey work may make the operator hesitant to call for survey work, even in some necessary occasions. In some tunnels for special purpose (e.g. particle accelerator in hadron collider), the accuracy for tunnel alignment is very high, and accuracy is the most prioritized task (W. T. Greening et al. 1993; Wei et al. 1993; Wei et al. 1999), but most civil construction concerns very much about time and cost. Some design philosophy in tunnel monitoring and inspection provides a few inspiring ideas (Berberan, Machado, and Batista 2007; Van Gosliga, Lindenbergh, and Pfeifer 2006; Pejić

2013), but they are more about as-built tunnels and the main focus is not time and cost of construction.

The last but not the least issue is about design, schedule and cost. In the design phase for a new tunnel, engineers ask surveyors for a rough estimation of survey time. In good geotechnical conditions, surveyors may give an estimation of "routine survey every ten meters, relocation survey every two hundred meters" (Lu, Shen, and Mao 2014). However, during the construction, surveyors may notice deformation and settlement of the liners and request for more time and higher frequency. The estimation and scheduling for survey is experience based, unpredictable and uncontrollable in the perspective of construction engineers.

This paper gives an answer to plan the reference network design during design phase. The proposed design algorithm tries to fill three gaps discussed in this section: it should be a reliable reference network for automated guidance systems (e.g. VLTB); it should integrate the reference network as part of the temporary facilities of the projects during design phase; eventually it should satisfy affordable time and cost while ensure necessary survey accuracy for quality control in construction.

2.4.3 First-order Optimization of Reference Network

The design algorithm in this thesis should ensure both low cost and standard abiding accuracy, it is necessary to find optimum locations for total station and prisms in the network. Previously survey researchers developed solutions to optimize their geodetic network. This topic is from traditional geodetic surveying, but in this thesis, the framework utilizes a variant of this method to optimize the optimum locations for reference prisms.

The researchers in geomatics started to study the concept of geodetic network optimization in 1882 (Schmitt 1982). The reference networks in

geomatics are always large scale, and they are built to set up a stable and high-quality reference datum for a large area. The applications include very-long-baseline interferometry, orbit correction of global navigation system of satellites (A. R. Amiri-Simkooei et al. 2012). In modern tunnel survey, it can help optimize the ground control for tunnel.

A typical case of geodetic network design can be described as Figure 32. Surveyors set up several to dozens stations (locations for survey observation). Each station is equipped with tribrach, upon which surveyors can mount either prism or theodolite on this station. When the tribrach is mounted with a prism, it works as reference station, and can be surveyed by other stations; when the station mounted with a theodolite, it can survey other stations. After all survey among these stations, the network (stations and the observations between each two stations) is set up as a geodetic reference, and will be treated as the authority of coordinates of local area by all other surveys, like civil survey.

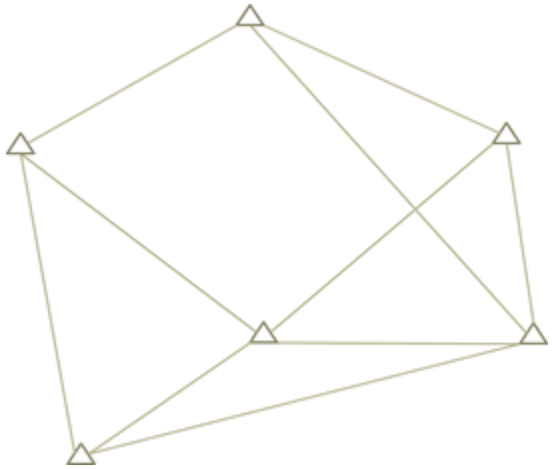

Figure 32. A geodetic network setup. The stations are presented by the triangles, and the observations are shown as the line.

Owing to the importance, the network is required to be stable and reliable (Seemkooei 2001). However, as all engineering problems, the setup survey is not

always ideal, and the shape of the network, which includes all relative positions between each stations, is not the optimal enough for the design purpose. Mathematically the geodetic network can be expressed as the following equation:

$$Q_x = (A^T \cdot P \cdot A)^{-1} \tag{3.2}$$

In equation (3.2), matrix A represents the configuration (the shape, all locations of stations and their mathematical relations); matrix P is the priori weight matrix from the observation process; matrix Q_x is the posteriori variance-covariance matrix of the network, recording the internal statistical relations between each two stations (Cross and Thapa 1979). Mathematically, the stability and reliability of the network can be quantified by the matrix Q_x, because smaller variances mean higher certainty in the locations of all stations, and therefore more reliable. The goal is to optimize the matrix Q_x and researchers developed four different optimization strategies for this problem: 1) zero-order design (ZOD), 2) first-order design (FOD), 3) second-order design (SOD), and 4) third-order design (TOD) (Schmitt 1982). (The ZOD is for free-net problem (Schmitt 1982) and will not be elaborated in here)

FOD manipulates the configuration A, and by moving the locations of the stations, it delivers an optimized shape with higher quality (Berné and Baselga 2004; Schmitt 1982). In comparison, SOD targets on the weight P of each observation and station in the calculation (A. Amiri-Simkooei 2004; Kuang 1992; Schmitt 1982; Kuang 1993). The reason for SOD optimization is that the weights are initially determined by the quality of the observation, and the common solution for high quality observation is repetitive measurement. However, as all stations are far away from each other on a large area, even up the mountains, the repetitive measurement is not easy especially from the cost aspect (Schmitt 1982). The TOD optimization is different from FOD and SOD, and it focuses on how to

improve quality of the network Q_x by adding a number of new stations to the network. TOD changes both configuration A and weight P, and there are not many researches on this topic and it is always solved by combination of FOD and SOD in a sequential process (Schmitt 1982).

In this paper, the design algorithm applies the FOD to choose the reference prism's location during every relocation of laser. This considers the future probable deformation on the liners of prisms and total station, and try to find optimum positions.

In optimization of geodetic network, the objective function is equation (3.2). To minimize the matrix Q_x in equation (3.2), there are several methods. Three popular strategies are A-optimality, D-optimality, and E-optimality (Berné and Baselga 2004), which minimize trace, determinant, and largest eigenvalue of covariance matrix Q_x. In this paper, the particular objective function is equation (43), and D-optimality is the chosen strategy.

2.5 OUTLINE OF THESIS

Considering all the factors, the proposed research focuses on innovating a general method of designing and optimizing tunnel guidance system for tunnel-boring construction. The research answers one question: how to integrate survey into tunnel-boring construction, with optimum construction time and cost. It reaches beyond the traditional guidance problem, which is largely defined from survey's perspective and focuses on the quality of the survey. However, from construction's perspective, the answers to questions like what is a feasible guidance problem, how to assess a guidance method, how to adapt the method to unideal conditions, are much different from survey's perspective. For

construction, the final question is always how the technologies help with the time and cost savings in construction of the projects.

The research approaches the problem in three steps: integrating automatic system into temporary facility of construction, adaptive trade-off of integration for extreme cases, and design phase integration and optimization for optimum construction time and cost.

Fundamentally, the integration demands automation of the survey system, it must work flawlessly with the current construction processes, and provide insightful information for decision making. The research provides a fully automated system for all-purpose tunnel-boring machine guidance. It tries to eliminate frequent intrusive survey activities, and make most of the automatic survey solution. The automatic guidance system is blended into the temporary facilities of the tunnel, and survey robots and wireless control network are mounted on the supporting brackets on the tunnel liner. This is the corner stone of the whole research, and enables the integrated survey to be general purpose.

The second step is to be adaptive. The integration must handle the extreme unideal conditions during construction. If the guidance system fails to provide guidance information in these scenarios, the intrusive survey will be brought back, which is always unexpected, therefore undermining the schedule and cost. The research studies how much survey accuracy can be sacrificed in order to deliver valid guidance information during harsh situations, as survey accuracy is an indicator and threshold of whether to introduce extra amount of work. The smart laser solution to be described, will make the trade-off in allocation of time and space between construction and survey.

Engineers of construction projects desire to precisely predict the time allocated for survey. Experienced surveyors can give them confident estimation,

and are less likely to introduce expected workload. However, the automatic system will introduce inaccuracy although it is convenient; adaptive solution to extreme scenarios sacrifices accuracy of survey as a trade-off for construction benefit; will the surveyors still be able to give trustworthy estimation? Can engineers assess the most suitable guidance methods during design phase? Can engineers schedule survey shutdown besides rough and experience-based estimation from surveyors? If there is unexpected change of design or extreme scenarios, can the schedule be automatically updated to reflect the necessary work? The answer is to devise the reference network design algorithm. The design algorithm plans for the establishment of reference networks, a quality control for guidance systems, during design phase. It can respond to different factors like tunnel settlement and displacement, different tunnel guidance methods, and change of design. The designed reference network can provide a foundation of quality control for all automatic guidance system (not just Virtual Laser Target Board system to be described), during the design phase. Engineers can clearly know where and when to setup prisms and survey robots based on a solid mathematical foundation.

Chapter 3. AUTOMATIC GUIDANCE SYSTEM

3.1 OVERVIEW

Automatic guidance system can be integrated seamlessly into the tunnel construction, without intrusive attendance. In this chapter, ideas and requirements of the automatic guidance system will be illustrated. The automatic guidance system should be invisible and intuitive, replacing the current methods silently. This requires the system to be reliable and user-friendly. Construction crew are conservative because the construction environments are complicated and demanding, reliability is the first step to persuade them to adopt the change of process. Moreover, reliable system requires much less attendance by the survey team, and construction crew will be less interrupted. User-friendly means automatic system presents a well-organized panel, providing only necessary information for control purpose. One of the major reasons that the conventional laser is still widely accepted is the laser spot on the target board is easy to comprehend and no information noise to increase the burden of understanding.

This chapter illustrates the Virtual Laser Target Board system (VLTB), the automatic guidance system applying three-point positioning algorithm. It can replace the conventional laser without compelling the operator to learn new knowledge, and it excels at self-maintaining and requires much less attendance comparing to the conventional laser. An automatic system requires the designer of the system carefully reviewing all corner cases the system may encounter in the tunnel, and designing proper responses to all possible emergent situations.

3.2 RESEARCH METHODOLOGY

The VLTB system integrates automated surveying, wireless communication, and 3D visualization in order to lend vital decision support to both tunnel surveyors and TBM operators under extremely limited "tunnel vision" scenarios. In addition, the data will be recorded in real time. Analytical results are transferred via wireless networks from the tunnel face to the aboveground office. The core idea of the method is to survey the TBM status in real time and visualize the most relevant information on a VLTB human interface, thus facilitating the operator and surveyor to make sound, timely decisions as tunnel boring operations continuously unfold.

As shown in Figure 33, the VLTB system is essentially based on a robotic total station plus three or more prisms. A tablet computer serves as the control console, which operates the robotic total station performing searching, locking, and surveying in wireless. The computer processes the surveyed data and renders the results in an intuitive way to help TBM operator makes proper decisions. The operations data are also transmitted to a server computer located at the site office above ground through a securely encrypted ZigBee wireless channel.

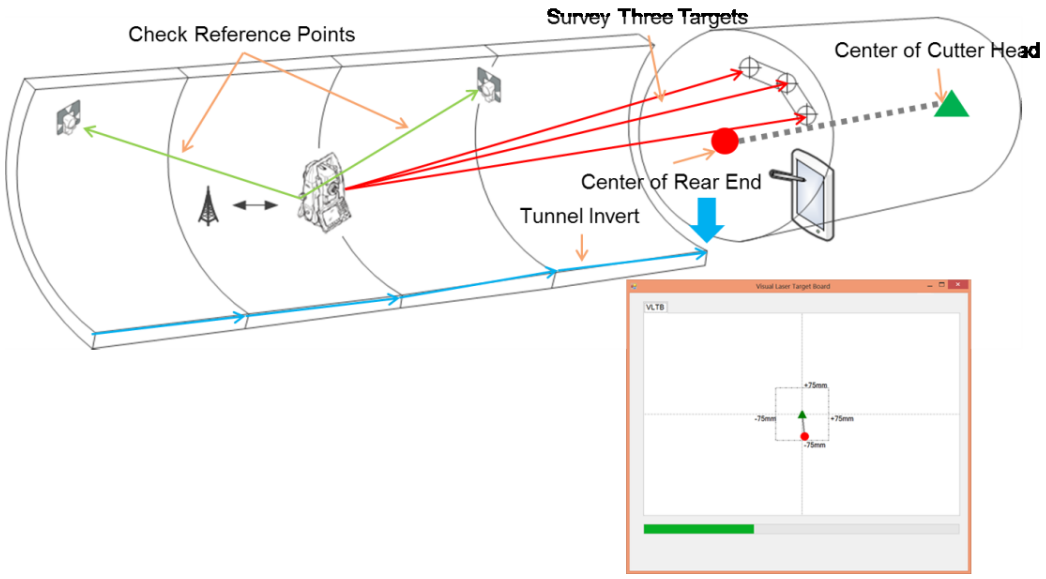

Figure 33. Virtual laser target board system design

The VLTB system improves the point-to-angle computing algorithm originally derived from developing the RTS-based Automatic Guidance System (Shen, Lu, and Chen 2011). The new algorithm requires three prisms, which can be located anywhere in a solid object such as in a limited survey window near the up-right corner of a TBM. Despite increased complexity, the computing performance of the enhanced algorithm in terms of accuracy and response time has been maintained. By pre-registering the relative positions of the cutter head and three selected targets at the rear end of the TBM (shown in Figure 33 as the green triangle and the red circle, respectively), the center of the cutter head can be determined with the accuracy in the order of 1-2 millimeters in near real time. A vector linking two invisible points in the underground space, namely the center of the cutter head and the center of the rear section of the TBM, are projected on a virtual laser target board interface of a tablet computer in order to visualize the TBM position and attitude. In addition, the tunnel invert (shown in Figure 33 as blue line) can also be automatically fixed by computing algorithms as the TBM advances (Xiaodong Wu, Ming Lu, and Xuesong Shen 2014). All the components

in the system are connected through wireless networks. Both the operator at the frontend and the site foreman above ground are kept current of the tunnel as-built alignment and the actual construction progress in real time.

3.3 COMPUTING ALGORITHMS

The algorithm to calculate the TBM's position and attitudes is similar to resection. There are three coordinate frames involved in the positioning algorithm, namely the prism frame (l), the TBM body frame (b) and the local geodetic frame (g). Also there are four points identified on TBM, including the three target points (C_1, C_2, C_3) and the cutter head (A). Before assembling the TBM in the underground space, all the four points are registered. Their coordinates in the TBM body frame are $(C_1, C_2, C_3)_b$ and A_b. As the algorithm solves framework rotation instead of translation, all symbols, include points, vectors, or matrices, are three-dimensional non-homogeneous values.

The prism framework is an ancillary frame to facilitate calculation, which is defined as following:

- Origin: C_2
- X-axis: $\overrightarrow{C_2C_1}$
- Z-axis: $\overrightarrow{C_2C_1} \times \overrightarrow{C_2C_3}$
- Y-axis: $\vec{Z} \times \vec{X}$

After defining the prism frame, the rotation matrix T_l^b and the translation vector V_l^b can be calculated based on the definition rules. Thus, the coordinates of (C_1, C_2, C_3) and A in the prism frame can be calculated as $(C_1, C_2, C_3)_l$ and A_l.

When the TBM is advancing in the ground, (C_1, C_2, C_3) are surveyed by RTS as $(C_1, C_2, C_3)_g$ in the local geodetic coordinate system, while the coordinates

of the cutter head in local geodetic coordinate system A_g are unknown. As shown in Figure 34, M_l^g can be calculated from $(C_1, C_2, C_3)_g$ and $(C_1, C_2, C_3)_l$, and therefore the unknown A_g can be calculated from M_l^g and A_l. In addition, the M_b^g can be calculated from known A_b and calculated A_g, thus the rotation angles ϕ, θ, ψ can be obtained by the decomposed T_b^g.

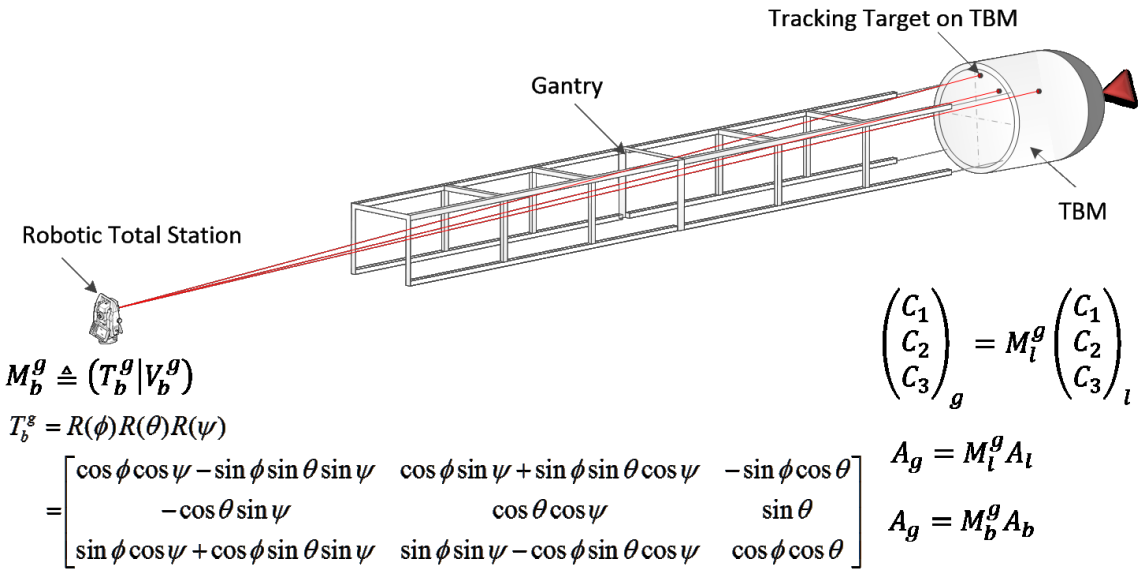

Figure 34. Calculating position and attitude of TBM based on three points

3.4 System Hardware and Software Architecture

The VLTB system is divided into three subsystems by functionality: the surveying subsystem, the communication subsystem and the control subsystem. The surveying subsystem comprises of target prisms and a robotic total station. The robotic total station is a total station enhanced with robotic control mechanisms and application programming interfaces (API). Users can control the robotic total station through the API and perform automation tasks, such as target searching, tracking and surveying. In the surveying subsystem, the robotic total station locks the coordinates of the prisms by a pre-scheduled plan or on

request from the control subsystem. The survey data are sent via the communication subsystem to the control subsystem.

As shown in Figure 35, the system is connected by the communication subsystem (ZigBee wireless network (Baronti et al. 2007)). Operator sends survey commands and receives surveyed results through tablet-based interfaces of the control subsystem (an industrial-class tablet computer). The relevant guidance information is also given on the tablet. On the other hand, the surveying subsystem (total station) receives survey commands, reads target prisms and broadcasts surveyed results via the ZigBee networks. On the site office aboveground, a server computer captures the broadcasted results, and submits the changes to the database, which triggers 3D visualization programs to re-render the time-dependent 3D models.

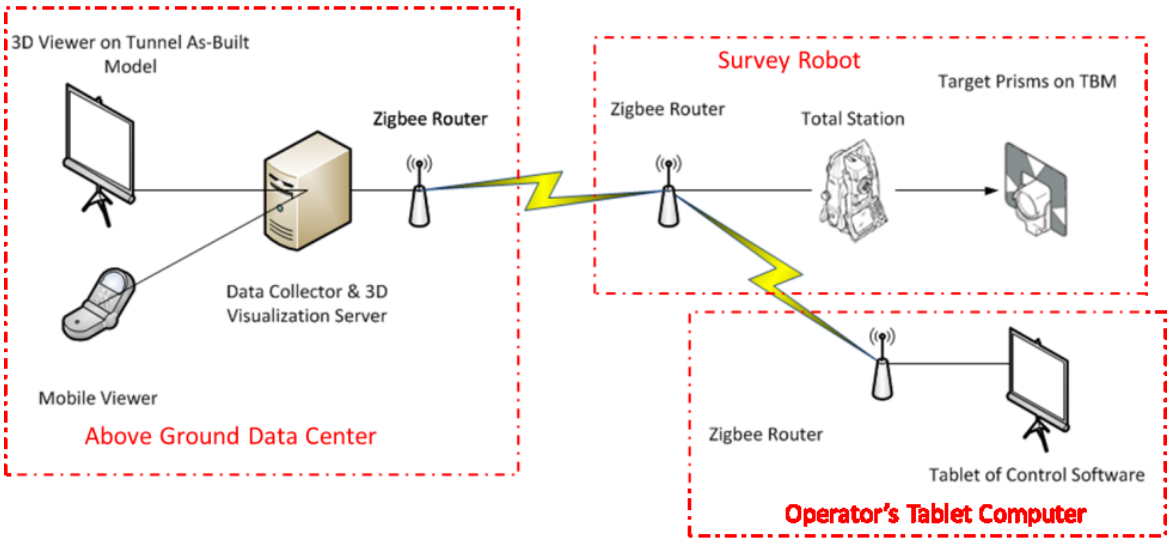

Figure 35. System components and architecture

The communication subsystem (as shown in Figure 36) is responsible for data communication, making the underground tunnel data available to the user on the surface and the other subsystems. The communication subsystem utilizes

mature, industrial standardized technologies as data link layer. For example, the ZigBee technology is the IEEE 802.15.4 –based low-power, secure network, which provides reliable data link on a range of 100 meters with proper line-of-sight (Baronti et al. 2007). By contrast, Bluetooth can provide high speed connection within 10 meters range. Thus, in different scenarios, the communication subsystem is configured differently. For example, for long-distance communication (more than 10 m), the ZigBee technology can be used, while for short-distance or low-latency scenarios (less than 10 m), the Bluetooth technology can be effectively employed. But to the other modules, the communication subsystem acts like a “black box”, and handles input/output data using standard input/output protocols. In tunnel construction, the survey location will gradually move deeper inside the tunnel along with the advance of the TBM. As such, the distance between the data source (the tunnel face) and the above-ground data receiver would gradually increase. The robotic total station is relocated once every 200 m tunnel advances in order to ensure the reliable and accurate performance by the RTS in terms of automatic prism recognition, tracking and surveying. The operator always works at the back of the TBM. As a result, the distance between the operator’s tablet computer and the robotic total station gradually increases up to 200 m. In consideration of these constraints, a communication technology that supports relay transmission (such as ZigBee) is more effective and provides the preferable solution.

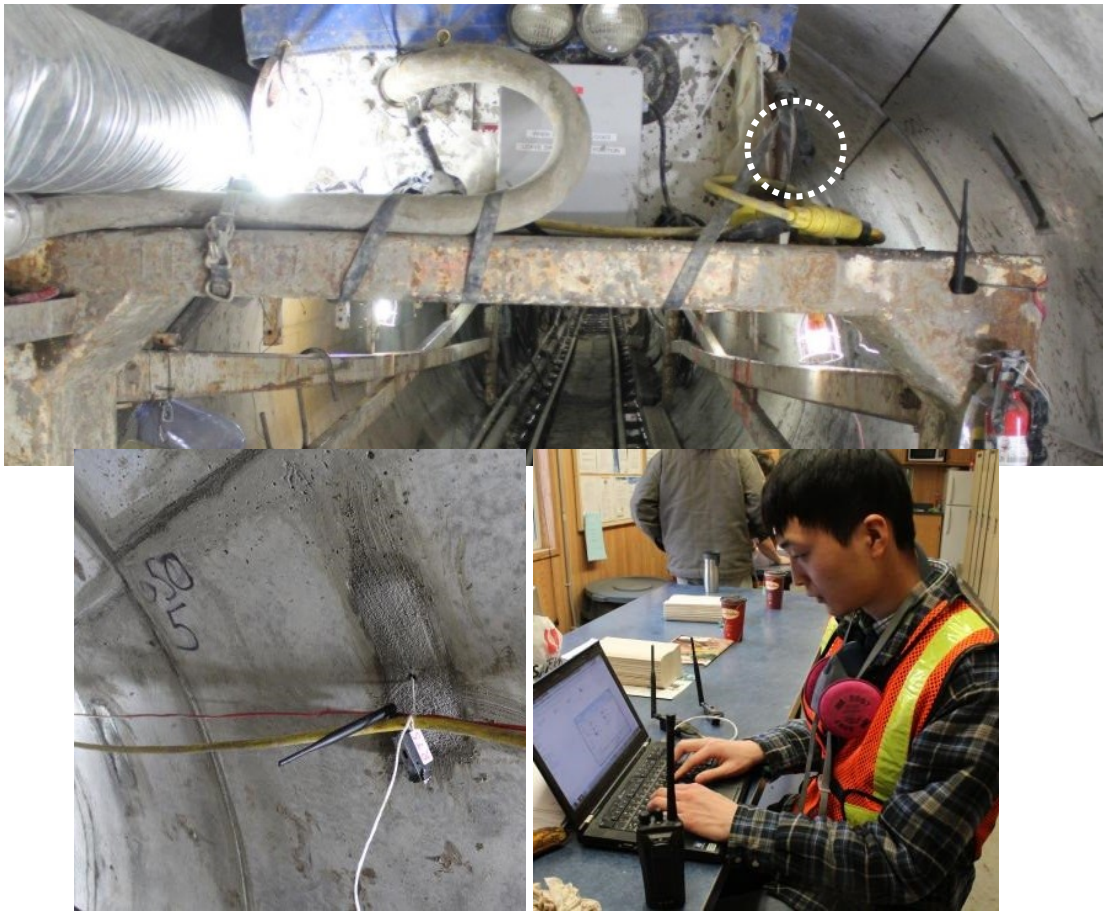

Figure 36. ZigBee relays deployed at end of gantry (Upper), on tunnel liner (Lower Left) and at above-ground trailer office (Lower Right)

The control subsystem is responsible for handling user interaction, survey control, data persistence and failure recovery. It interacts with both surveyors and operators. For instance, surveyors can set up the coordinates of robotic total stations and target prisms through the VLTB system configuration interface; on the same interface, they can also check alignment deviations and schedule the time events of automatic surveys. For operators, they interact directly with the VLTB interface and read the current tunnel alignment deviation and steering guidance information. It is noteworthy the VLTB hardware is a collection of inexpensive, mature, off-the-shelf technologies and its installation is simple and

does not require any physical laser target boards such as those special laser registration boards in VMT and *tacs* systems (tacs GmbH 2004; VMT GmbH 2003).

The software architecture of VLTB comprises of four different sub modules, and in the current version of the software system, all the four modules are implemented in the control subsystem. The four sub-modules are:

- Total station control
- Data serialization and logging
- Data processing
- Data visualization

All messages encoding commands or data are broadcasted over the ZigBee-based wireless sensor networks. The total station control module interprets the robotic total station control protocol, and the total station operates itself and is controlled by commands released from APIs. The data serialization and logging sub-module preserves all incoming and outgoing broadcast messages, and keeps track of all the events for further integrity check and debug purposes. The data processing module is the core, which processes survey data and produces results for supporting decision making by surveyors and operators. The data visualization sub-module utilizes the results from the data processing sub-module and renders them in more intuitive, role-specific interfaces in order to aid in decision making and project control.

3.5 USER INTERFACES

There are two "control panel" interfaces in the VLTB system, one is tailor designed for the operator and the other is for the surveyor. When the surveyor performs resection and enters tracking automation parameters for RTS (as show in left image of Figure 37), VLTB launches surveyor-specific user interface for

resection and parameter specification (as shown in the right image of Figure 37. Surveyor setting up RTS (Left) and surveyor-specific user interface (Right)

It allows surveyors to add and remove reference points and target points, survey the TBM, and perform system self-check. Each target is given a unique identification name; the associated raw surveying data (horizontal/vertical angle and slope distance) and its coordinates (East, North, and Zenith) are kept in a database. The surveyors' setup session can be preserved and reloaded when re-launching the interface. Every time the surveyors relocate the robotic total station, they need to recreate a session to preserve the working environment.

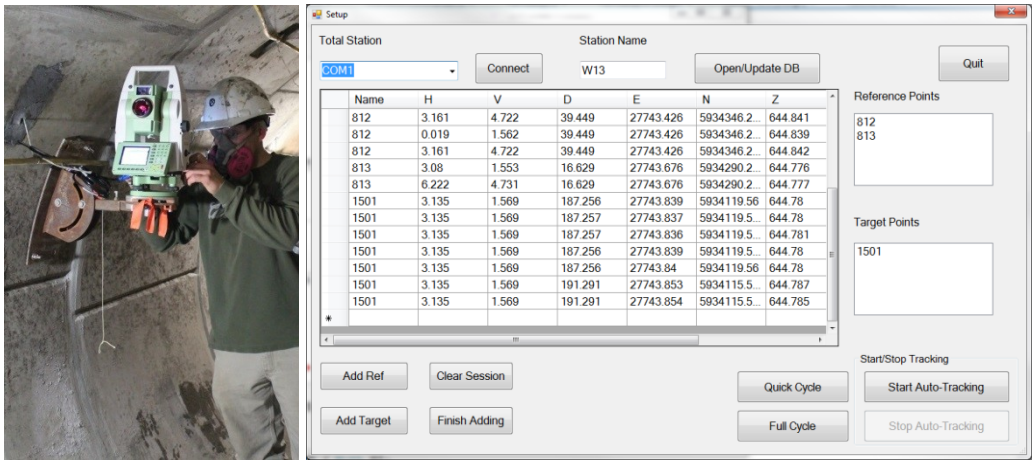

Figure 37. Surveyor setting up RTS (Left) and surveyor-specific user interface (Right)

The operator's interface is shown in the right image of Figure 38. The two-dimensional diagram shows the guidance information for the operator. In the diagram, the tunnel alignment should pass through the center of the cross and remains perpendicular to the observation plane (tunnel cross section). A red circle and a green triangle represent the center points at the rear end and the cutter head of TBM, respectively, while the vector connecting the two points represents the body axis of TBM. When the body axis of the TBM deviates from

the tunnel alignment, the red circle and the green triangle move away from one another and from the center of cross in real time. The steering guidance information is provided in terms of how to move the TBM in order to keep the red circle and the green triangle within the tolerance box while shortening the length of the body vector as much as possible. Note the red triangle arrows suggest the direction of the next maneuver by the TBM operator (turning right and downward as in Figure 38), assisting the operator in making decisions on steering control on the fly. The numbers on the right side of the interface show the current line/level deviations, yaw/roll/pitch angles, the advancing speed of TBM and the chainage distance the TBM has reached. Such real time operations information is crucial to keep track of the current tunnel alignment quality, the TBM position status and the construction progress.

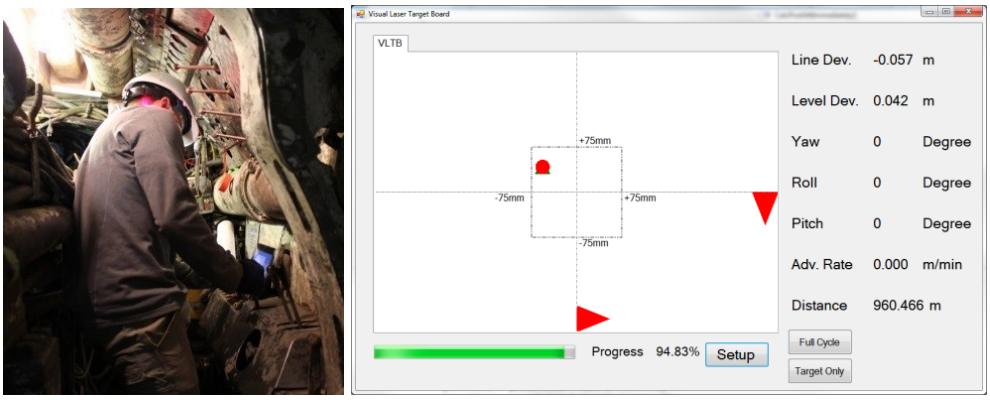

Figure 38. Operator reading deviation and guidance information (Left); operator-specific user interface (Right)

In addition to the user interfaces tailored for underground tunneling and surveying crews, a 3D visualization interface is also provided to show the real-time progress and deviations of tunnel boring operations along with the as-built tunnel invert for the site foreman and the management team working in the above-ground office (as shown in Figure 39).

Figure 39. Site foreman-specific 3D UI for project summary and visualization

3.6 ROBUSTNESS DESIGN

The underground tunnel construction environment is complicated, featuring confined space and high humidity. All these practical constraints negatively affect the robustness and reliability of the VLTB system. A single failure or mistake of the automation system may cause a huge impact on the progress and quality of construction.

The most critical constraints in connection with the VLTB system design are identified as (1) geometry of surveying, (2) battery life, (3) software logic, (4) communication quality, and (5) device installation and deployment. The robotic total station also relies on laser to track and survey the prisms installed on the TBM together with the two reference points with known coordinates fixed on the tunnel wall. One of the practical concerns is the dispersion of the laser. As the tunnel advances away from the robotic total station, the laser footprint grows larger. If the two prisms are too close to each other, the total station would be confused and the measurements taken by the total station could be incorrect. In reality, it is very difficult to install the three prisms at positions on the TBM

which are sufficiently apart from one another while all falling in the narrow field of vision of the total station.

To compensate, the processing program will automatically choose the corresponding algorithms based on how many target prisms are “surveyable”, as shown in Figure 40. Generally at least three surveyable prisms on the TBM allow the determination of exact spatial position and rotation of the TBM body in the underground space; one surveyable prism only yields the deviations of the end section of the TBM body. In order to achieve high accuracy results, the ideal geometric layout of prisms should be such that all the prisms fall in one plane perpendicular to the tunnel alignment (or the laser projection). In addition, the system is designed to be able to perform automatic self-check, report any possible displacement, and carry out regular self-calibration operations of the total station. To cope with the practical constraints of potential invisibility of the installed prisms, the automation system has been developed as per the operation logic given in Figure 40.

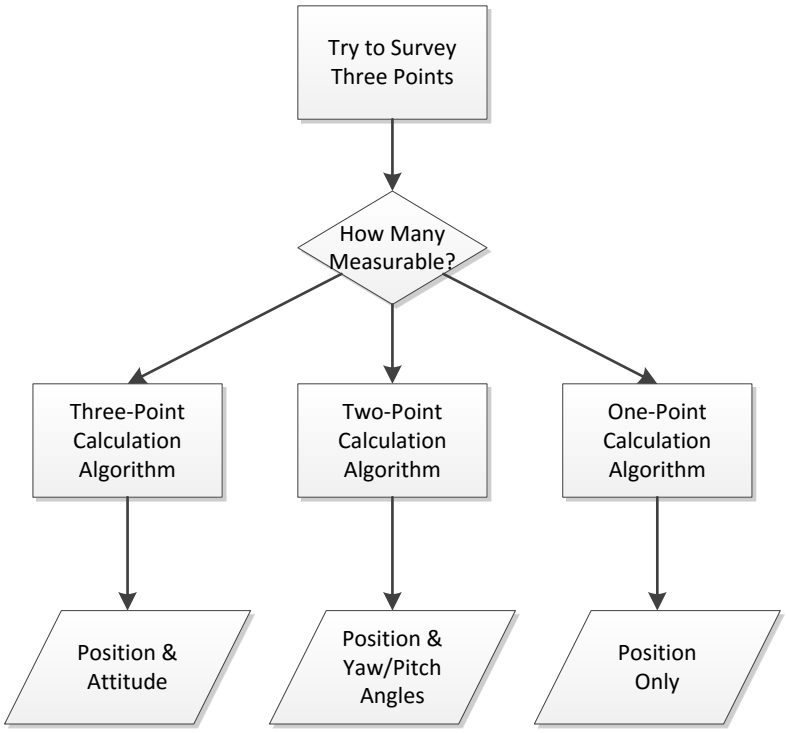

Figure 40. VLTB automatically chooses processing algorithm based on number of measurable targets

The second practical constraint is the battery management. The robotic total station, the tablet computer, and the wireless sensor networks are all powered by batteries. Currently, total station manufacturers provide external battery packs which can support the total station to continuously operate for over eight hours. Also, the tablet computer can be supported by the power supply inside the tunnel besides the TBM control panel. The universal serial bus (USB) ZigBee nodes are powered through the USB interface of a laptop computer, and the standalone ZigBee nodes use external batteries as the power source.

The third robustness problem is software logic. The software system uses both error codes and exceptions to protect system integrity (Goodenough 1975). The error codes are embedded in the logic of coding to handle known issues with the system. When the system receives error codes, it immediately triggers predefined actions, for example “waiting for next survey”. Exceptions are

expected for the events that are not clearly predefined. For example, when some workers or equipment block the line-of-sight of the robotic total station, the survey process would fail and the system will receive a corresponding error code. In this case, the system automatically reinstates to a safe mode and alerts the operator or the surveyors about the situation.

The fourth problem is communication quality. The performance of wireless sensor nodes is influenced by battery, software bug, and other factors of the application setting. Currently, the system monitors the processes of sending and receiving data over the wireless networks. Any time-out exceptions and message corruptions in communication are recorded for analysis. If errors and exceptions accumulate rapidly in a short time, the system probably suffers from a serious failure in one of the communication nodes. Immediately, a notification message will be sent to the operator. If the failure happens in a router node, it is more complicated to locate the node and it is not straightforward to identify which router has failed.

The last practical challenge is system installation and deployment. It is most difficult to mount the tablet computer in the congested steering chamber in the TBM. The body of TBM can be heated by electrical and mechanical systems. In the field testing, the tablet computer was temporarily fixed on the control panel but the overheating environment would potentially cause malfunction of the tablet computer.

3.7 LABORATORY TESTING

A mock-up TBM model (as shown in Figure 41) was built in order to validate the positioning algorithms underlying the VLTB system. The model is roughly one twentieth of the size of the real 2.4 m diameter TBM in the field.

Four survey prisms are mounted on the cutter head and the survey window at the back end. A RTS is set up 4 to 5 meters away, pointing at the round prism (the "ref" in Figure 41) as the north direction. The RTS surveys three points (Points "0~2" in Figure 41) and the VLTB system calculates the center point at the cutter head (Point "3" in Figure 41). Then the RTS directly surveys the cutter head center point and compares the resulting coordinates against the VLTB's computing outcome. The process is illustrated in Figure 42.

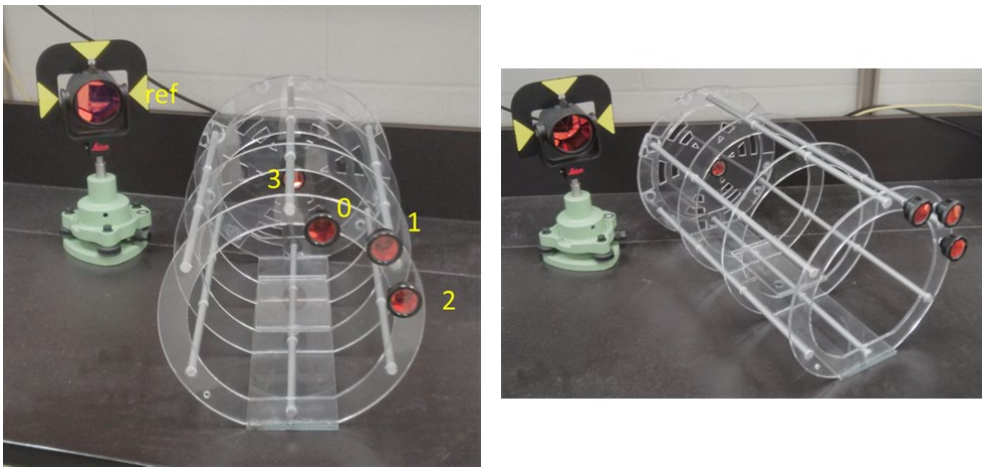

Figure 41. The mockup TBM model for algorithm validation

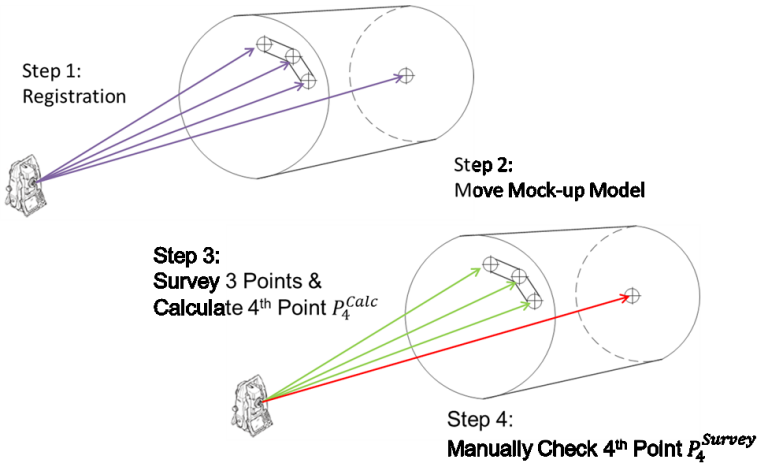

Figure 42. Four-step procedure for algorithm validation

Twenty-four groups of lab testing data from nine different RTS settings were collected. In each setup the RTS position was different and thus the bearing

varied accordingly. As given in Figure 43, the coordinate differences between the VLTB calculated vs. the RTS direct survey results were determined along the three axes, namely East, North and Zenith. The differences on North are negligible, while the differences on East and Zenith directions are larger, in the worst cases 7 mm difference was observed. The overall standard deviation of the differences on the east, north and zenith are 3 mm, 1 mm and 3 mm, respectively. The accuracy would be sufficient for the intended application of tracking and positioning a TBM in the tunnel project.

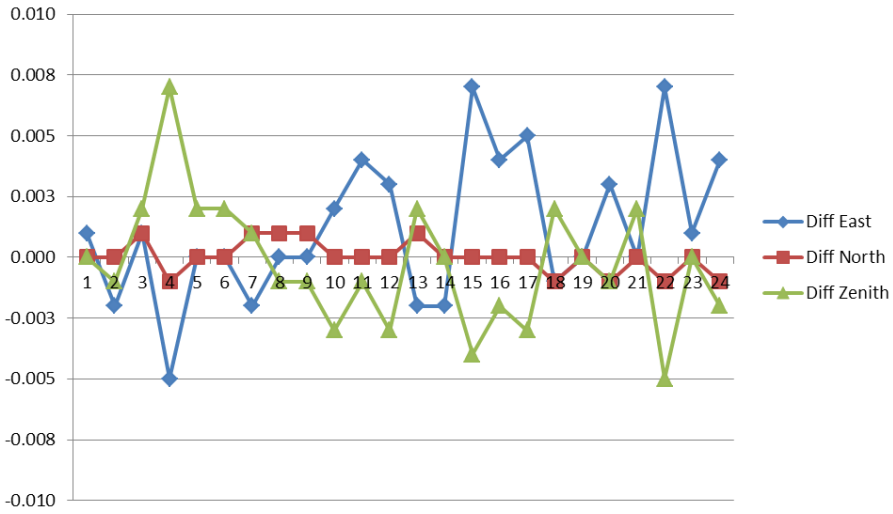

Figure 43. Differences between calculated and surveyed coordinates of the cutter head (unit of measure is meter)

3.8 FIELD TESTING

The system was successfully tested in a 1,000-m-long, 2.4-m-diameter drainage tunnel in Edmonton, Alberta, Canada during the seven-month period from August 2012 to March 2013. The visibility of the survey window varied during the construction phase. Occasionally, the trailing gantry squeezed the size of the survey window. A replaceable prism bracket (as shown in Figure 44) was utilized to make the installation of prisms flexible. The closest distance between

two prisms on the bracket is 293 mm. Therefore, the total station is recommended to locate within 200 m from the TBM to effectively distinguish each of the three prisms.

Figure 44. Prism bracket attached to TBM within visible window

RTS was mounted on a mobile bracket, which could be easily installed and removed from the tunnel liner, as shown in Figure 45. The arm of the bracket was adjusted to ensure the robotic total station is able to see through the survey window available at the back of the TBM while not being hit by fully loaded muck cars. After system setup and initialization, RTS performed pre-scheduled survey operations and reported survey data automatically. Based on field testing in the drainage tunnel, the TBM can advance as far as 200 m away from the RTS without the need to relocate the RTS; within 200 m, the automation and communication sub-modules of the VLTB system functioned with high reliability.

Figure 45. RTS mounted on a mobile bracket in the tunnel

The field testing of the VLTB system was conducted into two phases: in the first phase, the system surveyed the targets for several rounds and each round lasted for one hour, then the surveying results were regularly compared against surveyors' independent checking results, which were recorded directly from the offset of the laser spot on the target board. In this phase, the comparison between passive laser and VLTB is conducted to evaluate the accuracy and reliability of the VLTB system. The passive laser system serves as a valid reference though a 30-40 mm error is expected (Sheng Mao et al. 2013).

In the second phase, the system ran continuously in the tunnel while the tunnel crew and the TBM were working. The robustness of the system integration and automation in the field was tested in the second phase. System performance under practical settings was evaluated and key findings are summarized as follows:

The wireless network was always online during the tests. The wireless coverage, the interference, the delay and the batteries all functioned well and performed normally during the test. This test confirmed that design and setup of the wireless networks hardware system is valid under the practical tunnel settings. The total station surveyed the target prisms every five minutes. This test was to

make sure the total station's internal command server performs consistently with the wireless network and the control system.

The control and computing module handled data and exceptions properly, for example, when the line-of-sight is blocked, the total station halted the current survey cycle and scheduled a retry at a later time.

The data receiver captured the survey data and submitted the processed results to the database to run the 3D visualization program.

Table 1 shows consecutive testing results for two hours collected on March 13, 2013. According to the logging system, all messages during the two-hour test were successfully sent and received, which proves that the wireless networks and the total station worked well in the test. Meanwhile, it is found that the line-of-sight was blocked by workers and the expander of TBM between 10:29 AM and 11:01 AM. The control system handled the situation properly, resulting in a half-hour blank survey history as given in Table 1.

Table 1. Continuous survey results of one target prism (Hz, Vertical angles are in Radians, Distance, East, North, Zenith are in meters)

Time	Hz	Vertical	Distance	East	North	Zenith
13/03/2013 10:15:46 AM	3.135	1.569	165.272	27743.705	5934141.545	644.722
13/03/2013 10:21:36 AM	3.135	1.569	165.288	27743.704	5934141.528	644.722
13/03/2013 10:24:01 AM	3.135	1.569	165.34	27743.706	5934141.476	644.721
13/03/2013 10:25:07 AM	3.135	1.569	165.381	27743.703	5934141.435	644.721
13/03/2013 10:29:37 AM	3.135	1.569	165.502	27743.705	5934141.314	644.721
13/03/2013 11:01:26 AM	3.135	1.569	166.1	27743.714	5934140.717	644.719
13/03/2013 11:02:08 AM	3.135	1.569	166.123	27743.714	5934140.694	644.72
13/03/2013 11:04:16 AM	3.135	1.569	166.184	27743.713	5934140.633	644.718
13/03/2013 11:17:24	3.135	1.569	166.286	27743.715	5934140.53	644.721

AM						
13/03/2013 11:19:40 AM	3.135	1.569	166.286	27743.717	5934140.531	644.72
13/03/2013 11:33:35 AM	3.135	1.569	166.149	27743.713	5934140.667	644.72
13/03/2013 11:34:42 AM	3.135	1.569	166.149	27743.711	5934140.667	644.722
13/03/2013 11:36:15 AM	3.135	1.569	166.149	27743.713	5934140.668	644.721
13/03/2013 12:06:51 PM	3.135	1.569	166.152	27743.717	5934140.665	644.72
13/03/2013 12:12:58 PM	3.135	1.569	166.151	27743.715	5934140.665	644.722

The VLTB system is designed for rapid relocation and initialization in order to provide real-time guidance information even when the TBM is navigating curves, which requires frequent relocation of the laser station and presents the most difficult task for tunnel surveyors. A comparison in terms of accuracy and time efficiency between the proposed VLTB system against the traditional passive laser system is given in Table 2. It is found the VLTB system improves the surveying accuracy by 10 times (3 mm by VLTB vs. 30 mm by conventional laser), while eliminating the need of routine survey (for laser calibration) and reducing the relocation survey time from 7 h to half an hour. The survey time saved during tunnel-boring operations would easily add up to 10% savings in total project direct cost.

Table 2. Comparison of traditional passive laser and VLTB system

System	Accuracy	Routine Survey		Relocation Survey			
				Straight Tunnel		Curved Tunnel	
		Distance	Time	Distance	Time	Distance	Time
Passive Laser	30 mm	10 m	1 h	200 m	7 h	10 m	7 h
VLTB	3 mm	No	No	200 m	0.5 h	10 m	0.5 h

3.9 CONCLUSIONS

Researchers in construction engineering and management strive to devise ways of solving construction problems with clarity and ease, while always

thinking of the practical reality of how things should be done. This chapter describes such a product that stands as an example of what we can expect to see in the industry in coming years. It is an automated surveying robot that provides the position of a tunnel boring machine in real time. It has been field tested on a 1,000 m long sewage tunneling job inside the city of Edmonton, Alberta, Canada. The tunnel test bed showcases the future of technology integration and automation in construction.

In the coming 10 years, it's unlikely that we will see a revolution of means and methods as we are employing today. For example, TBM plus precast sections to build tunnels, crane plus prefabricated modules to install buildings or plants. We are not likely going to see robots replace humans in the field. Instead, we will see equipment operators, like the ones on our project, making decisions on the fly, assisted by "add-on" robotic instruments and sensors, which will lead to significant improvement in precision, efficiency and safety in field operations.

As field activities unfold, construction managers will have access to 3D platforms refreshed on a near real-time basis, consisting of as-built models alongside as-designed models, empowered by simulation and optimization analyses. This not only facilitates project control in terms of time, cost and quality, but turns the management of deviation corrections, design changes and schedule updates into a straightforward, transparent decision process for all the stakeholders involved.

The development of "add-on" technologies will enable people, but not replace people. The "add-on" technologies will also be instrumental in training equipment operators and field engineers and surveyors by readily capturing the technical knowhow and implicit knowledge of experienced field personnel. This potentially lays a fast-track solution to addressing the current and worsening

“skills crunch” and “manpower shortage” issues that present a bottleneck to the growth of construction industry in both developed and developing countries.

What’s more, this chapter builds up an automatic system, which is reliable, wireless controllable and applicable in real tunnel. These are the corner stones for the whole framework. The framework heavily relies on the system performing most the tasks by itself, and requiring rare manual interventions.

Chapter 4. SMART LASER PROJECTOR

4.1 OVERVIEW

VLTB is straightforward to set up and calibrate, which operates automatically in real time of construction; however, extreme visibility constraints can still hold VLTB back, as the actual survey window is much smaller subject to the blockage by the gantry sections and expansion rings. The visibility constraints are even more critical during the construction of curved tunnel sections, when the total station can barely identify and survey all the three prisms. In such difficult scenarios with compromised line-of-sight conditions, the three-point algorithm based VLTB system is no longer able to provide reliable TBM guidance information.

In this chapter, in order to address the identified limitation of VLTB, the authors introduce a one-point algorithm along with the associated automated laser projector system, which is able to deliver reliable guidance feedback to the operator even in those restricted survey window scenarios. The proposed method applies the similar strategy as the conventional laser: it projects a laser spot on the target board to indicate as-designed offsets from the alignment. Thus, this method seamlessly replaces the conventional laser-based tunnel guidance system, without introducing any change to the operator's current practice. Similar to the VLTB system, it can perform self-check automatically during "dark time". Moreover, it is easy and fast to set up the smart laser projector. The system can potentially save considerable cost in terms of the maintenance of tunnel guidance system, especially for curved tunnel construction.

4.2 METHODOLOGY

The basic design of the smart laser projector is to allow it to overcome the need for establishing a parallel laser beam to represent tunnel alignment. In addition to being easy to set up, the smart laser projector has a number of other benefits. One such benefit is that the high accuracy motor of total station provides the necessary mechanism to simplify the guidance methods. For example, the following two basic scenarios illustrate how a smart laser projector can help reduce risk and the amount of work needed to enable guidance.

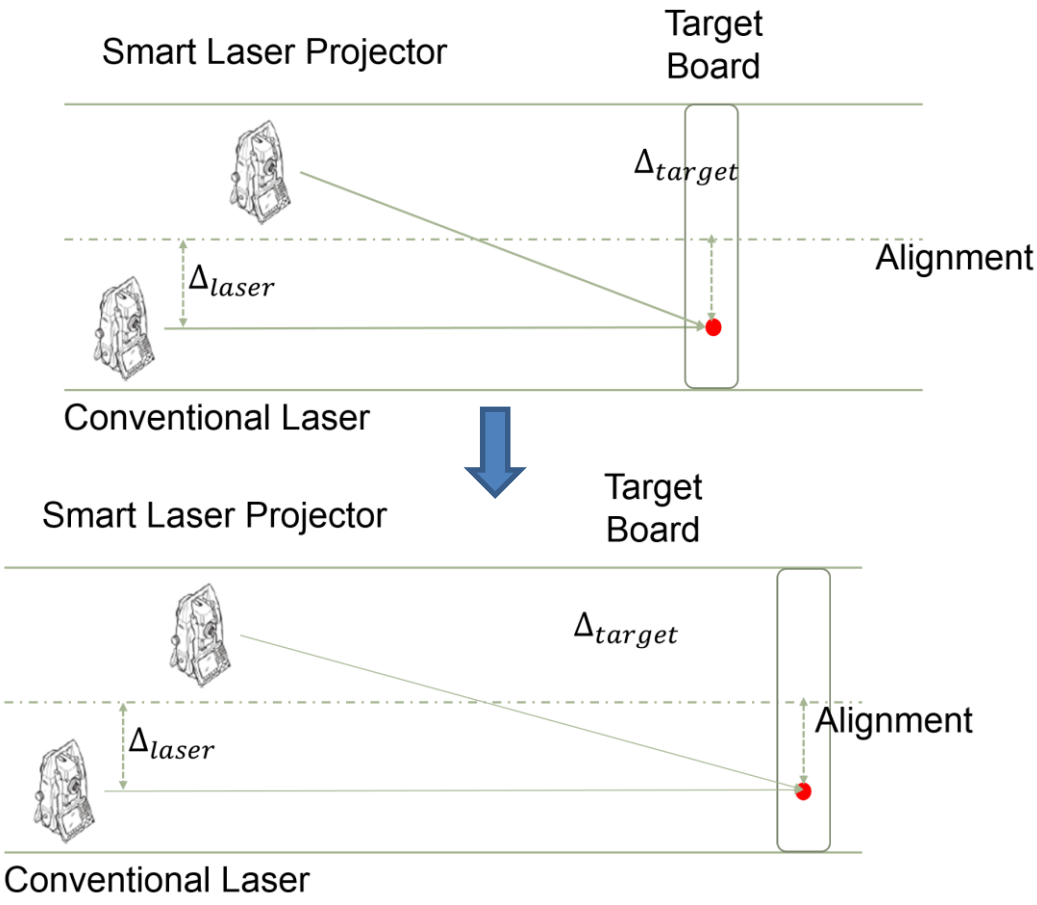

Figure 46. Smart laser projector shows the guidance laser spot

Instead of utilizing an always-parallel laser beam, the smart laser will always aim at the "right" orientation to emit a laser beam, and will leave a laser

spot at exactly the same location as the conventional laser. As is shown in Figure 46, as the target board advances with the TBM, the conventional laser beam — that is parallel to the tunnel alignment — leaves a new laser spot on the target board, indicating the deviation of the TBM from the as-designed alignment. The smart laser projector will calculate the as-designed position of the new laser spot, and emit the beam directly onto the new spot.

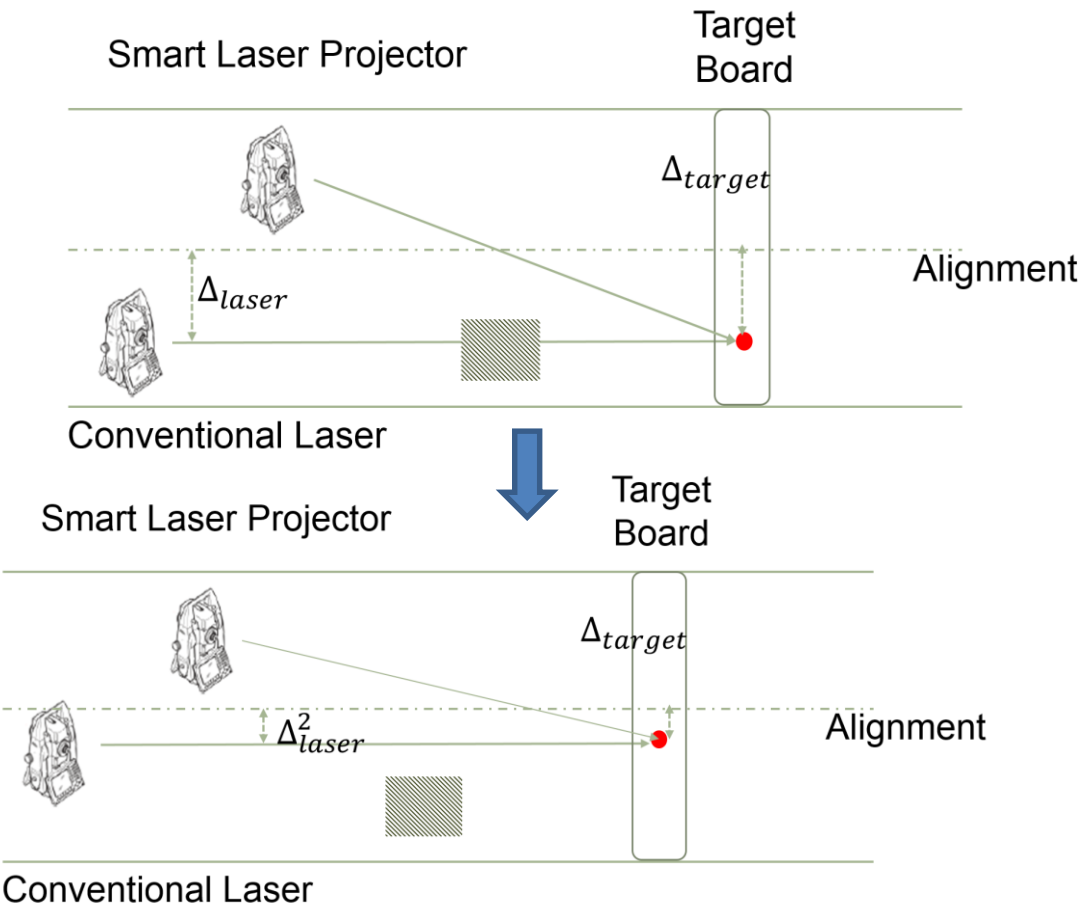

Figure 47. How the smart laser projector overcomes obstacles without requiring human intervention.

As illustrated in Figure 47, when the laser's sight line is blocked, the surveyors need to shut down the project and relocate the laser. After relocation, surveyors will determine a new offset between the alignment and the parallel

laser beam, and inform the operator. However, the smart laser projector can automatically search the board, find a new visible offset, and automatically inform the operator of its location through the tablet control interface.

4.2.1 Limited Visibility

One of the primary philosophical principles of surveying is to set up long-lasting coordinate references that can serve as solid, reliable benchmarks for construction. The goal and criteria of a survey is always accuracy, and this mindset is readily observable in conventional laser guidance setup where surveyors will spend an enormous amount of time to ensure the accuracy of the system. However, in real world tunnel construction, the time spent trying to maximize accuracy can be wasted due to the dynamic nature of site conditions. For example, the survey window becomes very limited when the gantry system and the supporting hoses of the hydraulic system are not set up well, and it can take around ten hours for surveyors to set up a conventional laser. However, only a few days later the TBM will have advanced another twenty meters, and the survey window will have changed because the gantry and hoses are in different places. Thus, the laser will need to be readjusted in order to pass through another visible window with a completely different line and level offsets, and it will take surveyors another ten hours to set it up, as they will need to perform a full survey and relocate the laser. Similarly, in a curved tunnel section, the laser must be relocated every four to five days. As shown in Figure 48, the survey window is crowded with obstacles, for example the expansion ring (upper left corner), hoses (in the middle of the picture), and some sections of gantry.

In the two examples, we can see that the setup is expendable and that the construction crew can easily discard the previous setup when new problems arise. VLTB is a perfect solution to these scenarios because it requires very little work to

setup, though it can still be limited by the extreme reduced visibility. For example, Figure 48 shows the actual survey window, which is much smaller and irregular due to the heights of different sections of the gantry and the positions of expansion ring and hoses. In curved tunnels, the curvature of the wall (tunnel liner) will also squeeze the survey window, while the three visible targets may never be visible. Although the one-point and two-point algorithm cannot achieve the same level of accuracy as the three-point algorithm, they provide a practically alternative for VLTB. In particular, the one-point algorithm is very space efficient (the prism can be set up directly on the back target board, which is the most visible place on TBM), time efficient (the total station only needs to survey one point, which can be done in roughly three seconds), and it has great potential for use in tunnels with extreme visibility limits. Furthermore, it is worth noting that two-point algorithm is very similar to three-point algorithm in that the angle of roll is always small and can be negligible much of the time; additionally, its ability to see the second point is not considerably higher than the three point algorithm's. Thus, the two-point method only works as a temporary substitute solution when the three-point method is not feasible.

Figure 48. Actual survey window.

The interpolation-based approximation of the one-point ad-hoc method is not solid or rigorous enough to provide a more serious one-point algorithm. In this paper, the one-point algorithm will be thoroughly examined in order to determine how accurate and reliable it is. First, it will be formalized in an analytical form for both straight and curved tunnel, and then it will be compared to lab tests using the three-point algorithm. If the one-point algorithm proves to be comparable to its three-point counterpart, it would establish the Smart Laser Projector as an indispensable field tool that can switch seamlessly between one and three-point algorithms, which would ensure optimal performance in actual job site conditions.

Traditionally, the VLTB is optimized for small-diameter tunnels because the receiving unit is not able to fit into the operator's chamber. It was originally intended to solve the extremely narrow survey window in small-diameter tunnel boring construction (e.g. microtunneling). In a typical eight-foot drainage or sanitary tunnel, windows account for about one quarter of the circle and have a radius of roughly half a meter, they are located about one-and-half meters above the bottom of the tunnel and on the rightmost side (looking along the alignment direction, as shown in Figure 49.) However, even such a small and narrow window cannot be always guaranteed, and the complexity of the TBM and its supporting system (expansion rings, installation arm, and hoses of the hydraulic system) may block the window (as shown in Figure 50). This effect gets worse as the distance between smart laser and the obstacles increases, as the laser spot will get bigger as it travels and the shadow will take up more space. In these compromised situations, the three target points are not always observable and the VLTB system needs a fallback solution.

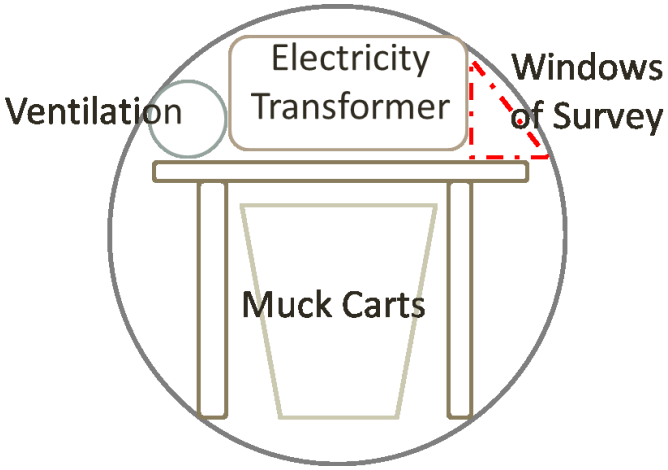

Figure 49. Survey windows (Looking along alignment).

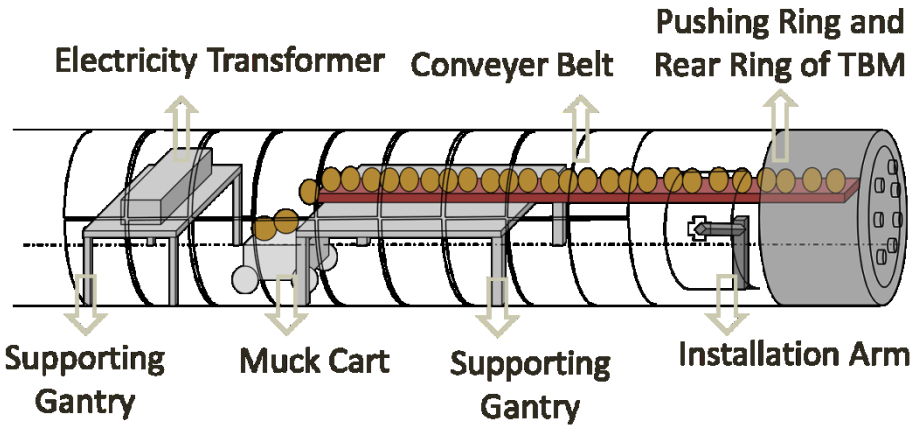

Figure 50. Tunnel boring machine and supporting facilities (Looking from side).

The three-point algorithm applied by the three-dimensional mode of the VLTB system requires at least three points, but the availability of more points is ideal as it enables the computation to be more robust and error-free. However, when the system cannot survey all three prisms, the three-point algorithm fails to compute the target coordinates due to a lack of sufficient input information. When this happens, there are two fallback solutions: the two-point solution and the one-point solution. The two-point solution utilizes the same calculation model as the three-point solution, while assuming that the roll angle of the TBM is zero. However, in curved tunnel construction, it is rarely guaranteed that it will

be possible to be able to have a clear view of at least three, or even two, prisms. Given this reality, the guidance system needs a well-modeled one-point solution to handle these challenging scenarios.

The smart laser projector that guides the tunnel-boring machine has two modes: three-point mode (VLTB mode) and one-point mode. The system will automatically adapt to the current survey conditions in the tunnel, and choose the right mode. In the three-point mode, the VLTB system is able to provide three-dimensional coordinates for every point on the tunnel-boring machine. Operators will be able to know the exact coordinates of the current centers of the cutter head and rear end, in addition to the three-dimensional pose of the TBM, and they can use this information to help them steer it. In the one-point mode, the survey data are not adequate for three-point computation and can only be utilized to compute the coordinate of the center of the rear end. In this mode, the smart laser will emit a laser dot on the target board which will coincide with the one projected by the conventional laser guidance system. Therefore, a well-trained and experienced operator can utilize their expertise with the conventional laser until the VLTB system can switch back to 3D mode when proper conditions are met.

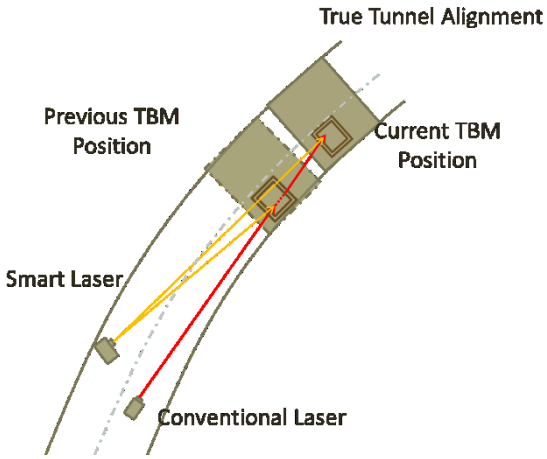

Figure 51. Smart laser projector is an advanced replacement for conventional laser.

The conventional laser utilizes parallel laser beam to indicate the tunnel alignment, and the smart laser directly emits laser spot onto the exact point on the target board as the conventional laser; however, whenever the TBM advances, the smart laser will recalculate the expected location of the laser spot on the target board—which will have moved—and re-emit a laser on the exact point with updated horizontal/vertical angles.

Although the smart laser system works similarly to conventional laser in the one-point mode, it is much more advanced. The smart laser is able to guide TBM, when visibility conditions are poor, which eliminates the need to set up a separate conventional laser system (the basic logic is described in Figure 52). Moreover, when the conventional laser is set up, the location of the target board is fixed, and adjusting the laser location when the line of sight is blocked can create an enormous amount of work. However, the smart laser can be easily relocated (minor relocations, for example, to bypass obstacles, only take about five minutes in the field), and will still shoot a laser beam onto the same target center (as shown in Figure 51); after relocation, the laser beam does not need to

remain parallel to the tunnel design alignment as is the case with the conventional laser guidance solution. It is much easier for surveyors to setup the smart laser system, as maintaining a parallel laser beam is a time-consuming and expertise-demanding process.

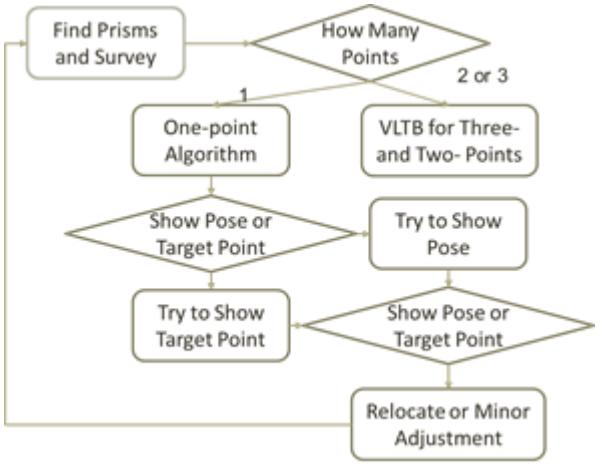

Figure 52. Logic of the Smart Laser Projector.

In some situations, the operator will want to know the pose information. When operator wants to know roughly the yaw angle, they can flip down the front board (the other board) and compare the dots on two boards.

Figure 53. Display position (left) and display pose (right).

The VLTB is ideal in that it is straightforward to set up and calibrate, and that it operates automatically in real time during construction; however, extreme

visibility constraints can still hold it back, as the actual survey window is much smaller and more irregular due to the heights of the different sections of the trailing gantry, and the positions of the expansion ring and hoses attached to the TBM. In extreme scenarios where visibility is greatly impaired, one-point and two-point algorithms ensure that continuing to run the VLTB remains feasible, despite lowered accuracy and reliability.

In this thesis, we introduce a one-point positioning algorithm for the automated laser projector system. This positioning algorithm continuously tracks one prism installed on the TBM, which has been surveyed in the shop, and, based on real-time calculations, the total station projects a laser beam onto the target board of TBM. The projected laser spot reflects the same guidance information as the conventional laser, and indicates the as-designed offset from the alignment. This method is advantageous because it seamlessly replaces the conventional laser without forcing the operator to change their current practice, it is space efficient as the prism can be set up directly at the most visible area on the TBM, and, like the VLTB system, it can automatically perform self-checks, thus eliminating “dark time”. The one-point algorithm has two analytical forms for both straight and curved tunnels. The author validated the algorithm for both straight and curved tunnel setups in a lab test in addition to performing a feasibility test in the field.

4.2.2 Local Alignment framework

This section first defines a local alignment framework, which will simplify the expression forms of equations, and help the reader to understand them in greater depth.

4.2.3 Basic Models for One-point Algorithm

The one-point algorithm surveys one prism fixed at a known point on the TBM and calculates the deviations of the TBM from as-designed tunnel alignment. To achieve this, it needs two mathematic models for calculation. One model is the TBM model, which reflects the geometric relationship between the known prism and the centre of rear end of TBM, and the other model is the alignment model, which defines the as-designed alignment. The one-point algorithm then computes the deviations of TBM from the as-designed alignment, based on the surveyed position of the prism.

The first step is to define the TBM model. It is assumed that the TBM is cylindrical in shape as shown in the left image of Figure 55. The cutter head center is P_h and the rear center is P_{bc}. The TBM framework is defined as F_t, the origin is P_{bc}, the Y axis is vector $P_{bc}P_h$, and the Z axis is zenith. Once the TBM's framework has been defined, surveyors can measure the coordinates of the prism with in it (offset) in the mechanical shop. The notation V_{pm}^t is taken as the offset of the prism, and this produces a relationship, which can be expressed as, $V_{pm}^t = P_{pm}^t - P_{bc}^t$ (the superscript t indicates that the point is in TBM framework).

After this has been done, the alignment framework can be defined as F_a. As shown in Figure 55, the start and the end of the alignment of this tunnel section are identified as P_s and P_e, and the center of the curve is P_c, with a radius of R. Thus the alignment framework F_a is defined as follows: the origin is P_s, the Y axis is vector P_sP_e, and the Z axis is the cross product of P_sP_c and P_sP_e.

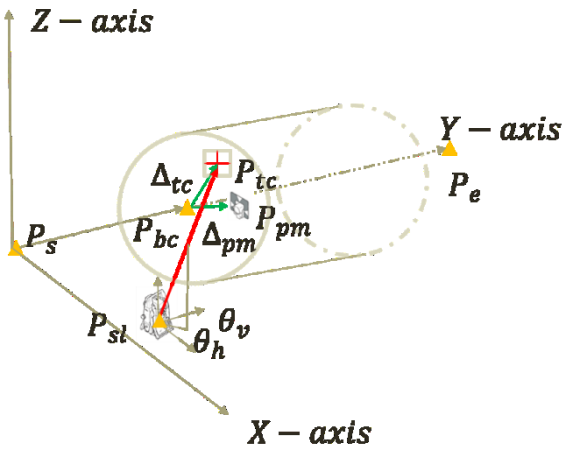

Figure 54. Mathematical definition for smart laser calculation

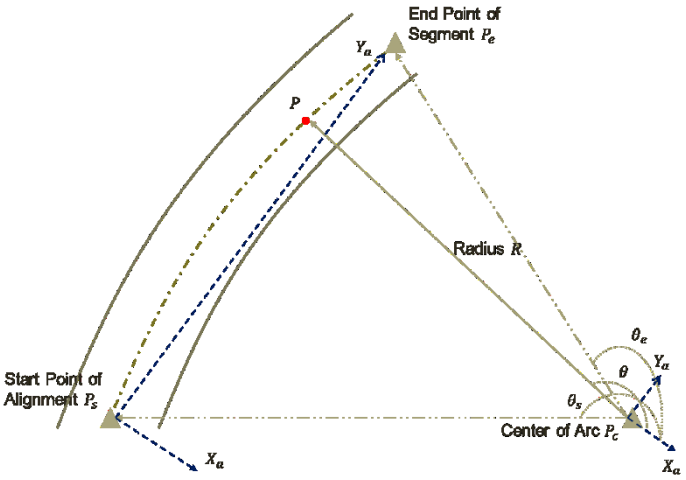

Figure 55. Basic Models for One-point Algorithm

The reason for defining an alignment framework is to simplify the expression of the alignment in a polar coordinate form, which helps to simplify the process of calculating deviations. For example, fixing any point P on the alignment only depends on one parameter, θ, which is the angle between the X axis and vector P_cP, as shown in Figure 55. This enables the position of point P on the alignment to be elegantly denoted as a linear problem, and it also allows for it to be easily converted back to its corresponding coordinates in the alignment

framework P^a (superscript a means the point is in alignment coordinate system) as per equation (3).

$$\begin{cases} x^a \leftarrow P_c^a + R\cos\theta \\ y^a \leftarrow P_c^a + R\sin\theta \\ z^a \leftarrow 0 \end{cases} \tag{3}$$

4.2.4 Calculating Deviations

After defining the two models, the one-point algorithm will start to track the prism in the field. At any given moment, total station (at position P_{ts}^a) surveys the prism as Q_{pm}^a (this notation indicates the actual coordinates of the prism in the alignment framework). Due to the limited information available to the one-point algorithm, it relies on two necessary assumptions to finish the calculation. The first assumption is where the X axis of the TBM framework falls on the radius of the arc P_c, as shown in Figure 56. The second assumption is where the as-designed rear ring center P_{bc} falls on the same radius as the actual rear ring center Q_{bc}.

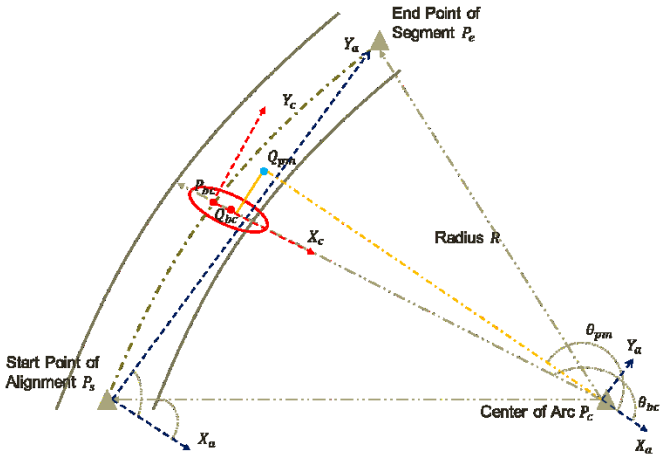

Figure 56. Calculate actual rear ring center

The algorithm first evaluates the angle parameter θ_{pm} of prism Q_{pm}, and then calculates the angle parameter θ_{bc} of the rear ring center Q_{bc}. The angle

difference Δ_θ between θ_{pm} and θ_{bc} can be determined by utilizing the Y axis offset of the prism as per the first equation in equation system (4), and then by deducing the parameter θ_{bc} from Δ_θ and θ_{pm}.

$$\begin{cases} \Delta_\theta \leftarrow \tan^{-1} \dfrac{Y(V_{pm})}{\overrightarrow{P_c P_{pm}}} \\ \theta_{pm} \leftarrow \tan^{-1} \dfrac{Y(\overrightarrow{P_c Q_{pm}})}{X(\overrightarrow{P_c Q_{pm}})} \\ \theta_{bc} \leftarrow \theta_{pm} + \Delta_\theta \end{cases} \tag{4}$$

The algorithm is consistently successful in calculating the as-designed rear ring center, which is the origin of the temporary TBM framework. Transformation matrix $M_{a\to t}$ can transform a coordinate in the alignment framework to a corresponding one in the TBM framework. This enables us to compute the coordinate of the actual prism in the TBM framework $Q_{pm}^t = M_{a\to t} Q_{pm}^a$, and eventually the coordinate of the actual rear center $Q_{bc}^t = Q_{pm}^t - V_{pm}^t$. Because the as-designed rear center P_{bc}^t is the origin of the TBM framework, the coordinate of point Q_{bc}^t is also the actual deviation of the TBM.

$$\begin{cases} x_{bc} \leftarrow P_c^a + R\cos\theta_{bc} \\ y_{bc} \leftarrow P_c^a + R\sin\theta_{bc} \end{cases} \tag{5}$$

4.2.5 Display Target Board Center

After computing the location of the as-designed target center, *smart laser projector* then emits a laser spot to display this location on the target board fixed on the TBM. Unlike the conventional laser, the smart laser's beam falls on the target board at exactly the as-designed position of the target board center in accordance with the as-designed tunnel alignment (the as-designed laser spot is called the target point). As shown in Figure 57, a conventional laser emits a beam that is parallel to the alignment, and leaves the laser spot on the target board. The alignment is generally defined based on the center axis or the bottom (invert) of

the TBM which is not visible to the total station during construction. Thus, it is impossible to emit the laser beam so that it coincides with the alignment. As part of the tunnel survey design surveyors always choose a fixed offset between the alignment and the laser beam. By design, the offset of the laser Δ_{laser} and the offset of the target point Δ_{target} from the alignment must be the same; at any two moments, T_1 and T_2, the actual offsets from the alignment $\Delta_{target,T1}$ and $\Delta_{target,T2}$ must be close to Δ_{target}. The difference between $\Delta_{target,T}$ and the fixed target Δ_{target} is the actual deviation of the TBM (deviations are not the fixed offsets, but the differences between as-designed and as-built tunnels). In practice, surveyors always take the center of target board as the target point, because it generally has a higher chance of being visible (often surveyors informally refer the "target point" as the "target center"). If the center of the target board becomes no longer visible, the surveyors will relocate the laser and choose another target point (and another fixed offset) that is not the center of the target board. However, on the next relocation of laser they will generally reassign the center of the target board as the target point.

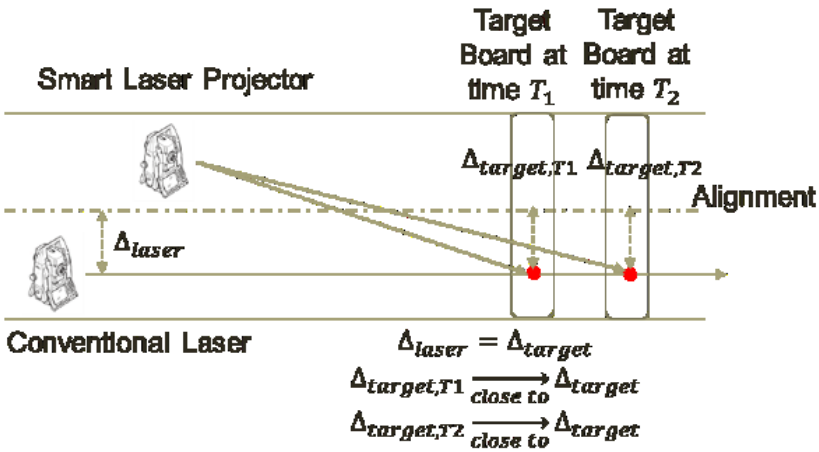

Figure 57. Comparison between conventional laser and smart laser projector

By contrast, the smart laser projector adopts a different method. It always emits a laser spot on the exact same position on the target board as the conventional laser, but the laser beam is not parallel to the alignment. The benefit of this design is its flexibility. The smart laser projector distinguishes the prism and the target point, and it can survey any known prism on the TBM and emit a laser spot on any target point with certain offset. Surveyors commonly choose several candidate points for mounting prisms on the TBM and survey their coordinates in the TBM framework before construction starts. In a scenario where the total station can no longer projects the laser spot onto the target point due to obstacles, the smart laser projector will automatically choose a new target point, redefine the fixed offset from Δ_{target} to Δ_{target}^{new}, and then utilize the tablet computer to notify the operator. In case the prism is blocked or no properly fixed offset is available, the system will inform surveyors that they must either change the mounting point of the prism or relocate the total station with the mounting bracket and eventually choose another proper fixed offset Δ_{target}^{new2}. This will substantially save time during setup and will prevent survey shutdown.

The implementation of the newly devised algorithm is a two-step process: the first step is to calculate the position of the target in the alignment framework, and the second is to calculate the horizontal and vertical angles on which the total station is desired to rotate. It is then necessary to define define another transformation matrix $M_{t\to a}$, which can transform a coordinate from the TBM framework and place it back in the alignment framework. Assuming the target point has a fixed offset V_{tgt}^{t}, and the algorithm can evaluate its coordinate in the alignment framework as $P_{tgt} = M_{t\to a}V_{tgt}^{t}$, the algorithm can then calculate the

vertical angle θ_{tgt}^{v} and the horizontal angle θ_{tgt}^{h} in order to fix the orientation of the laser projection:

$$\begin{cases} u \leftarrow P_{tgt}^{a} - P_{ts}^{a} \\ \theta_{tgt}^{v} \leftarrow \cos^{-1} \dfrac{Z(u)}{\|u\|} \\ \theta_{tgt}^{h} \leftarrow \tan^{-1} \dfrac{Y(u)}{X(u)} \end{cases} \tag{6}$$

The equation (6) calculates the vertical angle θ_{tgt}^{v} and the horizontal angle θ_{tgt}^{h}. After calculating the horizontal and vertical angles, the smart laser projector emits the laser in the direction defined by these two angles, and a laser spot will be visible on the target board. As mentioned above, the smart laser projector can easily change the offset V_{tgt}^{t} in order to adapt itself to different environments and conditions. The smart laser projector can potentially replace the traditional laser and work seamlessly as a complementary guidance solution for the VLTB system, when the size of survey window is substantially reduced during tunnel construction.

4.3 LAB TESTS

To further demonstrate the equations and to test the effectiveness of the one-point algorithm, a series of lab tests were conducted to compare the performance of the one-point and three-point methods in both straight and curved tunnels. The three-point algorithm is able to precisely calculate any point on the TBM, by surveying three visible prisms mounted on the rear of TBM.

The comparison test was conducted as follow: first, a registration survey was performed on a mock-up model and all points that would be utilized in later tests were collected, including the coordinates of all three prisms at the rear end and any other important points on the TBM (especially the cutter head center and

rear end center). Then, the model was firmly placed in a space that was designed to simulate the alignment of the tunnel. The automatic VLTB program continuously tracked all three points on the rear end of the TBM because they were the only visible points that could be surveyed by the total station. The three-point algorithm then was able to calculate the coordinates of any point (other than the three prisms) based on the three surveyed prisms. Meanwhile, the one point algorithm was intentionally linked with the coordinate of only one prism (any of the three surveyed), just as in the field. Using this limited data, the one point algorithm calculated deviations of the TBM at its rear end and predicted deviations at the cutter head. Because the three-point algorithm can calculate any point on the TBM (including the exact coordinates of the both the head and rear centers), it can also calculate accurate deviations at both the cutter head and rear end. Thus, we can directly compare the deviations between the two different algorithms in relation to the common survey and accurately assess the ability of one-point algorithm.

In order for the one-point algorithm to be considered viable, this comparison should yield two results: first, “one-point” must produce a reliable calculation of the rear end deviation; and second, “one-point” should be able to estimate a decent deviation at the cutter head. In addition, the results of both results must be consistent for two distinct tunnel setups, namely, a straight tunnel setup, and a curved tunnel setup. Although a straight tunnel can be considered a curved tunnel with an infinite radius in theory, in engineering practice the calculation of the as-designed alignment is considerably different. The one-point algorithm needs to determine how to project the laser beam back with a proper mathematical model of the alignment. Another key question that the tests must answer is how closely can the one-point algorithm estimate cutter

head deviation in curved tunnel; for example, for a typical 500m radius tunnel, will the one point algorithm arrive at an acceptable deviation estimation?

The lab tests were performed on a $1:20$ scale mock-up model of a real eight-foot TBM. The model was designed in AutoCAD and built by a two-dimensional printer (S. Mao, Shen, and Lu 2014). The lab test was designed to create an environment similar to a real tunnel. A total station was set up on one side of the lab (as in Figure 58), and a round prism, which is assumed to be north direction (as in Figure 59). A mock up TBM model was set beside the round prism, with its cutter head facing the wall and its rear ring facing the total station.

Figure 58. Total station controlled by VLTB and smart laser projector.

The mock up model had three prisms mounted at the rear ring (P_0, P_1, P_2) and one prism at the cutter head center (P_3), as shown in Figure 60. In the test, the VLTB first applied the three-point algorithm, measuring the three prims on the rear ring, and calculated the position of the cutter head; the VLTB then

measured the P_3 directly and compared it to the calculation. The validation of three-point comparison has already been illustrated in previous work (S. Mao, Shen, and Lu 2014), and will not be elaborated here. These steps were designed as a verification of the setup. The three point algorithm is capable of calculating any registered points (surveyed with three "visible prims" in registration setup), and if the coordinates for the calculated cutter head and the directly surveyed cutter head match, then it ensures that the equipment, the parameters, and the setup are reliable. After the verification, the comparison of the analytical results between the one-point method and the three-point method (whose results represent the "as-designed" positions) becomes more convincing.

The smart laser projector can take any prism as the "only visible" prism, and it can also choose any point as the target point because it can arbitrarily determine the offset of a target Δ_{target} to allow for optimal visibility. In this comparison test, the one-point algorithm assumed that the second prism, namely prism P_1, was the only prism visible. The one-point algorithm calculates the line and level deviations based on the survey results of prism P_1, and then the three-point algorithm will calculate accurate deviations for both the rear center and the cutter head center. In the test, the automatic program was instructed to relay only the coordinate of prism P_1 from total station to the one point algorithm, with no other information being provided. The reason for directly inputting the coordinate of prism P_1 is to ensure that both the one-point and three-point algorithms are using the exact same survey results, which ensures that the difference of the final results is solely attributable to the difference of the algorithms.

Figure 59. Mock up model and reference prism

Two sets of tests were conducted, one for straight tunnel and one for curved tunnel, and in each set the mock-up model was relocated five times, and five sets of data were collected for comparison.

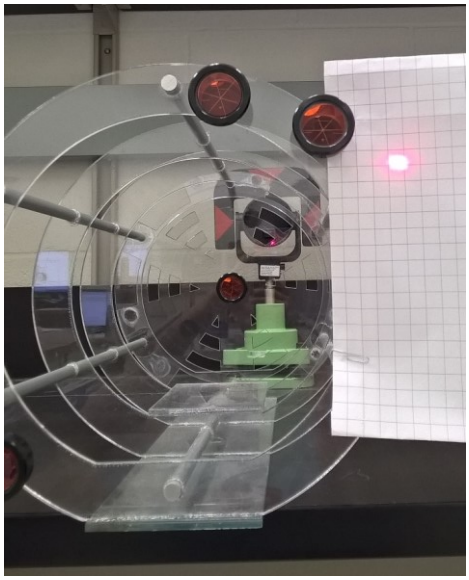

Figure 60. The lab setup of mockup TBM model.

4.3.1 Straight Alignment

In the lab test, the established coordinate system was a straightforward tunnel alignment framework. A Leica TPS 1203 total station is placed on one side of the lab, as shown in Figure 61, and it was assumed to have the coordinate of $(0m, 0m, 0.25m)$. A Leica round prism, as shown in Figure 60, was set up about eight meters away from total station. The direction from the total station to the round prism was assumed to be north (Y axis), and the Z direction (zenith) was the opposite direction of gravity. The start point P_s and end point P_e of the alignment section were invisible in the setup, and the coordinates were $P_s = (0m, 0m, 0m)$ and $P_e = (0m, 10m, 0m)$, respectively. Therefore, the alignment in this setup was the vector $(0m, 10m, 0m)$, the level and line deviations were simply interpreted as x and z coordinates of the cutter head and rear end of TBM, and the distance in the y coordinate.

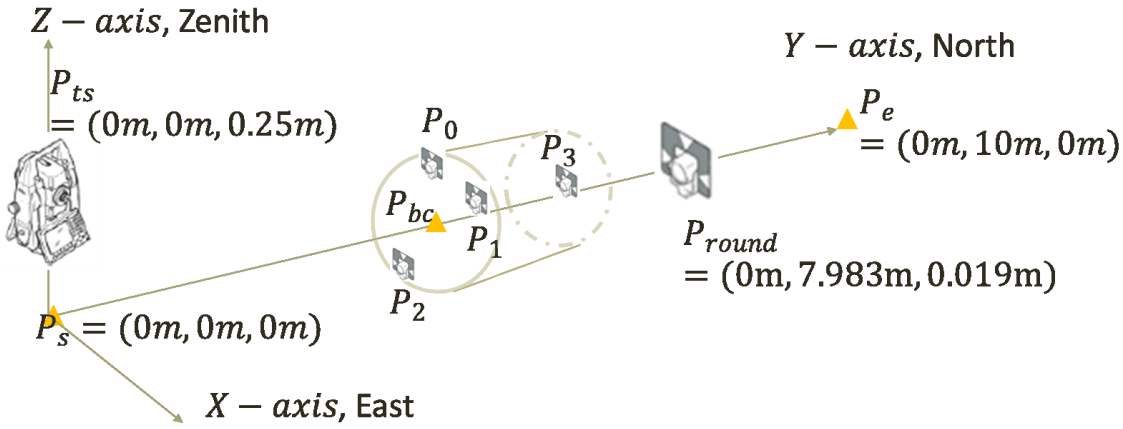

Figure 61. Total station is set up with "Azimuth Mode"

After the setup, the total station surveyed all four mini prisms on the mockup model for registration, as shown in Figure 60. Registration would then be validated by the three-point algorithm, which would compute the coordinate of the cutter head from the three prisms on the rear ring. The deviations could

then be calculated and displayed on the VLTB tablet (Figure 63). Next, the one-point algorithm calculated the as-designed location of P_1, and the total station emitted a laser onto a grid target board (a grid is $1cm \times 1cm$) on the mock-up model (Figure 63). The deviations between the as-built and as-designed locations of prism P_2 could be measured on the grid paper. The comparison between Figure 63 and Figure 63 is based on the first test in straight tunnel setup. The three-point method shows that the line deviation is $14mm$ and the level deviation is $19mm$. The one-point algorithm emitted a laser spot on the location of as-designed prism P_1, and the spot was about two grids (2cm) lower and one-and-half grids ($1.5cm$) left of actual P_1. This indicates that the two methods produce matching results.

Figure 62. Deviation calculation by three-point algorithm.

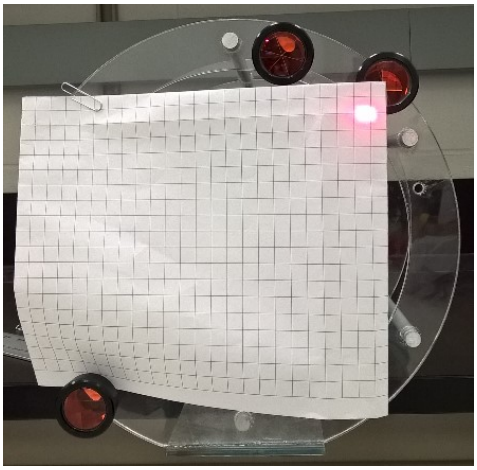

Figure 63. Deviation calculation by one-point algorithm (right).

The results are shown in Table 3. The three-point algorithm measured P_0, P_1, P_2 and calculated the position of P_3; the result was then compared with the direct survey of P_3. It can be observed that the differences between calculated and surveyed P_3 keep increasing when the TBM mock-up model advances away from its initial position, which is a typical pattern of error propagation in tunnel guidance survey (Sheng Mao, Duanshun Li, and Ming Lu 2015). After calculations of the three-point algorithm, the one-point algorithm took P_1 as an input to calculate the deviations of TBM, and computed the as-designed position of P_1.

Table 3. Three-point results for straight tunnel. (in meters)

		P_0	P_1	P_2	P_3	$Calc\ P_3$
Group 1	X	0.046	0.106	-0.078	0.030	0.030
	Y	7.166	7.166	7.171	7.623	7.623
	Z	0.132	0.111	-0.073	0.023	0.023
Group 2	X	0.057	0.117	-0.066	0.041	0.041
	Y	7.178	7.178	7.183	7.635	7.636
	Z	0.132	0.111	-0.073	0.023	0.023
Group 3	X	0.075	0.135	-0.048	0.059	0.061
	Y	7.222	7.222	7.227	7.679	7.676
	Z	0.132	0.112	-0.072	0.023	0.024
Group 4	X	0.078	0.138	-0.045	0.056	0.055
	Y	7.253	7.254	7.257	7.710	7.711
	Z	0.133	0.112	-0.072	0.023	0.026
Group 5	X	0.082	0.142	-0.041	0.040	0.043
	Y	7.317	7.320	7.315	7.772	7.773
	Z	0.133	0.112	-0.072	0.022	0.022

Table 3 shows the results directly measured by the three-point algorithm, which also serve as the benchmark for the one-point algorithm. In this table, P_0, P_1, P_2, and P_3 are the four mini prisms surveyed by total station, and "$Calc\ P_3$" is the position of P_3 as calculated by the three-point algorithm. The results confirm that the three-point algorithm could successfully calculate the cutter heads' positions based on three surveyable prisms on the rear section of the TBM model.

Table 4. Comparison of deviation calculation between three-point algorithm and one-point algorithm for straight tunnel setup (in meters)

		Rear Dev	One-point Dev	Diff Rear	Emit Angles	
Group 1	X (m)	0.014	0.014	0.000	H (◦)	0.013
	Y (m)	0.000	0.000	0.000	V (◦)	1.593
	Z (m)	0.019	0.018	0.001		
Group 2	X (m)	0.025	0.025	0.000	H (◦)	0.013
	Y (m)	0.000	0.000	0.000	V (◦)	1.593
	Z (m)	0.019	0.018	0.001		
Group 3	X (m)	0.045	0.043	0.002	H (◦)	0.013
	Y (m)	0.000	0.000	0.000	V (◦)	1.593
	Z (m)	0.019	0.019	0.000		
Group 4	X (m)	0.046	0.046	0.000	H (◦)	0.013
	Y (m)	0.000	0.000	0.000	V (◦)	1.592
	Z (m)	0.020	0.019	0.001		
Group 5	X (m)	0.050	0.050	0.000	H (◦)	0.013
	Y (m)	0.000	0.000	0.000	V (◦)	1.592
	Z (m)	0.020	0.019	0.001		

In Table 4, “Rear Dev” is the calculated deviations of the rear ring, with X representing line deviation and Z representing level (or grade) deviation. “One-point Dev” is the deviation calculated by the one-point algorithm. The reason for comparing “Rear Dev” and “One-point Dev” is that the one-point algorithm only possesses limited information about the TBM’s position, and thus it can only calculate the deviation at the rear end of the TBM.

“Diff Rear” are the differences of the calculated deviations between rear center and P_1. The deviation calculations produced by the three-point and one-point algorithms are very close, and this demonstrates that the one-point algorithm application would be reliable in straight tunnels. The smart laser projector can completely replace the conventional tunnel guidance method as it can provide highly accurate deviation calculations for the rear ring of the TBM. “Emit Angles” displays the horizontal (X) and vertical angles (Y) at which the total station aims its laser to project the laser spot on the as-designed P_1 (expressed as radian for direct total station control input).

The calculation of the three-point algorithm has been illustrated in prior studies (Shen, Lu, and Chen 2011), and in this paper the author only applied group 1 data to the one-point algorithm in order to clarify the calculation process. When the smart laser system surveyed P_1 , the indicated position was $(0.106m, 7.166m, 0.111m)$, which allowed it to assume that the rear ring was at the same chainage distance $7.166m$. According to equation (71), the as-designed coordinate of the rear ring is $P_s^a + d \times Y_a = (0m, 0m, 0m) + 7.166 \times (0m, 1m, 0m) = (0m, 7.166m, 0m)$. The offset between the rear center and the prism was measured during preparation, with the offset being $V_{pm} = (0.092m, 0m, 0.093m)$; thus, the as-built rear center is (72) $Q_{bc}^a = Q_{pm}^a - V_{pm} = (0.106m, 7.166m, 0.111m) - (0.092m, 0m, 0.093m) = (0.014m, 7.166m, 0.018m)$, which is exactly the same as in Table 4. The as-designed prism was then measured at $P_1^a = (0.092m, 7.166m, 0.093m)$, and, according to equation (6), the horizontal and vertical angles are determined as follows:

$$u \leftarrow Q_{tc}^l - Q_{ts}^l = Q_{pm}^l - Q_{ts}^l = \begin{bmatrix} 0.092m \\ 7.166m \\ 0.093m \end{bmatrix} - \begin{bmatrix} 0m \\ 0m \\ 0.25m \end{bmatrix} = \begin{bmatrix} 0.092m \\ 7.166m \\ -0.157m \end{bmatrix}$$

$$\theta_{tc}^v \leftarrow \cos^{-1} \frac{Z(u)}{\|u\|} = \cos^{-1} \frac{-0.157}{7.168} = 1.5927$$

$$\theta_{tc}^h \leftarrow \tan^{-1} \frac{Y(u)}{X(u)} = \tan^{-1} \frac{7.166}{0.092} = 0.1283$$

The calculated vertical and horizontal angles match “Group 1” in Table 4.

4.3.2 Curved Alignment

A second lab test using a curved tunnel setup was also conducted. The basic configurations of the total station, the round prism, and the start and end point of the alignment were exactly the same as the straight alignment test. In the curved alignment setup there was a center of a circle, which passed both the start and end points of the alignment. The center of the circle was set at the coordinate

of P_c = (499.975m,5m,0m), and its radius was $500m$. For this test, group 1 is again taken as the calculation exam, $P_1 = Q_{pm} = (0.027m, 7.277m, 0.133m)$.

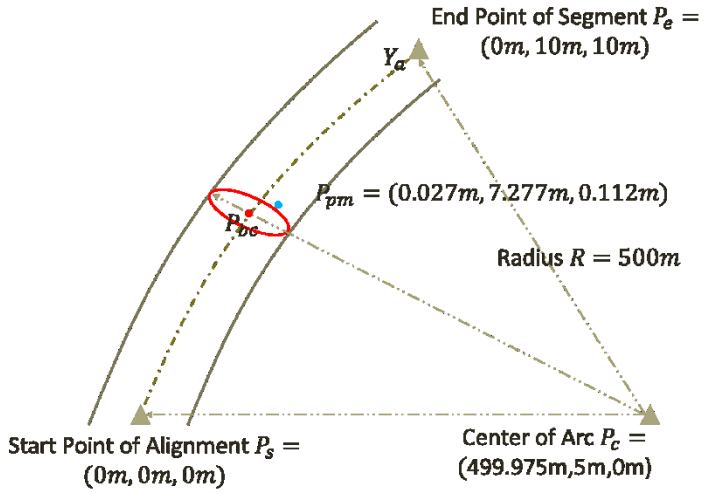

Figure 64. Curved alignment setup. The start and end points are the same, but the alignment between them is a curve. Prism P_1 is surveyed as P_{pm}.

As in the straight alignment test, the curved test was repeated five times, and the calculated results are shown in Table 5 and Table 6. Table 5 lists the reference results calculated by the reliable three-point algorithm, providing a benchmark for the comparison, and Table 6 lists the results of one-point algorithm. Table 5 provides all exact locations, either surveyed or calculated from three-point algorithm, and Table 6 shows the rear deviation as calculated by the one-point algorithm. Table 5 shows the results directly measured by the three-point algorithm, and sets the benchmark for the one-point algorithm. In this table, P_0, P_1, P_2, and P_3 represent the four mini prisms surveyed by the total station, and "$Calc\ P_3$" is the calculated position of P_3 by the three-point algorithm. The three-point algorithm was able to successfully calculate the cutter-head's positions from the surveyable prisms.

Table 5. Three-point algorithm calculation for curved setup (in meters)

		P_0	P_1	P_2	P_3	$Calc\ P_3$
Group 1	X	-0.033	0.027	-0.156	-0.046	-0.044
	Y	7.278	7.277	7.283	7.735	7.734
	Z	0.133	0.112	-0.072	0.022	0.021
Group 2	X	-0.021	0.039	-0.145	-0.035	-0.032
	Y	7.285	7.284	7.290	7.742	7.741
	Z	0.133	0.112	-0.072	0.022	0.021
Group 3	X	-0.010	0.050	-0.133	-0.024	-0.021
	Y	7.294	7.293	7.299	7.751	7.750
	Z	0.133	0.112	-0.072	0.022	0.021
Group 4	X	0.014	0.074	-0.109	-0.006	-0.005
	Y	7.311	7.311	7.314	7.767	7.767
	Z	0.133	0.112	-0.072	0.022	0.021
Group 5	X	0.051	0.111	-0.072	0.018	0.017
	Y	7.353	7.355	7.353	7.809	7.809
	Z	0.133	0.112	-0.072	0.022	0.023

Table 6. Comparison of deviation calculation between three-point algorithm and one-point algorithm for curved tunnel setup (in meters)

		Rear Dev	One-point Dev	Diff Rear	Emit Angles	
Group 1	X (m)	-0.045	-0.045	0.000	H (◦)	0.568
	Y (m)	0.000	0.000	0.000	V (◦)	91.236
	Z (m)	0.020	0.019	0.001		
Group 2	X (m)	-0.033	-0.033	0.001	H (◦)	0.568
	Y (m)	0.000	0.000	0.000	V (◦)	91.235
	Z (m)	0.020	0.019	0.001		
Group 3	X (m)	-0.022	-0.022	0.000	H (◦)	0.568
	Y (m)	0.000	0.000	0.000	V (◦)	91.233
	Z (m)	0.020	0.019	0.001		
Group 4	X (m)	0.002	0.002	0.000	H (◦)	0.567
	Y (m)	0.000	0.000	0.000	V (◦)	91.230
	Z (m)	0.020	0.019	0.001		
Group 5	X (m)	0.039	0.038	0.000	H (◦)	0.565
	Y (m)	0.000	-0.001	0.001	V (◦)	91.223
	Z (m)	0.020	0.019	0.001		

In Table 6, “Rear Dev” refers to the calculated deviations of the rear ring, while X represents the line deviation, and Z represents for the level (or grade) deviation. “One-point Dev” is the deviation calculated by one-point algorithm. The reason to compare “Rear Dev” and “One-point Dev” is that the one-point algorithm only receives limited information about the TBM’s position, and thus it can only calculate the deviation at the rear end of the TBM.

“Diff Rear” is the differences of calculated deviations between rear center and P_1. The deviation calculations produced by the three-point and one-point

algorithms are very close, and this demonstrates the effectiveness of the one-point algorithm's use in curved tunnels. The smart laser projector can completely replace the conventional laser as it can provide a highly accurate deviation calculation for the rear ring of the TBM. "Emit Angles" indicates the horizontal (X) and vertical angles (Y) at which the smart laser should be aimed in order to emit the laser spot on the as-designed P_1 (expressed as radian for direct total station control input).

The following is the simple calculation example for the group 1 data. According to equation (4), the polar coordinates of P_1 are:

$$\begin{aligned}
&\phi_{pm} \leftarrow \tan^{-1}\frac{Y(\overrightarrow{P_c^a P_{pm}^a})}{X(\overrightarrow{P_c^a P_{pm}^a})} = \tan^{-1}\frac{2.277}{-499.948} = 3.13704 \\
&\Delta_\phi \leftarrow \tan^{-1}\frac{Y(V_{pm})}{R} = \tan^{-1}\frac{0m}{500m} = 0 \\
&\phi_{bc} \leftarrow \phi_{pm} + \Delta_\phi = 3.13704
\end{aligned} \tag{7}$$

The first equation in the equation system (7) is to calculate the rotation angle of the prism in the curved tunnel. Because the tunnel is curved, every point on the curved tunnel can be expressed by polar a coordinate system expression, as described in equation (4). For the polar expression, every point is defined by a radius to the center, and the angle of rotation from the starting radius. In this case study, the first equation in equation system (7) is used to calculate the rotation angle.

The second equation in the equation system (7) is to calculate the difference of rotation angles between the prism and the TBM center. The reason for using this equation is that, in some cases, the center of TBM and the prism are offset along the TBM's *Y* axis, and this offset will cause a difference of rotation angle. In this case, this offset is zero, which means that the prism is on the rear ring.

Therefore, the third equation in the equation system (7) gives the rotation angle of the TBM center. The as-designed center of the rear ring can then be computed from the polar coordinate system, and the as-designed prism can be calculated as well. This step is to calculate the three-dimensional coordinate of the center of the TBM by using the polar expression, because the three-dimensional coordinate of the TBM center cannot be directly measured. Because P_c is the center of the curve, and the as-designed centre of the rear ring P_{bc} is on the curve, we can then calculate P_{bc} in the Cartesian coordinate system. The angle Φ_{bc} is the rotation angle of P_{bc} in relation to the curve center P_c, and it is the same as the prism, as in this setup the prism and the rear center are on the same ring. Therefore, the rotation angle of the rear center P_{bc} can utilize the same rotation angle as P_{pm}, which is calculated in equation (7). The calculation details are shown in (8).

$$\begin{aligned} P_{bc} \leftarrow & \begin{bmatrix} \cos\phi_{bc} \cdot R \\ \sin\phi_{bc} \cdot R \\ 0 \end{bmatrix} + P_c \\ = & \begin{bmatrix} \cos(3.13704) \cdot 500m \\ \sin(3.13704) \cdot 500m \\ 0 \end{bmatrix} + \begin{bmatrix} 499.975m \\ 5m \\ 0m \end{bmatrix} \\ = & \begin{bmatrix} -499.9948m \\ 2.2763m \\ 0m \end{bmatrix} + \begin{bmatrix} 499.975m \\ 5m \\ 0m \end{bmatrix} \\ = & \begin{bmatrix} -0.0198m \\ 7.2763m \\ 0m \end{bmatrix} \end{aligned} \tag{8}$$

However, the offset between the rear center and the prism cannot be directly applied, as it is currently along the direction of $P_{bc}P_c$; thus, the true offset is shown in the equation (8). The equations from (9) to (11) are to establish a TBM coordinate system. This system already includes the information of the curvature and the position of the center of the TBM. The equation (12) converts

the offset between the prism and the center of the TBM, which is measured in the TBM Cartesian framework, into local Cartesian coordinate system. Original offset V_{pm} is measured in the Cartesian coordinate system with P_{bc} as the origin. However, when the TBM model advances on the curved path, the Cartesian framework of the TBM model no long aligns with the Cartesian coordinate system of the total station; therefore, the offset V_{pm}, which is measured in the TBM's Cartesian framework, needs to be converted to the total station's Cartesian framework. We need to translate the offset into the coordinate system that can be understood by total station. The first step is to determine the direction of $x - axis$, and the determine a unit vector pointing along $x - axis$. The rear center of TBM P_{bc} is designed to stay on the alignment, and thus we choose a unit vector x pointing from origin to the position of P_{bc}:

$$x = Normalize(P_{bc} - \begin{bmatrix}0\\0\\0\end{bmatrix}) = Normalize(\begin{bmatrix}499.948\\-2.277\\0\end{bmatrix}) = \begin{bmatrix}-0.9998\\0.00455\\0\end{bmatrix} \quad (9)$$

The next step is to determine $z - axis$ unit vector. In this example, there is no grade in the design, and thus z unit vector z is chosen as $z = \begin{bmatrix}0 & 0 & 1\end{bmatrix}^T$. The third step is to determine $y - axis$ unit vector y. According to geometry, $y$can be calculated from cross-product operation as $y = z \times x$, thus:

$$y = z \times x = \begin{bmatrix}0.00455443\\0.99999\\0\end{bmatrix} \quad (10)$$

The transformation matrix m is simply a matrix containing the three unit vector x, y, z. It can be expressed as equation (9). The matrix m can transform a coordinate or vector in TBM framework to a corresponding coordinate or vector

in local Cartesian framework. We can use matrix m to convert offset vector V_{pm} in TBM coordinate system to corresponding offset vector V_{pm}^{c} in local Cartesian coordinate system. The converted offset can be directly utilized with the coordinates measured by total station.

$$m = \begin{bmatrix} x & y & z \end{bmatrix}^{-1} = \begin{bmatrix} 0.99999 & -0.00455443 & 0 \\ 0.00455443 & 0.99999 & 0 \\ 0 & 0 & 1 \end{bmatrix} \tag{11}$$

$$V_{pm}^{c} = m \cdot V_{pm} = \begin{bmatrix} 0.99999 & -0.00455443 & 0 \\ 0.00455443 & 0.99999 & 0 \\ 0 & 0 & 1 \end{bmatrix} \cdot \begin{bmatrix} 0.092 \\ 0 \\ 0.093 \end{bmatrix} = \begin{bmatrix} 0.091999 \\ -0.000419007 \\ 0.093 \end{bmatrix} \tag{12}$$

After applying equation (9) to (12), the original offset V_{pm} (measured with a measuring tape) is converted into the total station's Cartesian framework V_{pm}^{c}. Noticeably, when the TBM model advances further, the V_{pm}^{c} will keep changing, as the center of the rear ring follows the curved path. The difference between the corrected V_{pm}^{c} and the original V_{pm} is negligible, as the radius of the curve is very large compared to the offset, but the conversion or correction is very necessary for a reliable model. In real-world tunnels, the coordinate system may be arbitrarily chosen in order to cater to practical needs, so the correction may not be negligible. Eventually, the deviations of the prism can be computed from the deviations of the prism:

$$P_{pm} = P_{bc} + V_{pm}^{c} = \begin{bmatrix} -0.0198143 \\ 7.27721 \\ 0 \end{bmatrix} + \begin{bmatrix} -0.092 \\ 0 \\ 0.093 \end{bmatrix} = \begin{bmatrix} 0.0721857m \\ 7.27721m \\ 0.093m \end{bmatrix}$$

$$\Delta = Q_{pm} - P_{pm} = \begin{bmatrix} 0.027 \\ 7.277 \\ 0.112 \end{bmatrix} - \begin{bmatrix} 0.0721857 \\ 7.27721 \\ 0.093 \end{bmatrix} = \begin{bmatrix} -0.0451857m \\ 0m \\ 0.019m \end{bmatrix} \tag{13}$$

Equation system (13) consists of two steps: the first step evaluates the as-designed coordinate of the prism in the TBM coordinate system as P_{pm}, and the second step calculates the positional difference Δ (or deviation) of the prism in relation to the design position. The calculation in (13) shows the deviations calculated by the one-point algorithm for "Group 1" data in the curved tunnel setup. The corresponding result calculated by three-point algorithm is shown in Figure 65.

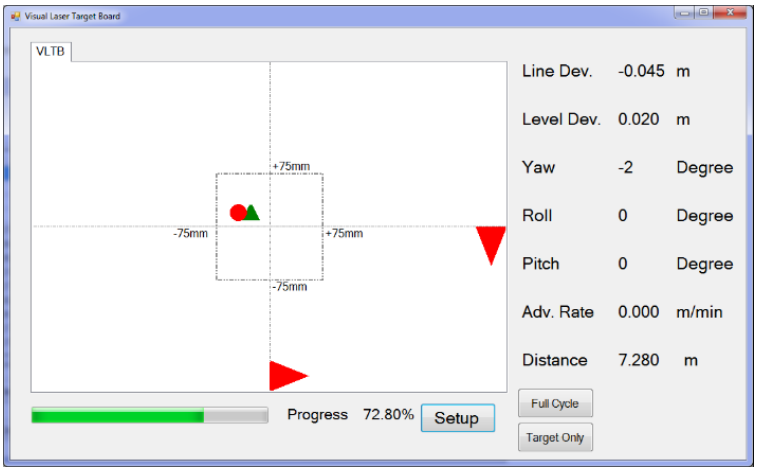

Figure 65. Deviations calculated by three-point algorithm in "Group 1" in curved tunnel setup.

We can also count the deviations of the one-point algorithm from the grid paper in Figure 66. The counted deviations totalled four-and-a-half grids horizontally, and two grids vertically, which match well with the calculated deviations by VLTB based on the three-point algorithm. A slight but important difference is that the "laser spot" in the screenshot and the real image are opposites of one another. The reason for this is that, in laser mode (as shown in Figure 66), the laser spot represents the as-designed alignment; in contrast, in the software interface, the as-designed alignment is shown as the center of the

crosshair, and the red dot represents the as-built position of the center of the rear ring.

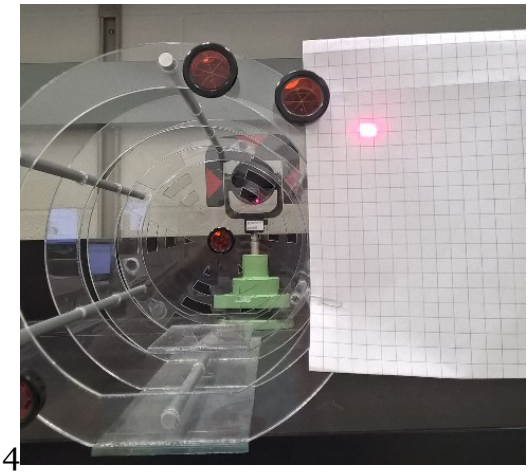

4

Figure 66. The emitted laser spot on the target grid paper, calculated by one-point algorithm in “Group 1” in curved tunnel setup.

4.4 PROOF OF CONCEPT IN THE FILED

The smart laser system was tested in a sanitary sewer tunnel in Edmonton between August 2014 and March 2015. Although the tunnel utilizes the same eight-foot TBM machine as the previous tunnel case (S. Mao, Shen, and Lu 2014), the survey window was much smaller than the previous one due to assembly problems. The tunnel was designed as a straight tunnel, but the alignment was later divided into several sections in response to geotechnical conditions, and to avoid having another sanitary tunnel in close proximity. This tunnel had almost the same design parameters as the previous tunnel, only it was designed for sanitary flow. The two tunnels shared the exact same TBM machine, and therefore the target prism bracket on the rear end was identical. The only difference was that the gantry system was not the same, and the survey window for this tunnel was even smaller due to the assembly.

The prism and target center were mounted at the back end of the gantry (referred as gantry test, on the left) and at the target board (referred as board test, on the right). The gantry test demonstrates the practical application of the theory, and the board test is to fit the smart laser in a real construction scenario. The results are shown in Figure 67 and Figure 68, and they show that the smart laser projector successfully emitted the laser spots at the expected location.

Figure 67. Gantry Test

In the gantry test, the total station was 46 meters away from the end of the gantry, and in the target board test, the total station was mounted in a safer position that did not block the conventional laser station. The distance between the board and the total station was approximately 84 meters. The VLTB system was able to fit into the current setup, and laser spot was reasonably small for the operator to tell where its center was.

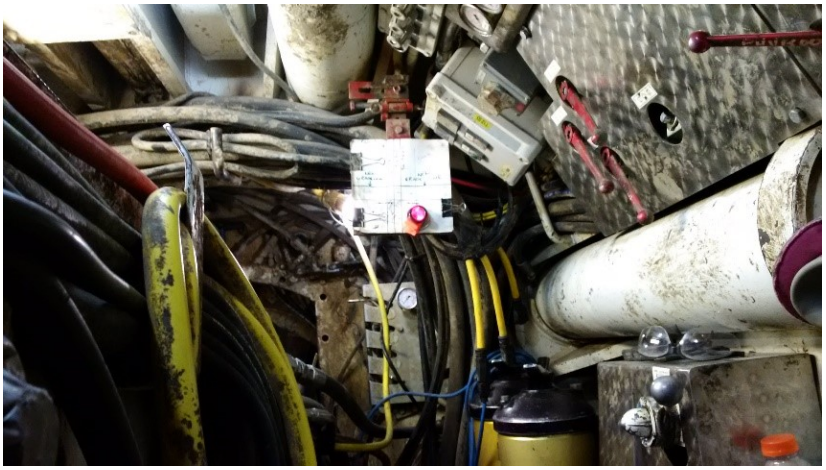

Figure 68. Target board test

4.5 TIME AND COST ASSESSMENT OF SMART LASER

The fundamental motivation for developing the automatic VLTB system and smart laser projector is to enhance efficiency and effectiveness of the guidance system for use in confined tunnels and extremely narrow spaces. The VLTB and the smart laser projector are not only designed to simplify the guidance system setup, but they also potentially save construction cost. The conventional laser requires tremendous resources of tunnel survey specialists for calibration and maintenance in straight tunnel section construction scenarios (Lu, Shen, and Mao 2014). However, in a curved tunnel section, the shortcoming of the conventional laser would be amplified, and the inconvenience and difficulty associated with its setup and maintenance can make their use significantly undermine construction productivity. The time and cost associated with the use of the original VLTB system was estimated on the basis of a one-kilometer straight tunnel by Monte Carlo simulation (Lu, Shen, and Mao 2014), which provides real-world cost data for tunnel construction. The cost analysis in this

paper will be based on the same cost information and crew hourly rates given in (Lu, Shen, and Mao 2014), including three main categories as follows:

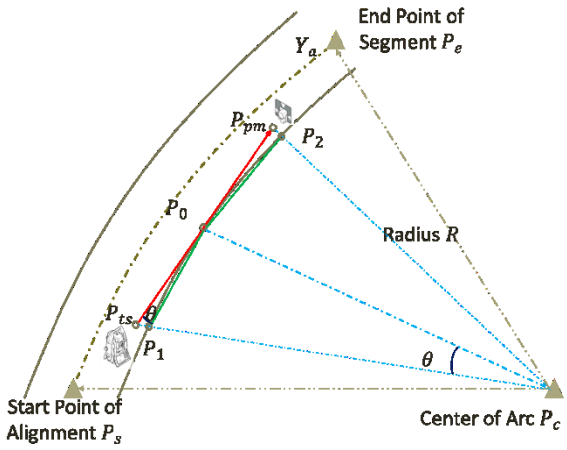

Figure 69. Visibility in curved tunnel

- Specialist tunnel survey crew man-hour cost
- Tunnel construction crew's direct production loss due to shutdown
- Indirect costs of the project
    - TBM equipment cost (normally a large capital investment like TBM cost is measured as cost per meter, so it is not directly calculated as laser maintenance events' cost)
    - Gantry and support system cost
    - Project management control cost

There are two primary reasons for including these three categories of costs in an assessment: firstly, the TBM relies solely on the guidance system to steer and advance and it cannot proceed without one; secondly, for municipal service tunnels, the maintenance and setup of the guidance system will entirely block construction and eventually prevent any tasks from being executed in parallel (for example, it is not possible to conduct conveyor belt maintenance in parallel with laser maintenance).

Therefore, by combining the three categories of costs, the hourly cost of "laser adjustment/maintenance/setup event" can be calculated, and the time spent on the each guidance system can be quantified. Moreover, the comparison of the VLTB system and the conventional laser includes both straight tunnel and curved tunnel scenarios, showing that the new technology can save more time and cost in the curved tunnel.

4.5.1 Hourly Cost for "Laser Maintenance Events"

The direct cost data are based on the management system of a North-American municipal construction department and the estimated costs provided by the management team (Lu, Shen, and Mao 2014). The hourly rate for an experienced surveyor is $77.30/*hour* (Lu, Shen, and Mao 2014), and at least three surveyors are required for a common relocation maintenance practice (one for front reference benchmark maintenance, one for back reference maintenance, and one for total station or leveling operation). Therefore, the hourly cost of surveyors alone is $231.90.

The second part of the cost is the production loss of the construction crew. During the survey, the whole construction team is idle. A typical tunneling crew include at least nine members: (Lu, Shen, and Mao 2014)

- Tunnel foreman I: one person
- TBM operator: one person
- Crane truck operator: one person
- Tunnel laborer II: two people
- Tunnel laborer I: four people

Different classifications of laborers are responsible for different tasks including, but not limited to, concrete loading and unloading, loading and

unloading muck cars, and concrete installation. The cost for each classification of laborers is given as below:

- Tunnel foreman I: $\$52.05/manhour \times 1man = \$52.05/hour$
- TBM operator: $\$65.44/manhour \times 1man = \$65.44/hour$
- Crane truck operator: $\$46.57/manhour \times 1man = \$46.57/hour$
- Tunnel laborer II: $\$47.295/manhour \times 2men = \$94.59/hour$
- Tunnel laborer I: $\$45.855/manhour \times 4man = \$183.42/hour$

On aggregate, the direct production loss due to survey shutdown is estimated to be $\$442.07/hour$ (Lu, Shen, and Mao 2014). The last part of the cost for laser maintenance events is the indirect cost. The indirect cost for the project management team—which consists of a tunnel supervisor, a projector manager, and a field engineer—is $\$73.383/manhour \times 3men = \$220.15/hour$. In addition, if the overhead in the field is estimated to be $\$2000/day$ for all the facilities, and a schedule consisting of $8hours/shift$ x $1shift/day$, the hourly overhead cost is $\$250/hour$. It is noteworthy the TBM equipment cost is treated as fixed project overhead which does not vary with the construction duration, hence is not taken into account in the cost estimate. In conclusion, the total hourly cost for a laser maintenance event is estimated as: $\$231.90/hour + \$442.07/hour + \$220.15/hour + \$250/hour = \$1144.12/hour$.

4.5.2 Time and Cost for Straight Tunnel

In the previous paper on tunnel guidance cost estimation, there are two types of survey: routine surveys and relocation surveys. In the original assumption, a routine survey was to be performed after every ten meters of TBM advancement, and took one and a half hours to complete; relocation survey events were to happen every two hundred meters, and took about five hours to finish. After the previous paper, the TBM was reassembled in another tunnel, and

operated by another team, who had equivalent skills and expertise in calibration of tunnel guidance system. However, in the second tunnel, due to the conditions of gantry installation, some gantry sections and attached hoses and wires were slightly higher than the adjacent sections, which eventually led to conditions wherein the survey window of the conventional laser was always blocked.

The standard procedure of the laser setup starts with horizontal adjustment, and makes the laser pass all three strings. The surveyors then tune the laser vertically, and make sure that the laser beam has the same grade as tunnel alignment. The author has worked with survey teams on tunnel maintenance events on five separate occasions, with three being for scheduled relocation, one being a routine survey, and the last one for an emergent adjustment. All the three relocations took no less than ten hours, and the last emergent adjustment took almost twelve hours.

After more discussion with tunnel crew and survey crew, the author realized that these situations are quite common. Given this, for the purposes of this thesis the shutdown time for a relocation procedure will be defined as ten hours. For a one-kilometer tunnel, there will be at least five relocation surveys, and about $\frac{1000m}{10m/routine} - 5 = 95$ routine surveys (minus five because these five routine surveys are substituted by relocation surveys). Therefore, the total time for maintenance of routine survey works out to $5 \times 10hour + 95 \times 1.5hours = 192.5hours$.

Considering the $\$1144.12/hour$ cost for the tunnel survey and collateral shutdown, the total cost works out to $\$1144.12/hour \times 192.5hours = \$220{,}243.10$, and the unit cost of conventional laser is $\frac{\$220{,}243.10}{1{,}000m} = \$220.24/meter$.

For the VLTB system, the basic unit of cost assumption remains the same as in the estimation paper (Lu, Shen, and Mao 2014). The estimation in this thesis will be built upon two shutdown categories: six relocations (utilizing $160m$ relocation interval) at two hours for each relocation; and the potential for an additional $31.60hours$ total shutdown time for the one-kilometer tunnel due to automatic system maintenance (Lu, Shen, and Mao 2014). Therefore, the total shutdown time for VLTB is $2hours \times 6 + 31.60hours = 43.60hours$. The total cost due to laser maintenance shutdown is $43.60hours \times \$1144.12/hour = \$49{,}883.63$, and the unit cost of the VLTB with regards to relocation maintenance is $\frac{\$49{,}883.63}{1{,}000m} = \$49.88/meter$.

4.5.3 Time and Cost for Curved Tunnels

The curvature of the tunnel liner will further diminish the survey window, and the relocation interval will be directly determined by the size of the open space in the survey window. In this section, the first step is to determine the maximum relocation interval.

As shown in Figure 69, the location of the prism reaches the position that cannot be measured by total station, based on the curvature of the alignment and ideal visibility conditions (i.e. there are no obstacles interfering with the line-of-sight; visibility is only constrained by the survey window size as illustrated in Figure 21 and Figure 49). According to Figure 69, if angle $\angle P_{ts}P_0P_1$ is equal to the angle $\angle P_{ts}P_cP_0$, then the length of $P_{ts}P_0$ is:

$$P_0P_{ts} = \tan\theta \cdot P_cP_0 = \tan\theta \cdot R \tag{14}$$

The length of $P_{ts}P_1$ is the window's size w; therefore, angle θ can be evaluated, and the maximum distance is expressed as:

$$\theta = \cos^{-1}\frac{R}{R+w}$$
$$P_{ts}P_{pm} = 2\tan\left(\cos^{-1}\left(\frac{R}{R+w}\right)\right)\cdot R \quad (15)$$

The above equation is the general equation for calculating the maximum relocation interval. If the radius of the tunnel is $R = 500m$ (Zhao, Shirlaw, and R 2000) and the survey window is $w = 0.5m$, then the maximum distance is:

$$P_{ts}P_{pm} = 2\tan\left(\cos^{-1}\left(\frac{R}{R+w}\right)\right)\cdot R = 2(R+w)\sqrt{1-\frac{R^2}{(R+w)^2}} = 44.733m \quad (16)$$

If the TBM keeps velocity as $5m$ in an eight-hour shift (Lu, Shen, and Mao 2014), the guidance system will lose the line of sight after about 8.95 hours due to the maximum visibility distance. However, the gantry system also takes up the space inside the tunnel being built, preventing the total station to be initially placed close to the prism. Assuming the gantry is $20m$ long, then, the maximum line-of-sight is no more than $24.733m$, the surveyors would need to relocate the conventional laser and the control strings every five days. The time spent on the relocation maintenance will be no less than the straight tunnel. In contrast, the smart laser system only requires two hours to be relocated.

The first setup step is to calculate the minimum relocation numbers required given 1km tunnel: $\frac{1000m}{24.733m/relocation} = 40.43\,relocation \approx 41\,relocation$. Immediately, we can observe that the frequency of relocation increases. For the conventional laser, the relocation shutdown is $41\,relocation \times \frac{10hours}{relocation} = 410\,hours$, and the routine survey (laser calibration) shutdown is $\left(\frac{1000m}{\frac{10m}{routine}} - 41\,routine\right) \times 1.5hours = 59routine \times 1.5hours = 88.5hours$. Thus, total

shutdown time is $410 hours + 88.5 hours = 498.5 hours$, total shutdown cost is $498.5 hours \times \$1144.12/hour = \$570{,}344$, ultimately, the unit cost of the laser maintenance event is $\frac{\$570{,}344}{1000m} = \$570.34/meter$. This price is almost double the price of the straight tunnel.

Conversely, for the smart laser projector solution being proposed, the total time is $41\ relocations \times 2 hours + 31.60\ hours\ = 113.60\ hours$, the total shutdown cost is: $113.60 hours \times \$1144.12/hour = \$129{,}972.03$, and the unit cost is $\frac{\$129{,}972.03}{1000m} = \$129.97/meter$.

The difference between the conventional laser solution and the proposed smart laser projector solution in the unit cost of laser maintenance events is much more significant in the curved tunnel scenario: the proposed smart laser projector system costs only 22% of the conventional laser.

Chapter 5. REFERENCE DESIGN METHODOLOGY

5.1 MOTIVATION

The previous chapters have introduced two tunnel guidance algorithms that survey prisms on the TBM at a given moment, and calculate the positions of any points on the TBM. For the operator, the algorithms are responsible for providing accurate guidance information throughout the construction process, and, for the surveyors, they need to provide an estimation of the accuracy of the guidance system. Therefore, it is essential to analyze the mathematical model of the TBM guidance, and provide an analytical tool to assess the accuracy.

The guidance algorithms are both based on survey, and thus the algorithms are affected by survey errors. For the past two hundred years, survey errors have been a significant problem for surveyors: even with all of the technological advances in survey equipment, the surveyors still cannot fully eliminate all errors. Luckily, survey errors—especially random noise—can be analyzed as statistical models. Surveyors can assess the errors in real survey practice, and develop plans to deal with them.

Take the VLTB for example: the total station surveys the prisms on the TBM with some errors, and the error models can quantify the impact on the guidance accuracy based on the survey errors. Surveyors can utilize these models to determine when the guidance is no longer accurate, and when they should perform maintenance on the guidance system. This survey technique can help construction engineers to better plan for guidance system and survey maintenance.

The errors models can be more helpful: a simple fact concluded from the models is that the accuracy and reliability of the system can be further improved

if a proper reference system exists. When the guidance system runs automatically, it relies upon several reference points (always prisms) to mark the correct positions and orientations of the TBM, and the system can perform self-calibration based on the positions of these references. A well-established reference system can greatly reduce the errors in the survey, and thus provide highly accurate guidance results.

From the construction engineer's perspective, the reference system is critical; however, surveyors also require time to maintain the reference points. It is important to determine the minimum number of prisms needed for a "healthy" guidance system. Moreover, construction engineers must design a plan to maintain the references with the guidance laser. Therefore, the error models of the guidance system, including the reference points and the guidance laser, must be fully understood.

Whenever the total station is relocated, the survey will introduce new errors. Whenever the TBM pushes the concrete liners, there will be new errors. A tunnel always takes at least one year to build, and errors in the guidance system accumulate slowly but steadily. The greater in length the tunnels are built, the larger the errors are. The solution to fix these errors is to set up a proper reference network. A proper reference network is the safety net for the system, and it ensures that the guidance equipment will perform the necessary self-assessment.

This chapter will elaborately study the error models and illustrate all aspects of the errors in the tunnel guidance system. After this has been done, it will introduce a design algorithm for the reference system based on error models, which will answer the question of "how to plan and maintain a reference system for TBM guidance in engineering design".

5.2 OVERVIEW

In this section, the visibility factor of the reference design will be discussed. The majority time during survey shutdown is allocated for laser relocation; thus, if the laser can guide the TBM as far as possible between shutdowns, the savings in cost and time will be greater. There are several constraint factors on the maximum guidance distance (relocation interval): visibility, minimum search window, and accumulated error. Visibility is the most straightforward constraint, especially in curved tunnel. In a tunnel with a radius of 500m, the total station can see no more than 49m ahead. Considering the length of the gantry system and unexpected obstacles in the survey window, the relocation interval is around 20m to 25m, which means that there is a survey shutdown every 4 to 5 days during construction (assuming 5m daily progress for a typical small-diameter tunnel).

The minimum search window is associated with the functioning of an automatic guidance system. Due to the dust and heat in the tunnel, the robotic total station is unable to identify two different prisms when their distance is less than 30cm. This limits the maximum distance over which the total station can work, and this distance is affected by many factors. The author and his team tested the limits of the total station's range by gradually moving a bracket with three prisms away from it; eventually, the total station surveyed two different prisms as the same one when the distance between the bracket and the total station reached 180m. This suggests that the maximum distance of the three-point algorithm is no more than 180m.

Accumulated error is tricky: errors from each survey will stay with the survey results, and the accuracy of the guidance system will gradually decrease as

errors accumulate. Surveyors need to determine a maximum survey interval, which is the point at which accumulated errors begin to prevent reliable guidance results. With the theory of error model and error propagation from survey engineering, we can estimate the stochastic properties of the survey, e.g. surveyors utilize the error model in open traverse to help design full survey (Chrzanowski 1981; S. C. Stiros 2009). We can apply the same theory to estimate the accuracy of guidance, and to assess the accuracy of the three-point algorithm in VLTB and other laser methods. Thus, we can calculate a different maximum distance between the total station and the TBM based on the desired level of accuracy.

After determining the maximum distance, the total station is always placed close to the gantry in order to reduce how often relocation is required (e.g. if the maximum distance is 180m and gantry is 20m, the actual relocation interval is 160m). Because the total station is very close to the boring front of the machine, deformation can affect its location. It is therefore necessary to determine proper locations for the reference prisms so they can safely serve as benchmarks for the total station. In one relocation, surveyors set up two prisms in the tunnel, which the relocated total station utilized to perform resection, error checking, and self-calibration (S. Mao, Shen, and Lu 2014). One prism will be mounted at the same spot on the total station before it is relocated, and this prism is called back sight; the other prism is mounted on the liner, and an optimization process helps to determine the best location.

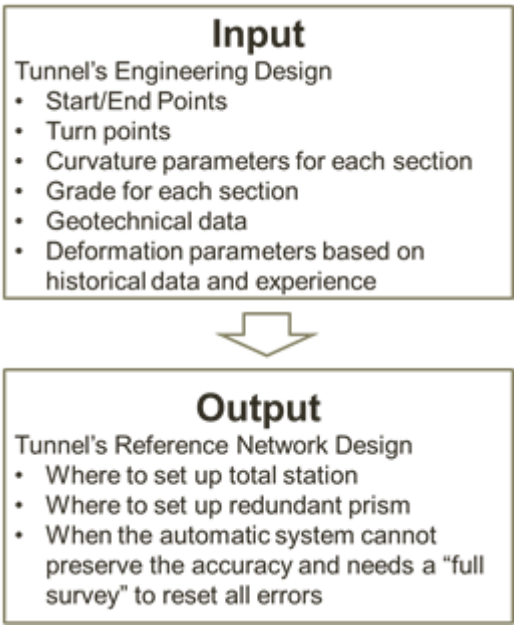

Figure 70. Input/output for the design and optimization algorithm of tunnel reference network

5.3 ERROR MODEL AND ERROR PROPAGATION

5.3.1 Error Model

In this section, the error model and error propagation theory from geomatics will be introduced, and the meaning of error models will be fully discussed.

The term, "observations", refers to the idea that results can be directly measured by survey tools. For example, measuring tape can measure the length of any line segment; in this case, the length is the observation and the measuring tape is the tool with which it is measured. The term, "parameters", refers to arbitrary variables that are selected to simplify the modeling process. This definition is somewhat abstract, but it simply means that the parameters are part of the modeling but are not directly surveyed.

The model connecting observations and necessary parameters is called the functional model. Take the mathematical model of the total station, for example. The total station is positioned at coordinate of (x, y, z) and surveys an unknown prism, marked as (p, q, r), producing survey results that include the slope distance d, and the horizontal and vertical angles θ and ψ. We can build a functional model to calculate the position of the prism from the total station and the measurements.

$$\begin{bmatrix} x + \cos\psi\cos\theta \\ y + \cos\psi\sin\theta \\ z + \sin\psi \end{bmatrix} = \begin{bmatrix} p \\ q \\ r \end{bmatrix} \tag{6.17}$$

The functional model is expressed as equation (6.17), in which variables x, y, z, d, θ, ψ are all observations: x, y, z are measured by surveyors and provided as known positions, and d, θ, ψ are measured by the total station itself. On the other hand, the coordinate of a prism p, q, r is chosen as parameters because it is not possible to directly get the coordinate of any prism, and the coordinate of a prism is calculated from a total station with known coordinates, a surveyed slope distance, and horizontal and vertical angles.

In real world surveying, errors exist in all observations. Depending on the source, errors can be categorized as random errors, which are purely unavoidable random noise that exists in all measurement, or as blunders and system errors, which are avoidable (Mikhail and Ackermann 1976). Mathematically, a measurement is regarded as a sample of a normal distributed variable $N(\mu, \sigma)$; μ is the mean of the distribution and presents the true value of measurement (Mikhail and Ackermann 1976). A single reading of the measurement will be affected by random error and can hardly be the true value; only a large quantity of repeated measurements on the same target can approximate the true value. In

statistics, this difference is referred as mean of sample and the mean of a population (Mikhail and Ackermann 1976).

This model also shows that the random error associated with the measurement is a variable of normal distribution $N(0, \sigma)$. However, if there are blunders and system errors in the measurement, then the model is biased (biased means that the mean in the statistical model is not zero) and the total error will be $N(\mu_{blunder} + \mu_{system}, \sigma)$. The blunder $\mu_{blunder}$ is caused by human errors and it is unpredictable; thus, in real practice, it should be eliminated by incorporating well-designed procedures and practices. System errors μ_{system} are either caused by deficits or the limitations of equipment or methods, and they are normally detected and eliminated during equipment calibration (Mikhail and Ackermann 1976).

During a survey task, there is always more than one survey target, and when establishing a functional model it is preferable to use the matrix form to simplify the expression. To represent a set of observations $x_1 \quad \cdots \quad x_n$, we assign a symbol X. Each observation has its own error, and sometimes two observations have some internal connections (these connections are called dependency). Traditionally, variance-covariance matrix is used to define the errors (variance) and inter-variable connections (covariance) (D. Li et al. 2015)

$$C_{XX} = \begin{bmatrix} \sigma^2_{x_1x_1} & \cdots & \sigma^2_{x_1x_n} \\ \vdots & \ddots & \vdots \\ \sigma^2_{x_nx_1} & \cdots & \sigma^2_{x_nx_n} \end{bmatrix} \tag{18}$$

The matrix (18) is marked as C_{XX}, and this symbol represents the variance-covariance matrix of all elements in observation set X. In this matrix (18), the diagonal shows the variance of each variable. Items that are not on the diagonal (e.g. $\sigma_{x_ix_j}$) show the covariance between observations x_i and $x_j (i \neq j)$; if

$\sigma_{x_i x_j} = 0$, the two variables are independent from the aspect of statistics; otherwise, the two variables are dependent.

The matrix (15) is very useful, and the quality of the survey can be assessed from it: when smaller (closer to zero) variance (values on the diagonal) and covariance (the other values) indicate less uncertainty in the survey, the result is more reliable.

5.3.2 Error Propagation

The survey process always starts from known points with a known variance-covariance matrix, and then propagates to unknown points. For example, the tunnel survey starts from accurate ground points, which are measured using either GPS or ground control points (Anderson and Mikhail 1998), and it will continue in the tunnel until it reaches of the rear end of the TBM. Errors exist in each step of the survey process and propagate from the beginning to the end. We only know the position error of the start point and the survey errors in each step, and we need to understand how the errors propagate during the process and how they affect the variance-covariance matrix of each surveyed prism (Mikhail and Ackermann 1976).

Let us start from error propagation using a linear model. We begin by defining a general linear model $Z = KX + K^0$, with a coefficient matrix K and a constant vector K^0 as defined in equation (19). In this model, there are two sets of values: parameters $Z = [z_1 \quad \cdots \quad z_m]^T$ and observations $X = [x_1 \quad \cdots \quad x_n]^T$. Observations are survey results, and they contain survey errors. The linear model evaluates the parameters based on the observations and propagates errors (uncertainties) from observations to parameters. The problem that must be

answered is whether or not we can quantify the statistical properties of the errors in the parameters.

$$K = \begin{bmatrix} K_{11} & \cdots & K_{1n} \\ \vdots & \ddots & \vdots \\ K_{m1} & \cdots & K_{mn} \end{bmatrix} \qquad K^0 = \begin{bmatrix} k_1^0 \\ \vdots \\ k_n^0 \end{bmatrix} \tag{19}$$

In statistics, the symbol $E(\cdot)$ is used to express the expectation of the random variable. If we want to calculate the expectation of Z, we can start from the known coefficients K and K^0, in addition to the expectation of X. We can also calculate the variance-covariance matrix of Z from the variance-covariance matrix of X. The equation (20) is the error propagation of linear models. The variance-covariance matrix contains the statistical properties of the parameters. This process is called error propagation.

$$\begin{aligned} E(Z) &= E(K \cdot X + K^0) = K \cdot E(X) + K^0 = K\mu_X + K^0 \\ C_{ZZ} &= K \cdot C_{XX} K^T = K\sigma_{XX} K^T \end{aligned} \tag{20}$$

In the field, nonlinear functional models are very popular; for example, the total station measuring model (the equation (6.17)) is a non-linear model, and it is the most popular model used in surveys. We need also to deduce the error propagation model for non-linear models. The most critical step for non-linear error propagation is “linearization”. The core idea of linearization is to apply the Taylor series (Mikhail and Ackermann 1976) to change a non-linear model into a linear-model around an approximation point $X^0 = [x_1^0 \quad \dots \quad x_n^0]^T$.

For a non-linear model $Z = [f_1(X_1, \dots, X_n), \cdots, f_m(X_1, \dots, X_n)]^T$, parameters Z and observations X are connected by non-linear functions $f_i(X_1, \dots, X_n)$. However, error propagation cannot work with these non-linear functions

$f_i(X_1, \ldots, X_n)$. The solution is to apply the Taylor series, and then to apply total derivative (Mikhail and Ackermann 1976) on each function $f_i(X_1, \ldots, X_n)$, which will result in each nonlinear model being expressed in linear form as $dz_i = (df_i/dx_1)_0 dx_1 + \cdots + (df_i/dx_n)_0 dx_n$. After linearization, the non-linear functions will have the same form as linear functions, and can thus be utilized in error propagation calculation. Using equation (21) allows for the easy estimation of the prism and total station errors during design phase.

$$\begin{aligned} \begin{bmatrix} dz_1 \\ \cdots \\ dz_m \end{bmatrix} \triangleq dZ = K \cdot dX \triangleq \begin{bmatrix} (\frac{df_1}{dx_1})_0 & \cdots & (\frac{df_1}{dx_n})_0 \\ \vdots & \ddots & \vdots \\ (\frac{df_m}{dx_1})_0 & \cdots & (\frac{df_m}{dx_n})_0 \end{bmatrix} \begin{bmatrix} dx_1 \\ \cdots \\ dx_m \end{bmatrix} \\ \mu_Z = E(Z) = \begin{bmatrix} f_1(E(X_1), \cdots, E(X_n)) \\ \vdots \\ f_m(E(X_1), \cdots, E(X_n)) \end{bmatrix} \\ \sigma_{ZZ} = K \cdot C_{XX} \cdot K^T = K \cdot \sigma_{XX} \cdot K^T \end{aligned} \tag{21}$$

5.4 RESECTION ERRORS

The previous section illustrates the fundamental knowledge of error propagation theory in survey. In this section, error propagation will be used to help determine the errors in resection. Resection is a process of calculating the total station's position and orientation in relation to the reference prisms, and it is a non-linear model (total station survey method) that is used to calculate parameters (position and orientation of total station) from observations (prisms, distances, and angles). It is also a good example for demonstrating error propagation.

For all guidance methods, a laser (survey robot, normal motorized total station, and conventional laser) must be placed into the tunnel. The most important aspect of the setup is to align the laser with the tunnel alignment. For

VLTB systems, the three-point algorithm utilizes the resection method (Anderson and Mikhail 1998) to calculate its own location and orientation.

Resection is a method used to locate and orientate the total station (laser station with motor and survey functionality). The total station, which is pre-set with an arbitrary unknown location and orientation, surveys two known prisms in the space and then calculates its own location and orientation, aligning itself to the coordinate system of the two prisms that are originally surveyed.

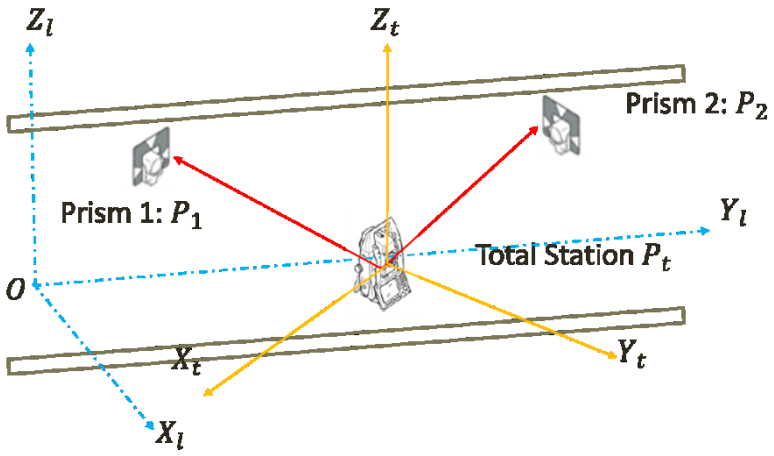

Figure 71. Resection of total station based on two reference prisms.

As shown in Figure 71, the coordinates of the two prisms in the local Cartesian coordinate system are P_{p1}^{l} and P_{p2}^{l}. The total station is taken out of the box and mounted on the bracket, but due to all these movements, its own coordinate system $X_tY_tZ_t$ is arbitrary and not aligned with the local Cartesian framework. First, the total station is levelled, and its Z_t axis is made parallel to the Z_l axis of local Cartesian framework. Then, the total station surveys the two prisms in its arbitrary framework, as P_{p1}^{t} and P_{p2}^{t}. In reality, the survey results are expressed as slope distances s_1, s_2 and horizontal/vertical angles $h_1^t, v_1^t, h_2^t, v_2^t$ in the total station temporary framework:

$$
\begin{aligned}
P_1^t &\leftarrow P_t^t + \begin{bmatrix} \cos v_1 \cos h_1 s_1 \\ \cos v_1 \sin h_1 s_1 \\ \sin v_1 s_1 \end{bmatrix} \\
P_1^t &\leftarrow P_t^t + \begin{bmatrix} \cos v_2 \cos h_2 s_2 \\ \cos v_2 \sin h_2 s_2 \\ \sin v_2 s_2 \end{bmatrix}
\end{aligned} \tag{22}
$$

The resection problem can be further simplified as a two-dimensional rotation problem, as the Z_t axis is parallel to Z_l axis; thus, $Z(P_t^l)$ is a fixed offset from the origin of the local Cartesian framework. To solve the two-dimensional rotation problem, we define horizontal distance d_1, d_2:

$$
\begin{cases} d_1 \leftarrow \cos v_1 s_1 \\ d_2 \leftarrow \cos v_2 s_2 \end{cases} \tag{23}
$$

Then solve the equations:

$$
\begin{cases} x_t \leftarrow X(P_t^l) \\ y_t \leftarrow Y(P_t^l) \\ X(P_1^l) \leftarrow x_t + \cos a_1 \cdot d_1 \\ Y(P_1^l) \leftarrow y_t + \sin a_1 \cdot d_1 \\ X(P_2^l) \leftarrow x_t + \cos a_2 \cdot d_2 \\ Y(P_2^l) \leftarrow y_t + \sin a_2 \cdot d_2 \\ a_1 - a_2 = h_1 - h_2 \end{cases} \tag{24}
$$

By solving the equations in (24), we can calculate the three unknowns x_t, y_t, a_1. In addition, if there is a third prism with a known location, the resection will have one redundancy, or one degree of freedom. The redundancy can provide two benefits: (1) it can help with the adjustment of the resection, which diminishes the effect of random errors; (2) it can improve system reliability, which helps to detect if any prism is disoriented or displaced.

However, there are two limitations for setting up prisms in a tunnel under construction. The first limitation is that the narrow shape of the tunnel causes prisms to be too close to each other in the X-Z plane, and the second limitation is

that the roof is the only area safe enough to mount prisms. These two limitations present a very weak geometry for reference network setup (Bossler 1984), and a network with weak geometry is comparatively weaker in limiting the propagation of errors.

In real world, equation set (24) cannot have exact results due to the errors in the survey. For instance, the known positions for the two reference points and the resection process inherently have errors. Thus, equation set (24) can only find an optimum solution based on the available information. As shown in Figure 72, the total station is located at P_r as given by the optimum solution, but the true position is at P_t. Thus, the calculated coordinate system for total station $P_r - X_rY_rZ_r$ deviates from the true coordinate system for total station $P_t - X_lY_lZ_l$ in terms of angle and position aspects. The angle error mainly occurs in the horizontal angle, as shown in Figure 72.

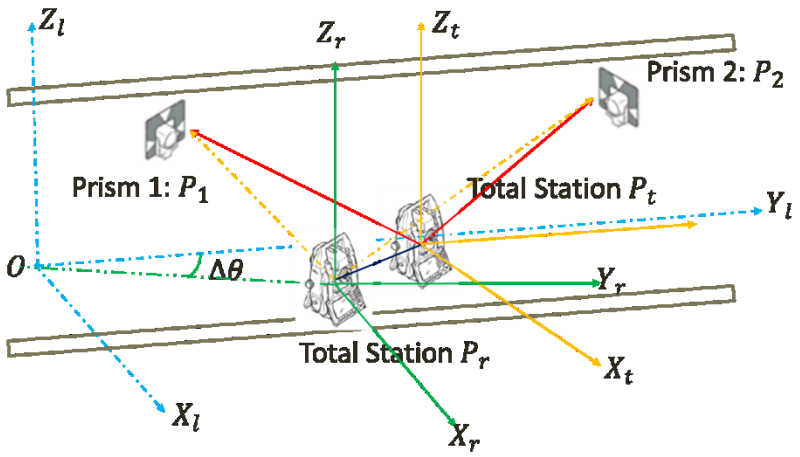

Figure 72. Total station resection error.

In the case of angle and position errors, the laser spot ends up in the wrong location when the total station tries to emit its beam parallel to the alignment. For example, assume the total station is supposed to emit the laser at

a point defined by the horizontal/vertical angle pair (h, v), but, due to the angle error $\Delta\theta$, the position of the laser spot on target board is:

$$P_{tc}^{l} \leftarrow P_{r}^{l} + \begin{bmatrix} \cos v \cos (h + \Delta\theta) s \\ \cos v \sin (h + \Delta\theta) s \\ \sin v \cdot s \end{bmatrix} \tag{25}$$

To further demonstrate how much error resection may cause, this subsection will give an example. Assume the true total station position is $P_t \leftarrow \begin{bmatrix} 0m \\ 0m \\ 0m \end{bmatrix}$, and calculated total station position is $P_r \leftarrow \begin{bmatrix} 0m \\ -0.005m \\ 0m \end{bmatrix}$, and one prism is located at $P_{pm} \leftarrow \begin{bmatrix} 20m \\ 0m \\ 0m \end{bmatrix}$. In the true coordinate system, the horizontal and vertical angles to the prism are $(0°, 0°)$. However, in the calculated coordinate system, the horizontal and vertical angles are:

$$\begin{aligned} v_{pm} &\leftarrow \frac{0}{\sqrt{0.005^2 + 20^2}} = 0° \\ h_{pm} &\leftarrow \tan^{-1} \frac{0.005}{20} = 0.0143° \end{aligned} \tag{26}$$

Equation (26) shows that there is 0.0143° difference between the calculated framework and the true framework. The calculated framework will be regarded as the true framework for the rest of the tunnel, and we will try to evaluate how much guidance error is due to this 0.0143° difference.

Let us assume that the one-point algorithm tries to position a prism, and the horizontal angle error is $\Delta\theta \leftarrow 0.0143°$, the slope distance is $200m$, the horizontal angle $h \leftarrow 87°$, and the vertical angle $v \leftarrow 1°$. By applying equation (25), the true target point without the horizontal angle error is $\begin{bmatrix} 10.466m \\ 199.695m \\ 3.490m \end{bmatrix}$. In comparison, the calculated target point with horizontal angle error is $\begin{bmatrix} 10.416m \\ 199.693m \\ 3.490m \end{bmatrix}$.

The difference between the true position and the calculated position is $\begin{bmatrix} 50mm \\ 2mm \\ 0mm \end{bmatrix}$, which shows the potential magnitude of the resection error's impact on guidance.

In a real tunnel, a $5mm$ resection error is not rare when the TBM is several hundred meters away from the entrance shaft (S. C. Stiros 2009). If we assume that the total station accumulates $2mm$ of resection error during every relocation and the interval between two relocations is 200m, after only 500 meters of construction the error would become so huge that the TBM would not be able to advance safely. Thus, it is imperative to control this error in order to achieve higher accuracy in TBM guidance.

5.5 GUIDANCE ERRORS

Each guidance methodology has its own mathematical model, and each model is computed from basic observations. For example, the three-point algorithm relies on the positions of three visible prisms, and the "laser with receiving units" relies on the positions of laser spots on receiving units.

5.5.1 Guidance Errors of Three-point Algorithm

Due to resection errors, the station framework is not fully aligned with the local Cartesian framework (or alignment framework, depending on the goal of resection). When the total station surveys the three prisms on the TBM in VLTB, the three prisms are actually measured within the station framework. Because the three surveys are performed in a short time, the results are very accurate within the station framework, which means that the three prisms are accurately positioned within the station framework.

This section will discuss the errors of the three-point algorithm in the station framework before turning its attention to the total station's orientation

error and position error. Finally, the guidance error will be measured in the alignment framework (the error in transformation between alignment framework and the local Cartesian framework is negligible, thus the transformation will not be discussed here).

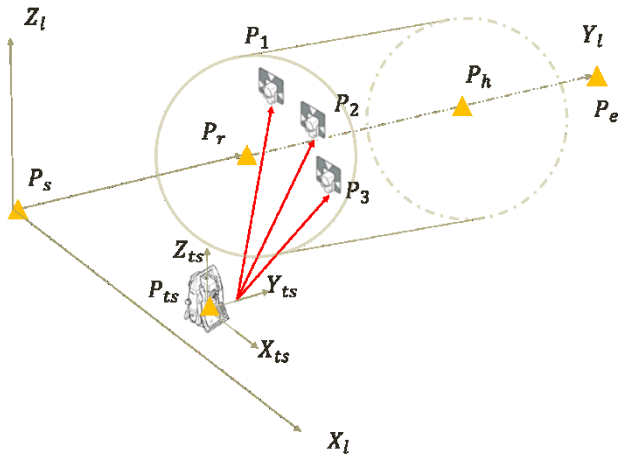

Figure 73. Total station surveys three prisms P_1, P_2, P_3 on the TBM, and calculates rear center P_r and cutter head P_h of TBM.

We assume P_1, P_2, P_3, P_h are the coordinates of the three prisms and the cutter head in the station framework during the registration survey (S. Mao, Shen, and Lu 2014; Shen, Lu, and Chen 2011), and that Q_1, Q_2, Q_3, Q_h are the corresponding points in the station framework in any survey during construction. The three-point algorithm first builds two temporary coordinate systems (referred to as a three-point framework), $P_2 - X_pY_pZ_p$ and $Q_2 - X_qY_qZ_q$: (Shen, Lu, and Chen 2011)

$$\begin{cases} X_p \leftarrow Normalize(P_1 - P_2) \\ y \leftarrow Normalize(P_3 - P_2) \\ Z_p \leftarrow X_p \times y \\ Y_p \leftarrow Z_p \times X_p \end{cases} \qquad \begin{cases} X_q \leftarrow Normalize(Q_1 - Q_2) \\ y \leftarrow Normalize(Q_3 - Q_2) \\ Z_q \leftarrow X_q \times y \\ Y_q \leftarrow Z_q \times X_q \end{cases} \tag{27}$$

The two coordinate systems are the same coordinate system, only with different reference bases (For example, a point can be expressed in both Cartesian (x, y, z) and polar (d, θ, ϕ) coordinate systems; it is the same point, but the coordinate expression is different). Equation (27) only preserves the relative positions between all points. In construction, the total station surveys Q_1, Q_2, Q_3 and then calculates Q_h by using (26): (Shen, Lu, and Chen 2011)

$$\begin{cases} m_p \leftarrow \begin{bmatrix} X_p^T \\ Y_p^T \\ Z_p^T \end{bmatrix} \\ m_q \leftarrow \begin{bmatrix} X_q^T \\ Y_q^T \\ Z_q^T \end{bmatrix} \\ Q_h \leftarrow m_q^{-1} \cdot m_p \cdot (P_h - P_2) + Q_2 \end{cases} \tag{28}$$

Equation (28) can be briefly illustrated as follows: because $P_2 - X_p Y_p Z_p$ and $Q_2 - X_q Y_q Z_q$ are the same coordinate system, we first calculate the coordinate of the cutter head in $P_2 - X_p Y_p Z_p$ by $R_h = m_p \cdot (P_h - P_2)$; then, after movement of the TBM, we calculate the cutter head's coordinate in the station by transforming it back to the station framework $m_q^{-1} R_h + Q_2$.

If there is no error, the calculation will be perfect and actual and calculated Q_h will be the same. However, errors in total station survey (angle error 1"~3", distance measurement error $1mm + 1ppm$ (Leica Geosystem AG 2010a)) can cause the calculation to be inexact. By applying the error propagation model in equation (21), we can analyze the error in the calculation of cutter-head position:

$$
\begin{cases}
Q_h = m_q^{-1} \cdot m_p \cdot (P_h - P_2) + Q_2 \\
K = dQ_h|_{P_{1x},P_{1y},P_{1z},P_{2x},P_{2y},P_{2z},P_{3x},P_{3y},P_{3z},P_{hx},P_{hy},P_{hz},Q_{1x},Q_{1y},Q_{1z},Q_{2x},Q_{2y},Q_{2z},Q_{3x},Q_{3y},Q_{3z}} \\
\quad = \begin{bmatrix} (\frac{dQ_{hx}}{dP_{1x}})_0 & \cdots & (\frac{dQ_{hx}}{dQ_{3x}})_0 \\ (\frac{dQ_{hy}}{dP_{1x}})_0 & \cdots & (\frac{dQ_{hy})}{dQ_{3x}})_0 \\ (\frac{dQ_{hz}}{dP_{1x}})_0 & \cdots & (\frac{dQ_{hz})}{dQ_{3x}})_0 \end{bmatrix} \\
\sigma_{Q_hQ_h} = \begin{bmatrix} W_{P_{1x}P_{1x}} & & \\ & \cdots & \\ & & W_{Q_{3z}Q_{3z}} \end{bmatrix} \\
\sigma_{Q_hQ_h} = K \cdot C_{Q_hQ_h} \cdot K^T
\end{cases}
\tag{29}
$$

In equation (29), K is the linearized coefficient matrix, and its dimensions are 3×21. In addition, symbol P_{1x} represents the x value of point P_1, and symbol $W_{P_{1x}P_{1x}}$ represents the variance of x value of point P_1. Assume we have a TBM and four prisms in the registration survey, and the coordinates for each point are as shown in Table 7. Because equation (27) does not preserve station framework-related information, and all error information is expressed in matrix $\sigma_{Q_hQ_h}$, we can simply assume the points are the same. Point P_2 is $1.5m$ deeper in the operator's chamber, and is always mounted on the back target board. With this established, all variances must then be determined. Utilizing a total station with an angle error of 1"and a distance measurement error of $1mm + 1ppm$ (Leica Geosystem AG 2010a), we can apply the same error propagation model to obtain the accuracy of single-point measurement. Both the horizontal and vertical angles are always small because of the constraints imposed by the survey window. In equation (30), v, h, d refer to the vertical angle, horizontal angle, and slope distance that are measured by the total station when it surveys the prisms. Angle measurements v, h have standard deviations of 1", and slope distance has a standard deviation of $1mm + 1ppm$. In addition, v *and* h are set to be 0°, as the total station always flatly surveys the targets, which are close to each other in a

small area (constrained by the survey window); d is set to be $180m$, as the maximum distance of VLTB.

$$\begin{cases} p = \begin{bmatrix} x \\ y \\ z \end{bmatrix} = \begin{bmatrix} \cos v \cdot \cos h \cdot d \\ \cos v \cdot \sin h \cdot d \\ \sin v \cdot d \end{bmatrix} \\ K = dp|_{v,h,d} \\ \sigma_{vhd} = \begin{bmatrix} \sigma_{vv} & & \\ & \sigma_{hh} & \\ & & \sigma_{dd} \end{bmatrix} \\ \sigma_{pp} = K \cdot C_{vhd} \cdot K^T \end{cases} \tag{30}$$

Over $180m$ of the survey distance, the standard deviations of the x, y, z values of a prism are $(0.0012m, 0.0009m, 0.0009m)$. Furthermore, the automatic aiming system of the total station has a $1mm$ aiming error in the three directions of XYZ, which can be equally distributed to each direction as $(\frac{\sqrt{3}}{3}m, \frac{\sqrt{3}}{3}m, \frac{\sqrt{3}}{3}m)$ variance; therefore, the final accuracy of the automatic prism survey over $180m$ is $(0.0018m, 0.0015m, 0.0015m)$. We set this variance for all $Q_1 \sim Q_3$ points. In comparison, all $P_1 \sim P_h$ points are measured during the registration survey where, over a short distance and without automatic aiming, the variance is only $(0.001m, 0m, 0m)$.

Table 7. The error information is expressed in matrix $\sigma_{Q_hQ_h}$. We can assume $Q_1 \sim Q_3$ are translated and rotated to the same place. Because there is no error in K matrix, this step is valid.

	X	Y	Z		X	Y	Z
P_1	0.2	0	2.2	Q_1	0.2	0	2.2
P_2	0.5	1.5	1.95	Q_2	0.5	1.5	1.95
P_3	0.8	0	1.8	Q_3	0.8	0	1.8
P_h	0	4.5	0				

We can now calculate the accuracy of the three-point algorithm over a $180m$ survey distance. The result is $(0.00957699, 0.00298439, 0.00801554)$, or

simply $E_{tpp} = (0.010m, 0.003m, 0.008m)$. According to construction standards (The City of Edmonton 2012), the limit for horizontal deviation is $150mm$, and the limit for vertical deviation is $89mm$. Thus, the results indicate that the three-point algorithm is accurate enough for the task.

The error of the three-point algorithm E_{tpp} is the error within the station framework. However, the station framework itself deviates from the alignment to some degree (see section 5.4) because the total station suffers from orientation error and position error. Thanks to the station framework and the three-point framework, we can handle the three-point algorithm's error E_{tpp} and the three-point framework's error E_{tpf} separately. Once again, we apply the error propagation model for point Q_2, which is the origin of the three-point framework, however this time we only apply the orientation error E_α and the total station position error E_{ts}.

$$\begin{cases} p = \begin{bmatrix} x \\ y \\ z \end{bmatrix} = \begin{bmatrix} \cos v \cdot \cos h \cdot d + X_{ts} \\ \cos v \cdot \sin h \cdot d + Y_{ts} \\ \sin v \cdot d + Z_{ts} \end{bmatrix} \\ K = dp|_{X_{ts}, Y_{ts}, Z_{ts}, h} \\ \sigma_{xyzh} = \begin{bmatrix} \sigma_{xx} & & & \\ & \sigma_{yy} & & \\ & & \sigma_{zz} & \\ & & & \sigma_{\alpha\alpha} \end{bmatrix} \\ \sigma_{pp} = K \cdot C_{xyzh} \cdot K^T \end{cases} \tag{31}$$

In equation (31), X_{ts}, Y_{ts}, Z_{ts} are the coordinates of total station in the alignment coordinate system, and h is the horizontal angle of the prism P_2. All other parameters are the same as equation (30), only this time the total station's errors will be considered. However, the solution of equation (31) depends on the resection errors, which are affected by relocations. This will be discussed later in section 5.7.

5.5.2 Guidance Errors in Laser-based Systems

The biggest problem for both conventional and smart laser systems is the precise pose measurement. As shown in Figure 74, the laser assumes that the rear ring has a perfectly as-designed pose, without any yaw/pitch/roll in the tunnel alignment coordinate system. However, the actual TBM may have a different pose, and the as-designed and as-built rear rings may intersect at the prism.

Assume α, β, γ are the yaw/pitch/roll angles of the TBM's pose, $V_{prism} = [\Delta X, \Delta Y, \Delta Z]$ is the prism's as-design offset from the center of the rear ring on the X, Y, Z axes, V'_{prism} is the as-built offset in the alignment coordinate system, and D is the error of the position of the center of the rear ring.

$$R = \begin{pmatrix} \cos(\gamma) & 0 & \sin(\gamma) \\ 0 & 1 & 0 \\ -\sin(\gamma) & 0 & \cos(\gamma) \end{pmatrix} \cdot \begin{pmatrix} 1 & 0 & 0 \\ 0 & \cos(\beta) & -\sin(\beta) \\ 0 & \sin(\beta) & \cos(\beta) \end{pmatrix} \cdot \begin{pmatrix} \cos(\alpha) & -\sin(\alpha) & 0 \\ \sin(\alpha) & \cos(\alpha) & 0 \\ 0 & 0 & 1 \end{pmatrix}$$

$$V_{prism} = \begin{bmatrix} \Delta X \\ \Delta Y \\ \Delta Z \end{bmatrix}$$

$$V'_{prism} = R \cdot V_{prism}$$

$$D = V'_{prism} - V_{prism}$$

(32)

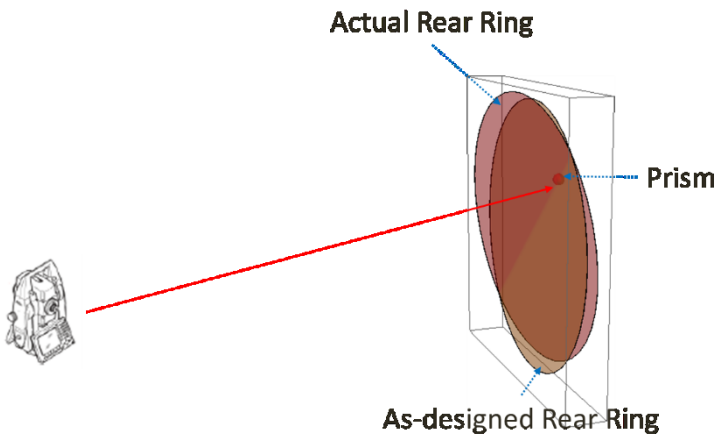

Figure 74. Pose error

Assume the yaw and pitch angles are both 1°, which equals a length of $\tan(1°) \times 1m = 17.5mm$ on the target board. The operator can always maintain deviations within this level, and therefore this assumption is rational. Then, assume that the offsets of the prisms in two different TBMs are $V_1 = [1m, 1m, 1m]$ and $V_2[1m, 0m, 1m]$. With this established, equation (32) can be applied to compute the pose error for these two TBMs:

$$\begin{cases} R = \begin{pmatrix} 0.999848 & -0.0174524 & 0. \\ 0.0174497 & 0.999695 & 0.0174524 \\ -0.000304586 & -0.0174497 & 0.999848 \end{pmatrix} \\ V_1' = R \cdot \begin{bmatrix} 1m \\ 1m \\ 1m \end{bmatrix} = \begin{bmatrix} -17.6mm \\ 34.6mm \\ -17.9mm \end{bmatrix} \\ V_2' = R \cdot \begin{bmatrix} 1m \\ 0m \\ 1m \end{bmatrix} = \begin{bmatrix} -0.152mm \\ 34.9mm \\ -0.457mm \end{bmatrix} \end{cases} \tag{33}$$

As shown in equation (33), the pose errors are very different. The error on the Y axis is spread along the alignment, and does not affect the steering. Moreover, errors the on the X, Z axes represent errors in line and grade deviations separately, and these two are most important. As we can see, the X, Y errors of V_2' are negligible, and the reason for that is that in TBM 2, the prism is mounted on the rear ring. The prism should be close to the center of the rear ring on the Y axis to reduce the harm caused by pose error.

5.6 Errors from Concrete Liners' Deformations

Tunnels all suffers different levels of deformation, due to changes in geotechnical conditions which put pressure on the hydraulic pushing system of TBM (V. A. Kontogianni and Stiros 2005). However, the concrete liners that the total station and reference prisms are mounted to should experience as little

displacement as possible. Conventional laser always rely on three strings of plummets ahead of them, but these plummets are closer to the TBM and have a larger chance of being affected by deformation. The laser itself will be placed as close as possible to the rear of gantry in order to increase the relocation distance. Therefore, all parts of the reference network in a conventional laser are affected by deformation (V. A. Kontogianni and Stiros 2005), yet, sadly, the deformation cannot be detected and amended without initiating a productivity-killing full survey. Modern lasers provide back sight prisms (tacs GmbH 2004; VMT GmbH 2003), but they either set up one prism as a back sight—which has a weak resistance to deformation error—or they set up the prism based on the surveyors' experience.

Deformation in tunnels is a very complex problem. There are methods for setting up control points to observe deformation and to calculate a time-dependent deformation ratio (V. Kontogianni, Psimoulis, and Stiros 2006) or to calculate the mean tensor of deformation based on all geodetic measurement (S. Stiros and Kontogianni 2009), and these methods can provide a tool that can be used to update the deformation model. In this paper, we get deformation data from the research done by Kontogianni and Stiros, and express the deformation as standard deviations of the positions of the total station and prisms. After this has been done, the design algorithm will update the reference network according to the adjustments.

In this section, we first assume that the deformation consists of time-dependent and excavation-dependent parts. All prisms and total stations experience time-dependent deformation D_t, which spreads on both the horizontal and vertical axes. Time-dependent deformation D_t starts from the day the section is built and stops after time T_{stable}, during which the standard deviation increases

from zero to $E_t^{\max}$. The equation for time-dependent deformation is: (V. Kontogianni, Psimoulis, and Stiros 2006)

$$D_t = E_t^{max} \cdot (1 - e^{\frac{-t}{T}}) \tag{34}$$

In equation (34), t represents the number of days since the section was built, and T is an adjustable parameter that enables design engineers to determine the stable time T_{stable}. When a tunnel section is built on day t_1 and a prism is mounted on day t_2 and on any day $t_3$after being mounted, the time-dependent deformation error is:

$$E_t = E_t^{max} \cdot (1 - e^{\frac{-(t3-t1)}{T}}) - E_t^{max} \cdot (1 - e^{\frac{-(t2-t1)}{T}}) \tag{35}$$

Similarly, the excavation-dependent error is a function of the distance between the section and the cutting face. If we define the distance x, and the maximum excavation-dependent error $E_{ex}^{\max}$, then the deformation can be expressed as: (V. Kontogianni, Psimoulis, and Stiros 2006)

$$D_{ex} = E_{ex}^{max} \cdot [1 - (\frac{X}{x + X})^2] \tag{36}$$

Equation (36) only connects the distance between the equipment and the cutting face, and in this section, we assume this deformation convergent to stable after the TBM departs. Similar to equation (35), when the prism is mounted x_1 meters away from cutter head, and when the TBM advances, increasing the distance to x_2, the excavation-dependent deformation is:

$$E_{ex} = E_{ex}^{max} \cdot [1 - (\frac{X}{x_2 + X})^2] - E_{ex}^{max} \cdot [1 - (\frac{X}{x_1 + X})^2] \tag{37}$$

Both equation (35) and (37) shows a simple fact: if the prism or any other equipment is mounted after stabilization, the standard deviation associated with the position is small.

The deformation in this section can be visually and conceptually described as shown in Figure 75, which shows that the two different deformations originate from two different sources: soil and TBM thrust.

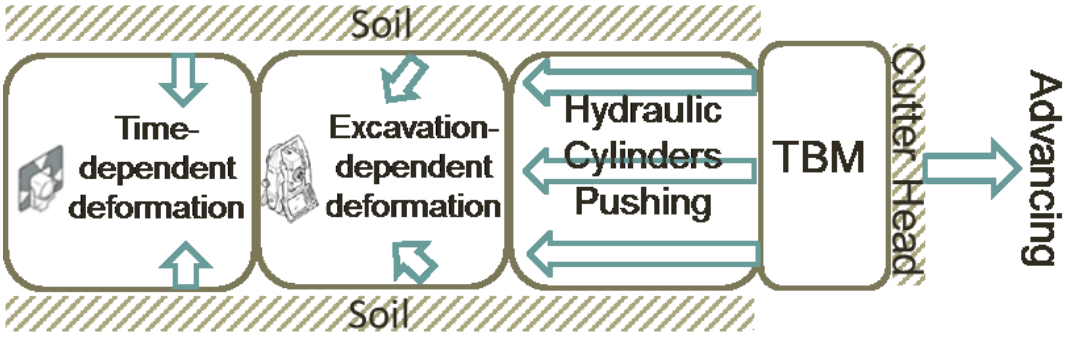

Figure 75. Time-dependent and excavation-dependent deformation

These two deformations will both be measured or estimated as two functions: the deformations increase quickly at the beginning, and the final deformations will stabilize around another value at some point. The two functions can also be visualized as Figure 76.

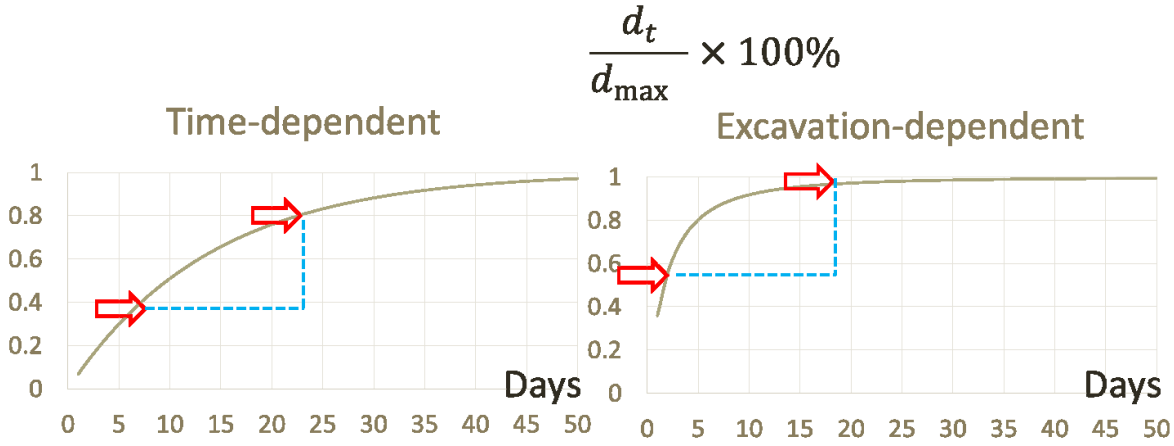

Figure 76. Two examples of deformation functions

5.7 REDUNDANT PRISM SETUP

5.7.1 General

When the total station is about to be relocated, surveyors will first set up a bracket near the rear of the gantry and then place a reference prism on it. This is the initial position of the next total station. The current total station will survey the prism and record an initial position. The total station and the prism will then be taken from the tribraches, which are mounted to brackets on the concrete liners. After this exchange, the total station will set up at a new position, while the prism remains at the previous position. A tribrach can ensure that the attached equipment will have the same coordinate (Leica Geosystem AG 2010b). A proper process can be described as following: the current total station at position P_{ts}^{i} will first survey a prism P_{ts}^{i+1} and is very close to the back of the gantry. The positions of the current total station and the prism will then be exchanged, leaving the tribraches on the mounting bracket (Leica Geosystem AG 2010b). Now, the current total station is at position P_{ts}^{i+1} and a back sight prism is at P_{ts}^{i} (referred as P_{0}^{i+1}). Once the total station is in the new position, the algorithm starts to compute the optimum location for prism P_{1}^{i+1} based on two existing prisms P_{0}^{i+1} and P_{1}^{i}.

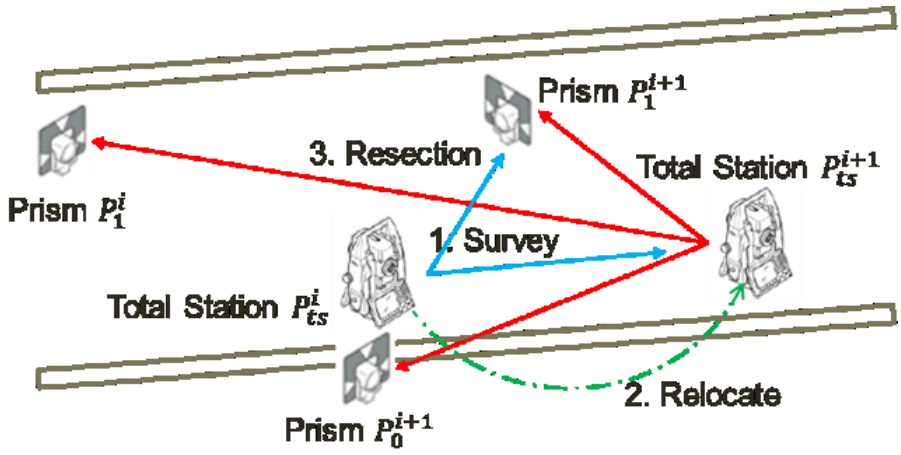

Figure 77. Total station relocation

The primary prism is the one on the previous total station's bracket, but it is common for surveyors to slightly adjust total station to avoid obstacles; thus, surveyors still need another prism for resection (at least two). The second prism is set up after the current total station has surveyed the next position but before relocation. The prism is supposed to be mounted on the concrete liner, thus its x, y, z values cannot freely change. A better way to address this location constraint is to utilize the polar framework shown in Figure 78. The first parameter of the prism's coordinate is the chainage distance, which indicates where the section prism will be set up. The second parameter is the rotation angle θ in the $O - XZ$ plane, and it is convenient to restrain θ based on the layout of the tunnel (ventilation, etc.). The third parameter is the prism's distance to the center L_r. In reality, the length of the mounting bolt, which firmly holds the prism, changes very little compared to the diameter $2r$. Therefore, we treat $L_r = r - L_b$ as a constant in the design. In summary, the mathematical mapping between the polar coordinate and the Cartesian coordinate of the prism can be expressed as:

$$f_{prism} : (D_c, \theta) \rightarrow (\sin\theta \cdot L_r, D_c, \cos\theta \cdot L_r) \tag{38}$$

The polar coordinate of the prism can easily express the geometric constraint; for example, in the right image of Figure 78, the ideal range of angle θ should be (θ_l, θ_u). The upper limit θ_u is placed by the ventilation pipe, and the lower limit is to make sure the redundant prism is not too close to the primary prism. In a typical $2.4m$ diameter tunnel, the $(\theta_l, \theta_u) = (\sin^{-1}\frac{0.8}{1.2}, \pi - \sin^{-1}\frac{0.8}{1.2})$.

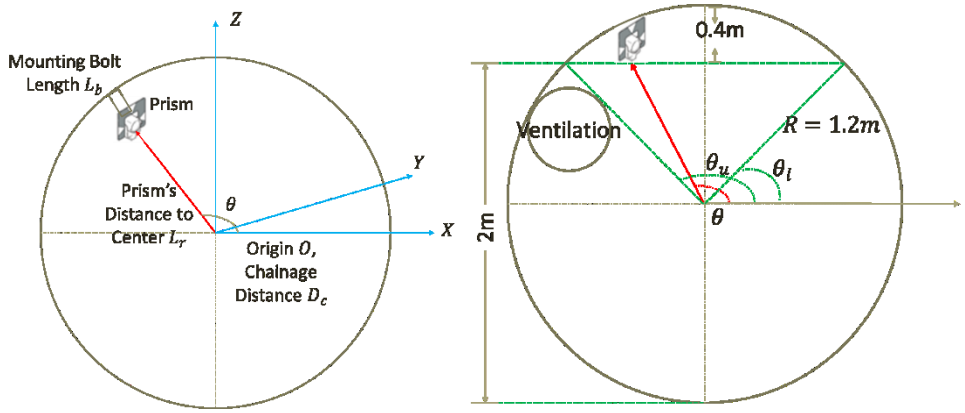

Figure 78. Redundant prism and its coordinate expressed in polar coordinate system.

After relocation, the total station will continuously survey the three prisms, and perform resection before guiding the TBM. The reason for this is that the total station is closest to the cutter head in the reference network. Besides the primary and redundant prisms, the redundant prism of the previous total station location is also utilized. The previous redundant prism is geometrically far away from the cutter head, and is only affected by time-dependent deformation. The primary and previous redundant prisms are well located, and the optimization algorithm is designed to find the optimum position for the current redundant prism, namely, a good (D_c, θ) pair.

5.7.2 Adjustment

The optimization method is entirely built upon the "adjustment" in the survey discipline. The idea for adjustment is simple: if we have multiple

observations, and each observation is naturally inaccurate at a certain level, how can we know the optimum result that is statistically close to the "true value". This technique was created by Gauss two hundred years ago, and has since been further developed by researchers from many fields.

Take a simple adjustment task as example: measuring three angles of a triangle. There are three conditions in the model, namely, the three angles. However, elementary trigonometry tells us that the sum of the three angles will be 180°. Thus, we only need to measure two angles, and the third can be calculated as $\phi_1 = 180° - \phi_2 - \phi_3$. Considering there are errors in both ϕ_2 and ϕ_3, and in this case we can still calculate ϕ_1, but ϕ_1 will contain errors. Luckily, ϕ_1 is deduced in other ways, and we can get a set of equations:

$$\begin{aligned} \phi_1 &= 180° - \phi_2 - \phi_3 \\ \phi_1 &= \alpha \end{aligned} \tag{39}$$

In equation (39), we have more information (three angles) than we need (two), and in solving equation (39) we can have a better estimation of all three angles ϕ_1, ϕ_2, ϕ_3. This is called adjustment. In equation (39), we call ϕ_2, ϕ_3 observations, because we observe them in direct measurement; as for ϕ_1, it is deduced through some method, and we call it parameter.

The basic idea of adjustment is to establish an equation system that takes in all observations made by the survey and all parameters that are utilized to simply the problem, and uses them to determine the statistical nature of all observations and parameters, and to eventually produce an optimum estimation for all observations and parameters.

For a complex model with both observations and parameters (Tao et al. 2003):

$$A\bar{L} + B\bar{X} + U = 0 \tag{40}$$

In equation (40), we have two model matrices A and B, they are coefficient matrices for observations and parameters separately. Both $\bar{L}$ and $\bar{X}$ are the true values of the observations and parameters, which means that they are exact numbers, and thus they exactly satisfy the mathematical relationship as in equation (40). (Tao et al. 2003)

$$\begin{aligned} L &= \bar{L} + v \\ X &= \bar{X} + x \\ Av + Bx + (A\bar{L} + B\bar{X} + U) &= 0 \\ W &= (A\bar{L} + B\bar{X} + U) \\ Av + Bx + W &= 0 \end{aligned} \tag{41}$$

However, in reality, both observation *L* and parameters *X* are measured or calculated with errors, and this is determined by the inaccuracy of the survey equipment. The corresponding errors are v and x for *L* and X. The exact mathematical relationship equation (40) can no long hold, and the model must be updated to take the errors into consideration. Therefore, the model is updated to equation (41).

Equation (41) is complicated but well studied, and we will not elaborate on it in this thesis. The solution for this equation can be found in equation (42) (Tao et al. 2003):

$$\begin{aligned} N_{aa} &= AQ_{LL}A^T \\ N_{bb} &= B^T N_{aa}^{-1} B \\ x &= -N_{bb}^{-1} B^T N_{aa}^{-1} W \\ v &= -Q_{LL}A^T N_{aa}^{-1}(Bx + W) \end{aligned} \tag{42}$$

The two vectors *x* and *v* are the corrections to the parameters and observations. Normally, some or all of the elements in the survey model will improve in accuracy during the adjustment because the combination of information can help refine the variance of the errors. Another important product of adjustment is the variance-covariance matrices of the parameters and

observations after adjustment. In this paper, these matrices will help in designing the optimum locations of the reference network. (Tao et al. 2003):

$$Q_{\hat{X}\hat{X}} = N_{bb}^{-1} \tag{43}$$

5.7.3 Optimization

Optimization for the reference network is built upon the adjustment. The first step in optimizing the reference network is to establish the adjustment equation system for all total stations and prisms. The values in this adjustment equation system are assumed, as it is in the design phase and no real tunnel has been built; however, the equation system itself is the target of optimization.

Let us assume that the current total station has its initial position at $P = (x, y, z)$, and the orientation error and position errors are $\sigma_\alpha, \sigma_x, \sigma_y, \sigma_z$; let us further assume that there are three prisms $P_1 = (x_1, y_1, z_1), P_2 = (x_2, y_2, z_2), P_3 = (x_3, y_3, z_3)$, and the corresponding position errors are $\sigma_{x1}, \sigma_{y1}, \sigma_{z1}, \sigma_{x2}, \sigma_{y2}, \sigma_{z2}, \sigma_{x3}, \sigma_{y3}, \sigma_{z3}$. P_3 is the to-be-established redundant prism, and its polar coordinate is $(cos\theta, y3, sin\theta)$. Moreover, the prisms are affected by time-dependent and excavation-dependent deformations; here we use $\sigma_{d1}, \sigma_{d2}, \sigma_{d3}$ as the notion for three prisms. Given this, the resection model can be expressed as:

$$f = \begin{bmatrix} f_1 \\ f_2 \\ f_3 \\ f_4 \\ f_5 \\ f_6 \\ f_7 \\ f_8 \\ f_9 \end{bmatrix} = \begin{bmatrix} \cos v_1 \cdot \cos(\alpha + h_1) \cdot d_1 + x - x_1 \\ \cos v_1 \cdot \sin(\alpha + h_1) \cdot d_1 + y - y_1 \\ \sin v_1 \cdot d_1 + z - z_1 \\ \cos v_2 \cdot \cos(\alpha + h_2) \cdot d_2 + x - x_2 \\ \cos v_2 \cdot \sin(\alpha + h_2) \cdot d_2 + y - y_2 \\ \sin v_2 \cdot d_2 + z - z_2 \\ \cos v_3 \cdot \cos(\alpha + h_3) \cdot d_3 + x - x_3 \\ \cos v_3 \cdot \sin(\alpha + h_3) \cdot d_1 + y - y_3 \\ \sin v_3 \cdot d_3 + z - z_3 \end{bmatrix} = \begin{bmatrix} 0 \\ \vdots \\ 0 \end{bmatrix} \tag{44}$$

We then apply linearization to equation (44) and establish a model of adjustment with conditions and parameters:(Tao et al. 2003)

$$\begin{aligned} A &= df|_{h_1,h_2,h_3,v_1,v_2,v_3,d_1,d_2,d_3,x_1,y_1,z_1,x_2,y_2,z_2,x_3,y_3,z_3} \\ B &= df|_{x,y,z,\alpha} \\ Av + Bx + f^0 &= 0 \end{aligned} \tag{45}$$

Equation (45) has the same form as equation (41). Thus, we can apply D-optimality to equation (45), to calculate the optimum location for P_3. One important note for equation (45) is that in real practice the prism at (x_3, y_3, z_3) is surveyed by the total station at (x_2, y_2, z_2); therefore, we can express the prism's location as $(x_3, y_3, z_3) = (x_2 + \Delta x_3, y_2 + \Delta y_3, z_2 + \Delta z_3)$, and equation (45) will be reformed as:

$$\begin{aligned} A &= df|_{h_1,h_2,h_3,v_1,v_2,v_3,d_1,d_2,d_3,x_1,y_1,z_1,x_2,y_2,z_2,\Delta x_3,\Delta y_3,\Delta z_3} \\ B &= df|_{x,y,z,\alpha} \\ Av + Bx + f^0 &= 0 \end{aligned} \tag{46}$$

The reason to deduct equation (46) is that $\Delta x_3, \Delta y_3, \Delta z_3$ are only affected by the total stations' orientation error and angle measurement accuracy, and is always much more accurate. Equation (46) reveals the internal dependency among the parameters in equation (45), and if we utilize equation (46) instead of equation (45) in D-Optimization, the optimized results will be more accurate. After adjustment, we can update the variance matrix of $\Delta x_3, \Delta y_3, \Delta z_3$, and then update the variance of x_3, y_3, z_3, which will be P_1 in the next relocation iteration. The updated matrix can be described as: (Tao et al. 2003)

$$\begin{cases} N_{aa} = A \cdot Q_{LL} \cdot A^T \\ N_{bb} = B^T \cdot N_{aa}^{-1} \cdot B \\ Q_{KK} = N_{aa}^{-1} - N_{aa}^{-1} \cdot B \cdot N_{bb}^{-1} \cdot B^T \cdot N_{aa}^{-1} \\ Q_{VV} = Q_{LL} \cdot A^T \cdot Q_{KK} \cdot A \cdot Q_{LL} \\ Q_{\hat{L}\hat{L}} = Q_{LL} - Q_{VV} \end{cases} \tag{47}$$

In the equation (47), Q_{LL} is the variance matrix of the observations, Q_{VV} is the variance matrix of the correction number, and $Q_{\hat{L}\hat{L}}$ is the updated variance matrix of the observations. The variance matrix of $\Delta x_3, \Delta y_3, \Delta z_3$ is a submatrix

of $Q_{\hat{L}\hat{L}}$, with the row and column ranges as 16~18. Later, the variance matrix of x_3, y_3, z_3 is:

$$Q_{X_3,Y_3,Z_3} = Q_{\Delta X,\Delta Y,\Delta Z} + Q_{X_2,Y_2,Z_2} \tag{48}$$

5.8 RELOCATION INTERVALS AND FULL SURVEY

5.8.1 Curvature Constraint

The most widely applied method for tunnel surveying is laser-based, with either the use of conventional lasers or one of the many varieties of improved models. However, visibility is the most vital limitation of the laser. As shown in Figure 79, the gantry system (including transforms, ventilation pipes, hoses of hydraulic system, etc.) and muck cars establish boundaries for the mounting zone for the laser equipment. In small-diameter tunnels, this is the only viable visible window to let a laser pass through. The survey window is a fan-shaped tube with a radius of about $37cm$, and the distance between each prism of VLTB system should be smaller than survey window. A practical size that the distance between each prism is no more than $25cm$ (leave some contingence space). Therefore, the total station cannot be more than 180m away from the prism, otherwise total station cannot distinguish two adjacent prisms.

Figure 79. Extreme Narrow Visible Window for Laser-based Guidance System.

Figure 80. Survey window size

However, even this narrow zone can be always guaranteed. The tunnel-boring machine is driven by hydraulic cylinders that push back upon as-built liners, and due to geotechnical conditions and the way the pushing system works, operators cannot accurately steer the machine to a specific location. This results in an as-built tunnel path, which sways horizontally and vertically around a designed alignment. But the gantry consists of multiple sections which are chained together and linked to the tunnel-boring machine. When the chained sections pass through the as-built tunnel, each section will scatter around the as-built alignment either higher/lower, and right/left, as shown in Figure 81. In tunnels with designed curvature, window will be even narrower, as the tunnel liner and gantry will squeeze the visible windows, as shown in Figure 82. Ultimately, the laser will soon fail to project a guidance laser spot for steering purposes.

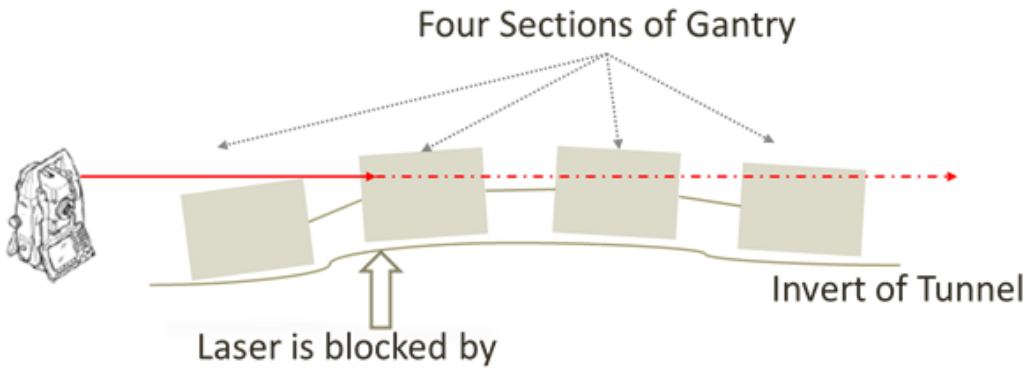

Figure 81 How As-built Vertical Curvature Affects Laser Guidance

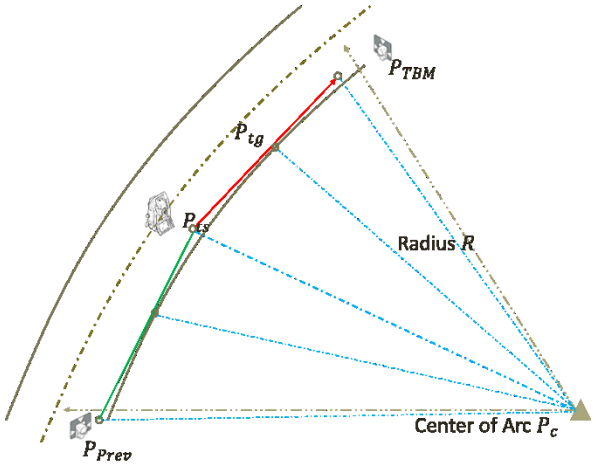

Figure 82 How As-designed Curvature Affects Laser Guidance

In Figure 82, the total station is within the survey window (as in Figure 80) and can see forward no further than P_{TBM}, and backward no further than P_{prev}. The length of $P_{ts}P_{prev}$ can be easily calculated as:

$$P_{ts}P_{prev} = 2 \cdot R \cdot \tan\left[\cos\left(\frac{R}{P_{ts}P_c}\right)^{-1}\right] \tag{49}$$

Similarly, the distance of $P_{ts}P_{TBM}$ can be computed as:

$$P_{ts}P_{TBM} = R \cdot \tan\left[\cos\left(\frac{R}{P_{ts}P_c}\right)^{-1}\right] + R \cdot \tan\left[\cos\left(\frac{R}{P_{TBM}P_c}\right)^{-1}\right] \tag{50}$$

Based on the discussion in the previous sections, we can conclude that the relocation interval of the total station is a trade-off between visibility, search window, and accumulated errors. We can streamline the whole design process in the manner outlined in diagram in Figure 83. In the beginning, surveyors set up the first two prisms and total station in the tunnel. These pieces of equipment have very small variance on their positions because they are close to the shaft, and they are mounted to the wood structure of the hand-digging tunnel sections (normally the tunnel crew first construct hand-digging sections, which are long enough to assemble the TBM and gantry system). Later, the TBM is assembled and advances to the maximum interval, whereupon the surveyors need to survey the new total station's position and set up the redundant prism. This process is repeated until the whole tunnel is completed.

Although the majority of the design is determined by the algorithm, there are still two critical decisions that surveyors must make. First, surveyors need to determine the confidence interval. For example, if the vertical deviation limit is 89mm, the allowed vertical deviation is within $(-89mm, +89mm)$. If the certainty level is 95% and TBM must not exceed the tolerance, then the boundary for guidance deviation should be $(-89mm, +89mm) = (-2\sigma, 2\sigma)$ and $\sigma = 45mm$; or if the certainty level is 99.7%, then deviation boundary is $(-89mm, +89mm) = (-3\sigma, 3\sigma)$ and $\sigma = 30mm$. The second decision that surveyors must make is when to introduce a full survey. A full survey is a time consuming process, and is traditionally decided based solely on the surveyors' expertise and experience during construction. With the design algorithm, surveyors can easily decide whether to introduce a necessary full survey based on these calculated stochastic properties. The full survey will reduce the orientation error, which is the major factor in the horizontal coordinate error; moreover, the full survey will decrease

the time-dependent and excavation-dependent deformations, as shown in equation (35) and (37).

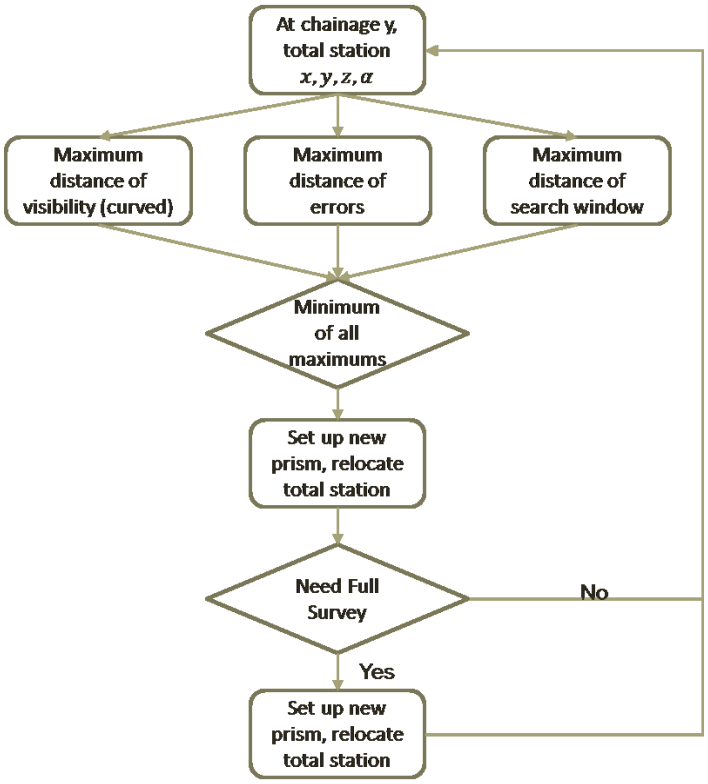

Figure 83. Diagram of the reference network design.

A full case study will be discussed to demonstrate how to apply the algorithm in designing reference network for a 1.1km tunnel.

5.9 CASE STUDY

5.9.1 General

In this section, the author presents a case study. The case study shows a simplified tunnel reference network design, and the reader is treated as an engineer who wants to deliver this design. The author will take the reader through the process of designing an optimum tunnel reference network step by step.

In the case study, the algorithm is assigned to design a reference network for a 1.1km straight tunnel. Since a straight tunnel can always be treated as a curved tunnel with an infinite radius, and the diameter is much smaller than the length (diameter roughly equals 0.2% of the length), the algorithm treats the tunnel as a linear problem. In this context, the term "linear" means that the optimization and design are mainly related to the chainage distance at which the reference prisms should be set up. As shown in Figure 84, the position of the prisms in the cross section of the tunnel is referred to as "non-linear" design, and, compared to the chainage distance (along the direction of tunnel alignment), the "non-linear" factors are relatively less important. In a tunnel, operational constraints are the major factors in the "non-linear" design; for example, the left-lower boundary of the prism is the ventilation pipe, and the right-lower boundary is the total station. The position of the prism varies within one meter in the cross section view, which is much smaller than the chainage direction.

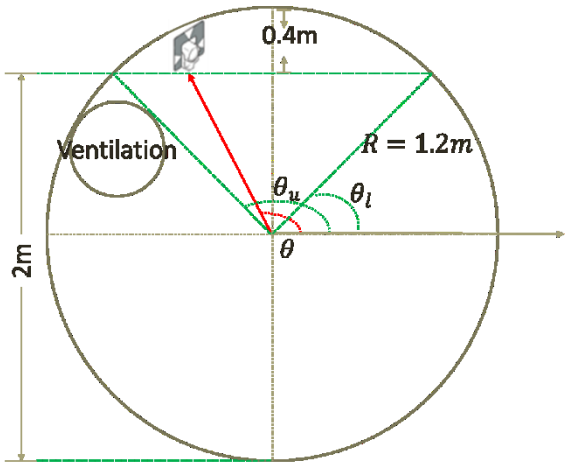

Figure 84. "Non-linear" Design of Reference Network

The diameter of the tunnel is chosen to be 2.4m, which is the same as other normal service tunnels. This optimization method is general and small diameter service tunnels can benefit from it better than larger diameter tunnels.

Service tunnels are built for municipal infrastructures, and they are very sensitive to the cost and time. The small diameter of service tunnels also means that only one crew—either a survey crew or a construction crew—can occupy the space at any given time. The method can greatly ensure the guidance quality without relying too much on the survey crew, and thus will leave more time for the construction crew. The characteristics of the sample tunnel is such that "horizontal deviation must be less than $150mm$ and vertical deviation less than 89mm". This is a common and reasonable standard for 2.4-meter diameter tunnels.

With the maximum deviation determined, it is now necessary to link the deviation and survey error. We choose confidence level of 99.7%, which empowers the operator with accurate measurement and high confidence even in the harshest situations.

By statistical definition, the 99.7% confidence level can be translated as three times the standard deviation of the actual guidance error, and we can therefore know that the standard deviations calculated by the guidance system cannot exceed $50mm$ horizontally and $30mm$ vertically. These two values are the error limit for the design, which means that, if the algorithm detects that the standard deviations exceed these two limits, the algorithm should either:

- Introduce a full survey to reduce the error
- Reduce the relocation interval for decreasing the speed that errors accumulate.

The algorithm will leave this choice to the engineers and experts in the construction field. The algorithm is built to provide the optimum design for the reference network, and the detailed managing decisions should be handled by engineers. As of today, much knowledge relating to design and construction is not

parameterized and cannot be comprehended by the algorithms; thus, algorithms should not take over the responsibility of design.

5.9.2 Details on Parameters

The basic structure of the tunnel and reference network is illustrated in Figure 87. The tunnel as drawn consists of three parts: the shaft on the left, the tunnel liners in the middle, and the TBM machine and gantry system on the right. The three parts are three different environments for the reference network setup:

- Shaft: in the guidance system, the shaft is the only place where the reference network is connected to the ground. On the ground, the reference network is controlled by the GPS and control points that are firmly fixed to the ground. The prisms that are mounted in the shaft sections will be not affected by the deformations of time and TBM movement. There are two reasons for this:
    - As shown in Figure 85, the shaft and its adjacent hand-dug sections are built with wood structures, and the prisms and total stations are mounted on the wood ceilings. There is a clear boundary between the wood structured sections and the concrete sections, as shown in Figure 86. The pushing pressure from the hydraulic cylinders cannot be transferred to the wood parts.

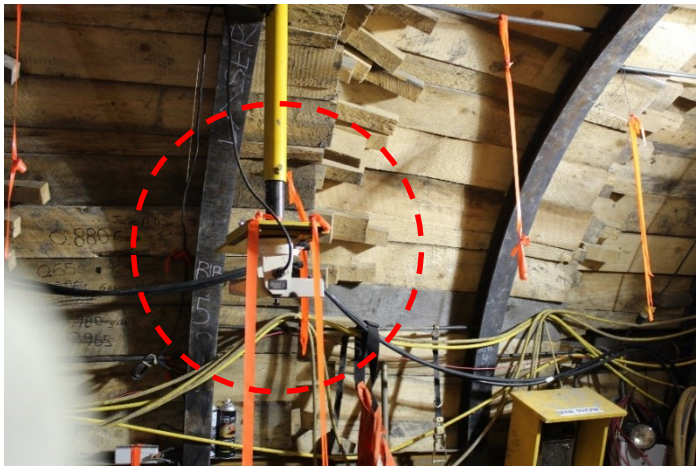

Figure 85. Wood ceiling in the shaft and hand-dug tunnel sections

- The other reason is that the hand-dug tunnel takes a very long time to finish, and, after it is completed, it takes days for the TBM to be assembled in the hand-dug section. The impact from time-dependent deformation fades during this process.

- At the end of shaft and hand-dug sections, it starts the concrete sections. Concrete sections suffer both time-dependent and pushing-dependent deformations.

Figure 86. The start of tunnel sections with concrete liners

- Finally, the third part is the TBM and gantry part. Tunnel sections close to the TBM and gantry are most vulnerable to both time-dependent and pushing-dependent deformations, because these sections have been recently built and are very close to the TBM. To reduce the amount of survey work and to ensure maximum intervals between relocation, the total station needs to be set at the very end of gantry. Thus, the total station is required to continually survey the reference prisms to perform self-locating.

The first prism and total station were set up in the wood area near the shaft. As shown in Figure 87, prism P_1 is the current redundant prism directly set up by surveyors in the initial survey, and P_2 is the first location of the total station. The first prism is set in the tail tunnel, which is very stable for the first prism. Practically, surveyors can put the first prism at any place within the specific ring in the tail tunnel, and it should be both safe and visible for the following operations.

After the TBM advances 160 meters, the distance between current (first) total station's position and the prism(s) reaches the maximum 180 meters. The 20 meters difference is accounted for by the length of the gantry and the TBM. The algorithm then needs to determine the position P_0, which is the next position that the total station should be moved to. To support the total station at P_0, the algorithm must also determine the position P_3 for the next redundant prism. In reality, to reduce the amount of survey work and to ensure a maximum interval between relocation, the position P_0 is chosen at 160 meters ahead of the current total station P_2.

Thus, the first optimization task is for the algorithm to determine the position P_3 for the redundant prism. The engineers can choose a proper height

according to their experience, and, in this case, the prism is set directly in the middle of the tunnel. In addition, because of the mounting pole and size of the prism itself, the center of prism is set at a height of 2.3 meters (as shown in Figure 87). The initial position for P_2 is $(0.8m, -20m, 1.8m)$. This is because, when the TBM starts at the first section the concrete sections, which is regarded as $y = 0\ meter$; the beginning of the gantry is at -20 meters.

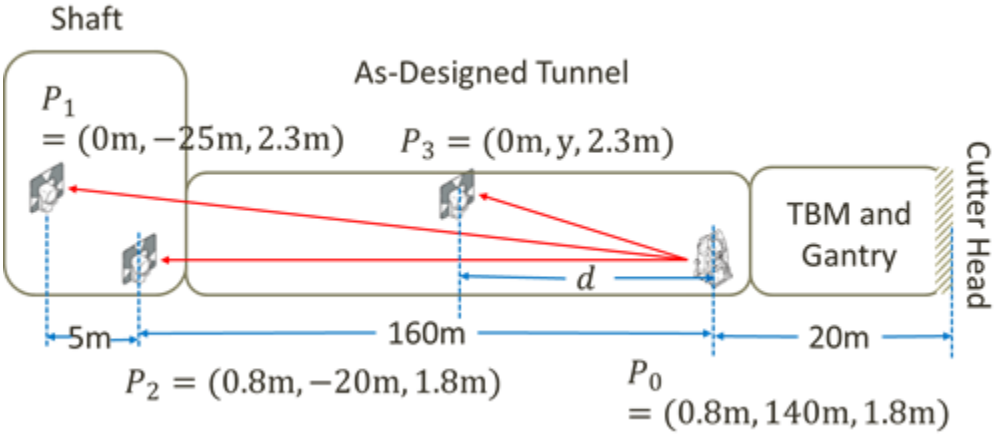

Figure 87. The first relocation.

The reason for fixing the x, z values of P_3 is that the changes of x, z are too small compared to y. If engineers really want to optimize x, z, they can first fix y, and then optimize x, z based on the optimized y. The searching step for the optimum y can be one meter. Since the prism is mounted in the as-built tunnel manually, it is impossible to mount it at an exact point. Therefore, in practice, it is not that useful to optimize x, z, and so this case study only focuses on the chainage distance optimization.

The formal description of the optimization program can be illustrated as follows. There are two pre-set prisms, P_1 and P_2, in the tail tunnel (tunnel sections on the other side of the shaft towards in the opposite direction of alignment) and shaft respectively that are measured and fixed by utilizing

plummets with high accuracy GPS static survey. The position errors for both points are $1mm$ on each axis of X, Y, Z. The point P_2 is the initial position of total station, and the total station guides the TBM between $20m$ to $180m$ (180m is the furthest prism's chainage distance). The total station must then be moved to a new position just besides the gantry at the chainage distance of 140m. Assume we have an expected position P_0, and the optimization algorithm needs to find the optimum position (the optimum chainage distance) of redundant prism P_3, which stays between P_2 and P_0. Then, when the TBM advances another $160m$ ($180m - length\ of\ gantry$), the total station relocates again, and the redundant prism P_3 becomes the new P_1 in the model and the total station itself becomes the new P_2 . The algorithm must iteratively find all optimum locations for the redundant prism for the whole tunnel.

Table 8. Parameters for Design Algorithm

Aiming Error	0.58mm	No Deformation		Small Deformation		Large Deformation	
Distance Error	$1mm + 1ppm$	$\mathrm{E_t^{max}}(x,y)$	$0\ mm$	$\mathrm{E_t^{max}}(x,y)$	$8\ mm$	$\mathrm{E_t^{max}}(x,y)$	$25\ mm$
Angle Error	1"	$\mathrm{E_t^{max}}(z)$	$0\ mm$	$\mathrm{E_t^{max}}(z)$	$3\ mm$	$\mathrm{E_t^{max}}(z)$	$25\ mm$
Daily Advance	$5m$	$\mathrm{E_x^{max}}(x,y)$	$0\ mm$	$\mathrm{E_x^{max}}(x,y)$	$8\ mm$	$\mathrm{E_x^{max}}(x,y)$	$25\ mm$
Interval	$160m$	$\mathrm{E_x^{max}}(z)$	$0\ mm$	$\mathrm{E_x^{max}}(z)$	$3\ mm$	$\mathrm{E_x^{max}}(z)$	$25\ mm$
T	14						
X	4						

The summarized parameters are shown in Table 8. In the design example, the algorithm is tested against three scenarios and is expected to produce three design plans for each scenario. The only differences between the three scenarios are the deformation parameters. The four deformation parameters $E_t^{max}(x,y)$, $E_t^{max}(z)$, $E_x^{max}(x,y)$, and $E_x^{max}(z)$ are defined in previous sections. The core idea is that deformation can be categorized as being either time-dependent or

excavation-dependent. Time-dependent deformation is due to the pressure of the earth on the outside of the tunnel, the weight of which gradually changes the shape of the liners to which the prisms are mounted. The deformation will gradually approach a max value, and the liners deform slower and slower as time passes. We categorize the time-dependent deformation as vertical $E_t^{max}(z)$ and horizontal $E_t^{max}(x, y)$. Excavation-dependent deformation is similar in concept. The TBM pushes the liner to move forward, and this push generates pressure on the liners. The farther away the TBM is from any specific liner ring, the less the pressure will cause deformation in it.

In the "no deformation" scenario, all of the four deformation parameters—including maximum time-dependent horizontal deformation, maximum time-dependent vertical deformation, maximum excavation-dependent horizontal deformation, and maximum excavation-dependent vertical deformation—are all zero. This setup of parameters is identical to the "full survey" traverse, which is done by surveyors in a breakdown of continuous hours, and is reserved for survey practice. During the short time (compared to weeks of construction), it is assumed that there will be no deformation. This setup is what engineers and surveyors already know, and it is a benchmark for the other two setups.

In the "small deformation" scenario, the parameters are 8 mm for horizontal deformation and 3 mm for vertical deformation. The time-dependent and excavation-dependent deformations share the same assumption (V. Kontogianni, Psimoulis, and Stiros 2006). The author try to make a reasonable assumption. The same applies for the large deformation: the parameters are assumed from a comprehension of previous work in the field, and are only supposed to present the impact from the deformation.

The optimization algorithm assumes the following constants: angle measurement is 1"; distance measurement is $1mm + 1ppm$ (ppm means 1 part per million); total aiming error is $1mm$; the time constant of time-dependent deformation is 14 , and the distance constant of excavation-dependent deformation is 4 (these two constants are taken from (V. Kontogianni, Psimoulis, and Stiros 2006)). A quick overview of how these parameters affect the calculation can be found in the following several cases. For example, in the "Small Deformation" setting, the final time-dependent deformation equation on the Z direction can be expressed as:

$$\begin{aligned} E_t &= E_t^{max} \cdot (1 - e^{\frac{-(t3-t1)}{T}}) - E_t^{max} \cdot (1 - e^{\frac{-(t2-t1)}{T}}) \\ &= 3mm \cdot (1 - e^{\frac{-(t3-t1)}{14}}) - 3mm \cdot (1 - e^{\frac{-(t2-t1)}{14}}) \end{aligned} \tag{51}$$

If we assume that the concrete section is installed on day 12 ($t_1 = 12$), the prism is mounted on day 23 ($t_2 = 23$), and the survey is performed on day 33 ($t_3 = 33$), then the time-dependent deformation error on Z direction can be calculated as:

$$E_t = 3mm \cdot (1 - e^{\frac{-(33-12)}{14}}) - 3mm \cdot (1 - e^{\frac{-(23-12)}{14}}) = 0.698mm \tag{52}$$

Deformation equations of excavation-dependent deformation are similar to equations (51) and (52), so the case will not be demonstrated here. For the guidance error, the previous section has already given a thorough calculation example. The second equation in equation system (53) is a complex symbolic calculation, and the expansion of the equation is very long and not helpful in understanding the case. Only the third equation is closely connected to the input parameters.

$$\begin{cases} p = \begin{bmatrix} x \\ y \\ z \end{bmatrix} = \begin{bmatrix} \cos v \cdot \cos h \cdot d \\ \cos v \cdot \sin h \cdot d \\ \sin v \cdot d \end{bmatrix} \\ K = dp|_{v,h,d} \\ \sigma_{vhd} = \begin{bmatrix} \sigma_{vv} & & \\ & \sigma_{hh} & \\ & & \sigma_{dd} \end{bmatrix} \\ \sigma_{pp} = K \cdot C_{vhd} \cdot K^T + \begin{bmatrix} \sigma_{aim} & & \\ & \sigma_{aim} & \\ & & \sigma_{aim} \end{bmatrix} \end{cases} \tag{53}$$

When the survey distance is $180m$, and angle accuracy for both horizontal and vertical angles is 1", and aiming error is $\sqrt{\frac{1}{3}}mm$ on each direction of x, y, z, then the third equation can be expressed as:

$$\begin{aligned} \sigma &= \begin{bmatrix} \sigma_{vv} & & \\ & \sigma_{hh} & \\ & & \sigma_{dd} \end{bmatrix} \\ &= \begin{bmatrix} (1")^2 & & \\ & (1")^2 & \\ & & (1mm + 180m \times 10^{-6})^2 \end{bmatrix} \end{aligned} \tag{54}$$

The calculated result is a matrix, and, in this case, we are most concerned with its diagonal. This calculation is purely symbolic and is provided for the purpose of illustration. Eventually, the square root of the diagonal of σ_{pp} is $(0.0012m, 0.0009m, 0.0009m)$, and they are the errors on the X, Y, Z axes respectively. Furthermore, the automatic aiming system will have an extra $(\sigma_{aim}, \sigma_{aim}, \sigma_{aim}) = (\frac{\sqrt{3}}{3}m, \frac{\sqrt{3}}{3}m, \frac{\sqrt{3}}{3}m)$ on each direction; therefore, the final accuracy of the automatic prism survey over $180m$ is $\sqrt{diagonal(\sigma_{pp})} + (\sigma_{aim}, \sigma_{aim}, \sigma_{aim}) = (0.0018m, 0.0015m, 0.0015m)$.

5.9.3 Process in Detail

To fully illustrate the calculation process of the algorithm, a short example will be applied to the "minor deformation" tunnel, which will be used to help in designing a proper reference network. At the beginning, as shown in Figure 88, the total station is placed at chainage -20 meters inside the shaft, and its corresponding redundant prism is set at chainage -25 meters in the tail tunnel. These two chainage distances are selected based on the design of the tunnel, but the engineers and surveyors are free to change the initial positions and replace them with a more suitable set of values. Indeed, the X coordinate of 0.8 $meters$ is also an estimation by the author, and is based on his survey experience in the tunnel. The selection of height (Z coordinates) can be found in Figure 78. Simply put, the engineers and surveyors are entitled to change all these initial parameters, and, as a general design algorithm, the results will reflect the change of these values.

$$P_1 = \begin{bmatrix} 0 \\ -25 \\ 2.3 \end{bmatrix} P_2 = \begin{bmatrix} 0.8 \\ -20 \\ 1.8 \end{bmatrix} P_0 = \begin{bmatrix} 0.8 \\ 140 \\ 1.8 \end{bmatrix}$$
$$Q_1^{xyz} = \begin{bmatrix} 1.33333 \times 10^{-6} & 0 & 0 \\ 0 & 1.33333 \times 10^{-6} & 0 \\ 0 & 0 & 1.33333 \times 10^{-6} \end{bmatrix} = Q_2^{xyz} \quad (55)$$

The initial positions for the three points are already set. Prism P_1 and total station P_2 are set within the hand-dug tunnel, and their positions are chosen by an experience surveyor. The only rule is to ensure good visibility for the following survey and guidance. (The unit for all equations in this section is meters). The surveyors can calculate the initial position errors through their aboveground survey from the municipal's survey control point, and the alignment surveying from the plummets. The initial errors include two parts: aiming error, and positioning error. The aiming error is defined by the Leica total station manual

(Leica Geosystem AG 2010a), and is assumed to be $\frac{1}{\sqrt{3}}\ mm$ on each direction of X, Y, Z. The positioning error comes from survey errors that accumulate from the municipal control points to the tunnel, which are here defined as $1mm$ on each direction of X, Y, Z. Thus, the initial parameters for this test are set as equation (55).

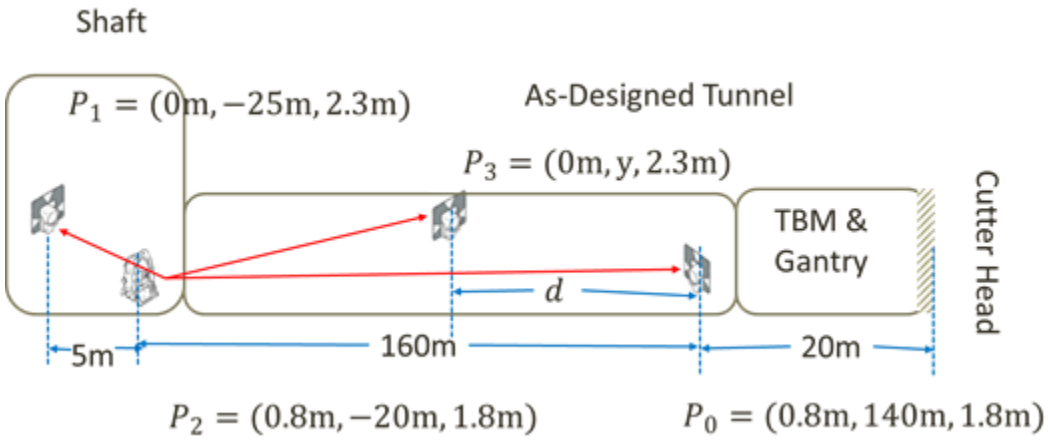

Figure 88. Initial setup of total station and redundant prism

The next total station's location P_0 is determined based on the maximum survey length. The problem to be solved is where to put reference prism P_3, which will support the total station at position P_0 during construction. The two variance-covariance matrices Q_1^{xyz} and Q_2^{xyz} reflect the initial position error of location P_0 and P_1. This initial position error is equal to $1mm$ error on all three axes of X, Y, Z, and we assume this error is unavoidable and introduced while setting up the prisms.

The algorithm will search all possible positions for the redundant prism, as the P_3 prism in the Figure 88. The position of P_3 is set as:

$$P_3 = \begin{bmatrix} 0 \\ y \\ 2.3 \end{bmatrix} \tag{56}$$

There is an unknown parameter y in P_3's coordinate. The range of y for searching is between the current total station at P_2 and the next total station at P_0. In this case, it is between -20 (Y coordinate of P_2) and 140 (Y coordinate of P_0). The search is handled by a for-loop structure in the C# program, where the program will increase 1 $meter$ in each loop. Every time the for-loop produces a new y, the algorithm will evaluate a "score" for this y, and at the end of the for-loop, the y value with the best "score" will be chosen and the redundant prism P_3 will be set at the chainage distance y.

The definition of the "score" has already been illustrated in previous sections; however, the meaning of the score in this numeric example needs to be emphasized. The total station will stay at new position P_0 to guide the tunnel boring machine for the next $160 meters$, and, a time goes by, the excavation and earth pressure will deform the tunnel section where the total station is mounted. Therefore, the coordinate of P_0 varies with the time. The total station is responsible for guiding the tunnel-boring machine, so its position is critical. The total station will give up on its pre-set position, and instead calculate its own position by performing resection on the three prisms P_1, P_2, P_3. This is because the total station is closer to the TBM than it is to the three prisms, and thus, the coordinates of the three prisms are more reliable than the coordinate of the total station. However, in reality, the positions of P_1, P_2, P_3 may vary due to deformation, and the initial survey on P_1, P_2, P_3 may also contains errors. Therefore, the resection of the total station at P_0 on the three prisms P_1, P_2, P_3 also contains errors. The challenge is how to choose a proper P_3 to ensure minimum errors in the resection of the coordinate of P_0 (P_1, P_2 are inherited from previous step, so it is only necessary to find an optimum P_3). The score is simply the

determinant of variance-covariance matrix Q_{xyza}, which is calculated during resection. Therefore, the goal can be modeled as finding a P_3, which can ensure a minimum determinant of variance-covariance matrix Q_{xyza} from resection.

The deduction of this calculation can be found in equations (41) and (42). The model is very complex, and the first step is to determine parameters and observations. In a resection over three points, the observations include: coordinates of the three prisms (X, Y, Z separately), survey results of the three prisms (horizontal and vertical angles, and slope distances). The parameters to be calculated are the total station's coordinate and orientation error.

By utilizing Mathematica, the most important matrices A, B (equations (41) and (42)) can be calculated. Matrix A is described as partitioned as four matrices in equation (57), and the symbol $M_{1,2\to3,4}$ should be interpreted as "this matrix represents the partition of rows 1 to 3 and columns 2 to 4 of the original matrix A". In matrix A, α is the orientation error of the total station, and it is set as the calculated orientation of the total station after resection. This orientation error is only an estimation of the current "true" orientation error, and the optimization process will update the orientation error based on resection. Symbols v, h with subscripts 1,2,3 are the vertical and horizontal angles of prisms P_1, P_2, P_3.

$$M_{1,1\to3,3} = \begin{pmatrix} \cos(\alpha + h_1)\cos v_1 & -d_1 \cos v_1 \sin(\alpha - h_1) & -d_1 \cos(\alpha - h_1)\sin v_1 \\ \sin(\alpha + h_1)\cos v_1 & d_1 \cos v_1 \cos(\alpha + h_1) & -d_1 \sin(\alpha - h_1)\sin v_1 \\ \sin v_1 & 0 & d_1 \cos v_1 \end{pmatrix}$$

$$M_{4,4\to6,6} = \begin{pmatrix} \cos(\alpha + h_2)\cos v_2 & -d_2 \cos v_2 \sin(\alpha - h_2) & -d_2 \cos(\alpha - h_2)\sin v_2 \\ \sin(\alpha + h_2)\cos v_2 & d_2 \cos v_2 \cos(\alpha + h_2) & -d_2 \sin(\alpha - h_2)\sin v_2 \\ \sin v_2 & 0 & d_2 \cos v_2 \end{pmatrix}$$

$$M_{7,7\to 9,9} = \begin{pmatrix} \cos(\alpha + h_3)\cos v_3 & -d_3 \cos v_3 \sin(\alpha - h_3) & -d_3 \cos(\alpha - h_3)\sin v_3 \\ \sin(\alpha + h_3)\cos v_3 & d_3 \cos v_3 \cos(\alpha + h_3) & -d_3 \sin(\alpha - h_3)\sin v_3 \\ \sin v_3 & 0 & d_3 \cos v_3 \end{pmatrix}$$

$$M_{1,10\to 10,18} = \begin{pmatrix} 1 & & & & & & & & \\ & -1 & & & & & & & \\ & & 1 & & & & & & \\ & & & -1 & & & & & \\ & & & & -1 & & & & \\ & & & & & -1 & & & \\ & & & -1 & & & -1 & & \\ & & & & -1 & & & -1 & \\ & & & & & -1 & & & -1 \end{pmatrix} \tag{57}$$

The expanded form of matrix B is much simpler. Matrix B is the coefficient matrix for unknown parameters, namely the X, Y, Z coordinate of the total station, and orientation error α. Matrix B is configured as shown in matrix (58). The symbol d with subscript 1,2,3 is the slope distance of prisms P_1, P_2, P_3, respectively.

$$\begin{pmatrix} 1 & 0 & 0 & -\mathrm{d1}\cos(\mathrm{v1})\sin(a + \mathrm{h1}) \\ 0 & 1 & 0 & \mathrm{d1}\cos(a + \mathrm{h1})\cos(\mathrm{v1}) \\ 0 & 0 & 1 & 0 \\ 1 & 0 & 0 & -\mathrm{d2}\cos(\mathrm{v2})\sin(a + \mathrm{h2}) \\ 0 & 1 & 0 & \mathrm{d2}\cos(a + \mathrm{h2})\cos(\mathrm{v2}) \\ 0 & 0 & 1 & 0 \\ 1 & 0 & 0 & -\mathrm{d3}\cos(\mathrm{v3})\sin(a + \mathrm{h3}) \\ 0 & 1 & 0 & \mathrm{d3}\cos(a + \mathrm{h3})\cos(\mathrm{v3}) \\ 0 & 0 & 1 & 0 \end{pmatrix} \tag{58}$$

Besides these two coefficient matrices, there is a variance-covariance matrix Q for all observations as shown in equation (59). The submatrix Q_1^{dhv} is the variance-covariance matrix for errors on slope distance, and the horizontal and vertical angle measurements of prism P_1; Q_1^{xyz} is the variance-covariance matrix of the errors on coordinate of prism P_1. Q_1^{xyz} contains two errors: survey error and deformation error. Survey error is introduced during setup, and

deformation errors are brought forward by time-related and excavation-related deformations. A detailed example of calculating time-dependent deformation has been demonstrated in equation (51), and will not be elaborated here. After calculating survey error and deformation errors, the total error of Q_1^{xyz} is a direct sum as $Q_1^{xyz} = Q_1^{survey} + Q_1^{time\ deformation} + Q_1^{excavation\ deformation}$.

$$Q = \begin{bmatrix} Q_1^{dhv} & & & & & \\ & Q_2^{dhv} & & & & \\ & & Q_3^{dhv} & & & \\ & & & Q_1^{xyz} & & \\ & & & & Q_2^{xyz} & \\ & & & & & Q_3^{xyz} \end{bmatrix} \tag{59}$$

All the slope distance, and horizontal and vertical angles are calculated during iteration. The equation (61) shows the slope distance, horizontal and vertical angles for the first iteration. The positions of P_1, P_2, P_0 are defined by the initial parameters, and P_3 changes in each new iteration, but all of them are unknown values with an iteration. The values in equation (61) involve no real total station, but ideal calculation without considering errors can be calculated as equation (61). For example, assuming the total station is set on P_0, and survey the prism on P_1:

$$\begin{aligned} u_1 &= P_1 - P_0 = \begin{bmatrix} 0 \\ -25 \\ 2.5 \end{bmatrix} - \begin{bmatrix} 0.8 \\ 140 \\ 1.8 \end{bmatrix} \\ d_1 &= \|u_1\| = 165.003 \\ v_1 &= \sin^{-1} \frac{u_1^z}{d_1} = 0.00303 \\ h_1 &= \tan^{-1} \frac{u_1^y}{u_1^x} = -1.57564 \end{aligned} \tag{60}$$

Following the example of (60), we can calculate the slope distance, and horizontal and vertical angles of the remaining two points in this iteration.

$$\begin{aligned} d_1, h_1, v_1 &= \begin{bmatrix} 165.003 & -1.576 & 0.003030 \end{bmatrix} \\ d_2, h_2, v_2 &= \begin{bmatrix} 160 & -1.571 & 0 \end{bmatrix} \\ d_3, h_3, v_3 &= \begin{bmatrix} 160.3 & -1.576 & 0.003125 \end{bmatrix} \end{aligned} \tag{61}$$

After calculating matrices A, B, Q, we can calculate the Q_{xyza} error matrix of the resection. In the first run, the unknown chainage distance y of P_3 is set as $-20\ meters$ in the for-loop, and the corresponding value is shown in equation (62).

$$Q_{xyza} = \begin{bmatrix} 0.00384176 & -1.26481E-05 & -6.16032E-07 & -2.36526E-05 \\ -1.26481E-05 & 1.23352E-06 & 1.48288E-09 & 7.78948E-08 \\ -6.16032E-07 & 1.48288E-09 & 9.31442E-07 & 3.73172E-09 \\ -2.36526E-05 & 7.78948E-08 & 3.73172E-09 & 1.45657E-07 \end{bmatrix} \tag{62}$$

The final step is to calculate the determinant of variance-covariance matrix Q_{xyza}, for the first iteration, the value of which being $1.27568043109634 \times 10^{-25}$. The whole process involves trying all 160 values of y between $-20 meters$ and $140 meters$, and to find the minimum determinant. In "minor deformation" setup, the minimum determinant appears as $y = 69\ meters$. A graph of the process like the one shown in Figure 89 helps to better understand the process:

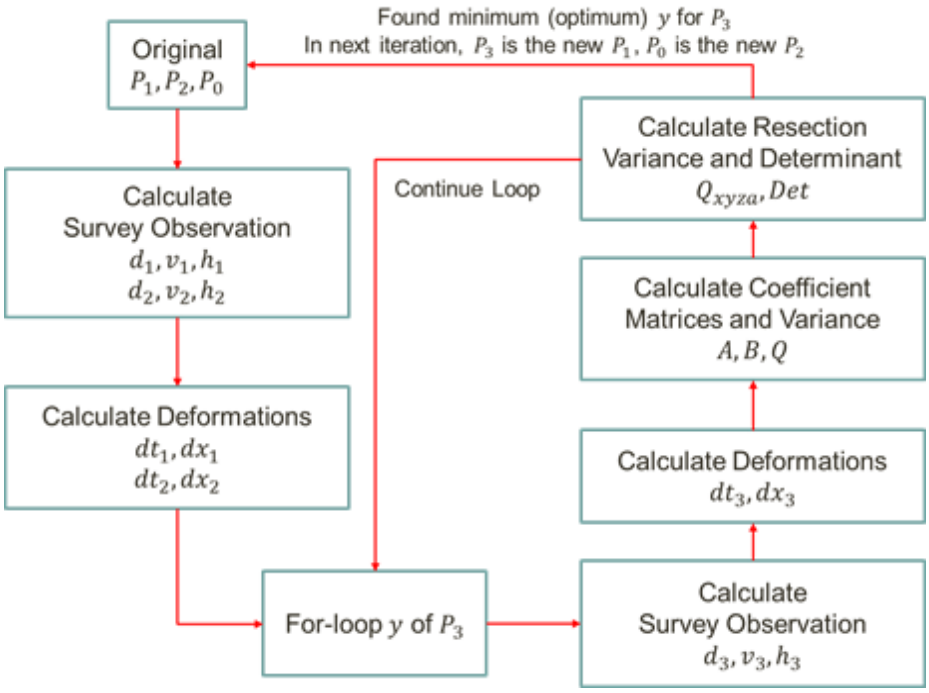

Figure 89. Flow of temporary facility design algorithm

The process demonstrates the optimizing of the minor deformation setting in detail. Given the construction of a $1.1km$ tunnel, the maximum survey distance is $160m$, and therefore in ideal cases (no errors exceed limit), there should be at least six relocations. The first relocation is at chainage distance $140m$, and the last relocation then sets up the total station at chainage distance $940m$. The diagram in Figure 90 contains six lines (1st, 2nd, 3rd, 4th, 5th, and 6th) of the final determinant of the variance-covariance matrix of resection, and each later line is higher than previous one in the graph. The values in X direction are the distance between prism P_3^i in relocation i and the previous total station P_0^{i-1} in relocation $i-1$ (in other words the P_2^i in iteration i).

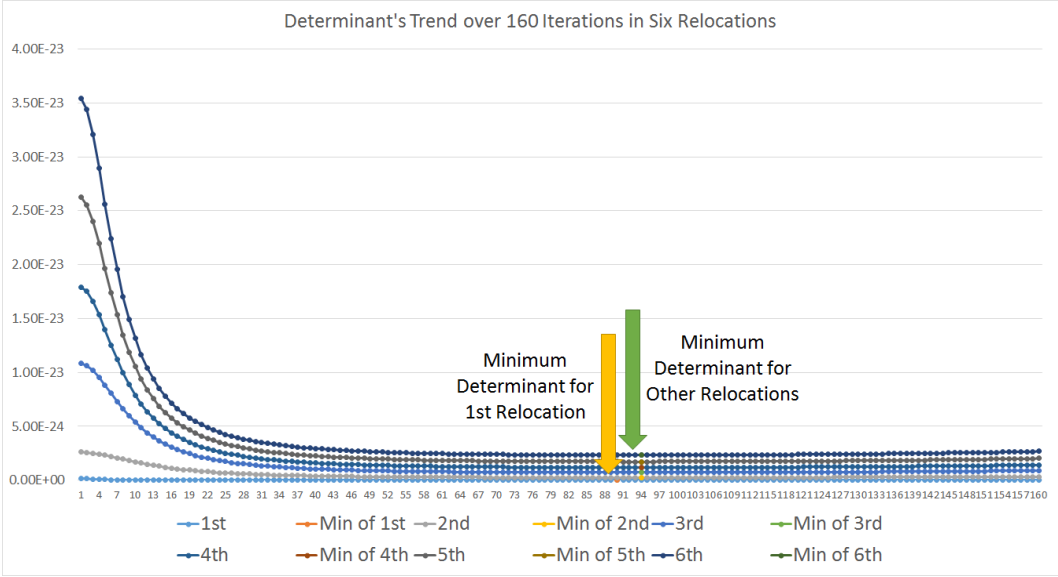

Figure 90. Optimization result for minor deformation setting for six relocations

Aside from the 1st relocation, whose minimum determinant is at a relative distance of $90m$ from P_2^0 (P_2^0 is the same point as P_2 in Figure 88), the other relocations all have their minimum determinants at a relative distance of $94m$. The reason for this difference is that there is no deformation in P_1^0 and P_2^0, and in the other relocations all prisms are affected by deformations. Moreover, as the design assumes a daily advancing distance of 5 $meters$, and the default relocation interval is 160 $meters$, the relocation date interval is fixed in this case. Therefore, the deformation factors affect the prisms in the same pattern in the last five relocations, and the relative position of P_3 to the total station is the same. However, the algorithm enables the engineers and surveyors to adjust the parameters. For example, the relocation date interval can vary, and engineers can determine a series of proper advancing rates for each day. If this is done, the results and the positions of prism P_3 will change according to the new parameters.

5.9.4 Connection with Guidance Method

The previous section discusses how errors from resection are calculated in the design algorithm, and how the optimization process is intended to find the optimum position for prism P_3. The errors from resection are only one part of the final errors of the guidance system; the other part comes from survey error. Survey errors have already discussed in section 5.5 (Guidance Errors), but, briefly put, these errors come directly from the total station survey method.

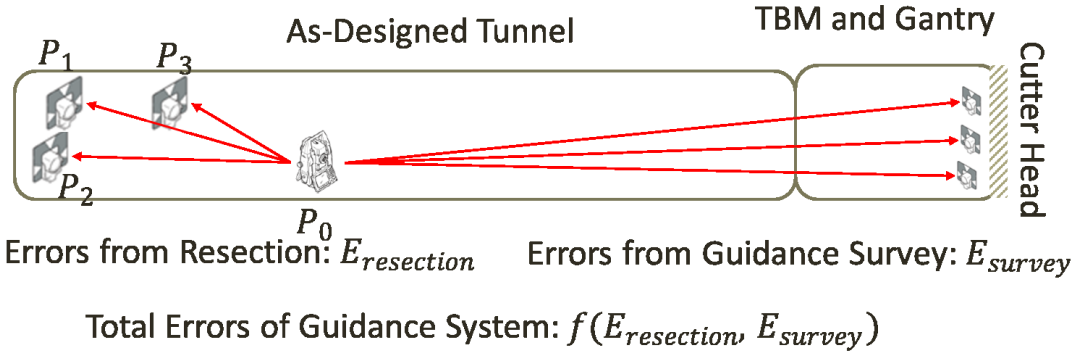

Figure 91. Total errors of guidance system as a whole

As shown in Figure 91, when prism P_3 is chosen, the total error is solely dependent on guidance survey error. In the case study, we have two different guidance methods: three-point based VLTB, and one-point based smart laser projector. Both methods survey the prism(s) on the TBM, and calculate the TBM's deviation. The difference between the two methods with regards to the guidance survey is that the VLTB can directly calculate the position of the TBM's cutter head based on the surveyed three points, whereas the smart laser projector cannot; consequently, surveyors need to estimate a range of possible boundaries for the cutter head based on the TBM operator's performance evaluation (the TBM guidance system keeps tracking its attitude when three-prisms are available, and evaluates how the operator can control the TBM as it advances along the alignment). As stated in section 5.5 (Guidance Errors), the guidance errors

consist of two parts: the error to position the prism on the rear end of TBM (end-point), and the error to position the cutter head based on the end-point error.

Table 9. Errors of end-point, three-point, and cutter-head in minor deformation scenario

	Rel 1			Rel 2			Rel 3			Rel 4			Rel 5			Rel 6		
	EP	TE	CH	EP	TE	CH	EP	TE	CH	EP	TE	CH	EP	TE	CH	EP	TE	CH
Err X (mm)	6	10	16	10	10	20	13	10	23	14	10	24	16	10	26	17	10	27
Err Y (mm)	2	3	5	3	3	6	4	3	7	4	3	7	4	3	7	4	3	7
Err Z (mm)	2	8	10	2	8	10	2	8	10	2	8	10	2	8	10	2	8	10

If Table 9 is taken as an example, the total guidance errors approach the maximum at the end of each relocation (shown as term *Rel n* in Table 9) because the distance between the total station and the TBM are also reaching the maximum. Engineers need to know if these maximum total guidance errors exceed the limit of the design specifications. If the maximum total guidance errors are still within the limit of the design standard, then engineers can safely eliminate full survey for these relocations; otherwise, engineers need to schedule a full survey for those relocations where total guidance errors are too big.

Total station will first survey one prism in both VLTB and smart laser projection. This point is called end-point, and the errors of surveying the end-point come from both resection errors and survey error. In Table 9, all end-point errors are marked as *EP*, and it is evident that, with the construction unfolding, the end-point errors keep increasing as the errors accumulate in resection. End-point is only the rear end point, and to properly position the cutter head, more calculation will be introduced. As discussed in section 5.5 (Guidance Errors), the author calculates the error of "transferring" position information to the cutter head, and these errors are marked as *TE* (transferring error) in Table 9. In the three-point algorithm, the end-point errors determine the mismatch between the

true coordinate system of the TBM and the coordinate system of the three-point algorithm; and, within the coordinate system of three-point algorithm, the error of calculating the cutter head is always $(0.010m, 0.003m, 0.008m)$. Therefore, the total errors, which are marked as CH, can be calculated as $EP + TE$ for each relocation.

This step is the second connection between the design algorithm and the automatic guidance system. The first connection is that the automatic guidance system can provide resection and resection errors for iterating the design algorithm for the next relocation; the second connection is that different guidance methods will provide different transferring errors. For example, if the layout of the three prisms on the TBM has changed, a new transferring error can be calculated following section 5.5 (Guidance Errors). Since the smart laser projector cannot directly calculate the cutter head position, the transferring error can be determined as follows: first, the automatic guidance system (VLTB) can calculate the average performance of the TBM operator based on data when three prisms are available; and second, in addition to the average performance given by the guidance system, engineers and surveyors can jointly set a contingency buffer.

In the next section, only the total guidance error for the cutter head CH will be given. Engineers need to analyze the output report of the design algorithm, and they have to schedule a full survey whenever total guidance errors exceed the limit. After a full survey, the design algorithm simply restarts from the relocation station, and keeps iterating to next relocation station.

Moreover, all the initial parameters that are input into design algorithm can be either from previous projects or from surveys in the current project. In other words, the design algorithm can work for both new projects in the design stage and for changing the plans in ongoing projects. This flexibility is very

important for tunnels with unstable geotechnical conditions because it allows engineers to keep collecting deformation data, and, whenever the as-designed deformation parameters differ from those collected during the construction, they can easily change the relocation plans for the rest of tunnel.

5.9.5 Results

Table 10 is the calculated results from the three setups. Theoretically, “no deformation” is the ideal case because the tunnel liners would have no deformation after being built. This is a benchmark result. “Small deformation” is an example of prism setup in a hard-rock geotechnical condition; the liner is firmly built and neither earth pressure nor push pressure from the TBM will cause too much deformation in the liners. Finally, there is “large deformation”, which is an example of when prisms are set up in softer geotechnical conditions, where displacement of all concrete sections are much larger.

Table 10. The results of three different scenarios.

No Deformation						
$P_0\ Chainage\ (m)$	140	300	460	620	780	940
$P_3\ Chainage\ (m)$	136	296	456	616	776	937
$\sigma_X\ (m)$	0.0017	0.0024	0.0031	0.0037	0.0042	0.0047
$\sigma_Y\ (m)$	0.0011	0.0012	0.0013	0.0013	0.0014	0.0014
$\sigma_Z\ (m)$	0.0010	0.0010	0.0010	0.0010	0.0010	0.0010
$\sigma_\alpha\ (°)$	2.01629	2.68791	3.22889	3.69403	4.10802	4.48536
$TBM\ \sigma_X\ (m)$	0.0128	0.0136	0.0144	0.0150	0.0157	0.0163
$TBM\ \sigma_Y\ (m)$	0.0049	0.0050	0.0050	0.0050	0.0051	0.0051
$TBM\ \sigma_Z\ (m)$	0.0096	0.0097	0.0097	0.0097	0.0097	0.0097
Small Deformation						
$P_0\ Chainage\ (m)$	140	300	460	620	780	940
$P_3\ Chainage\ (m)$	69	233	393	553	713	873
$\sigma_X\ (m)$	0.0042	0.0082	0.0106	0.0126	0.0143	0.0157
$\sigma_Y\ (m)$	0.0011	0.0027	0.0048	0.0053	0.0057	0.0060
$\sigma_Z\ (m)$	0.0010	0.0016	0.0021	0.0023	0.0024	0.0025
$\sigma_\alpha\ (°)$	5.37794	7.19514	8.74924	10.05152	11.18111	12.18471
$TBM\ \sigma_X\ (m)$	0.0165	0.0204	0.0231	0.0254	0.0273	0.0290
$TBM\ \sigma_Y\ (m)$	0.0049	0.0062	0.0080	0.0085	0.0089	0.0092
$TBM\ \sigma_Z\ (m)$	0.0096	0.0101	0.0105	0.0106	0.0107	0.0108
Big Deformation						
$P_0\ Chainage\ (m)$	140	300	460	620	780	940
$P_3\ Chainage\ (m)$	0	214	374	534	694	854
$\sigma_X\ (m)$	0.0098	0.0235	0.0283	0.0337	0.0381	0.0420
$\sigma_Y\ (m)$	0.0011	0.0021	0.0135	0.0149	0.0168	0.0176
$\sigma_Z\ (m)$	0.0010	0.0020	0.0135	0.0149	0.0168	0.0175
$\sigma_\alpha\ (°)$	12.62020	16.18989	20.93650	24.65783	27.74565	30.42022
$TBM\ \sigma_X\ (m)$	0.0248	0.0375	0.0437	0.0500	0.0552	0.0597
$TBM\ \sigma_Y\ (m)$	0.0049	0.0056	0.0166	0.0180	0.0199	0.0206
$TBM\ \sigma_Z\ (m)$	0.0096	0.0104	0.0216	0.0230	0.0249	0.0256

As shown in Table 10, when there is no deformation, the optimum prism locations are always around three to four meters behind the total station ("behind" means closer to the direction of entrance shaft). The reason for this is that, when there is no deformation, a shorter measurement distance produces smaller survey error, which increases the accuracy of the resection.

In comparison, when there is deformation, the distances between the total station and the prism are much further. This is because the closer prisms are mounted to the total station, and the liners are relatively newly built which makes the deformation much less stabilized. The deformation greatly affects the reference network design based on the three different plans.

In this tunnel, the alignment framework and local Cartesian framework are identical, and the horizontal alignment deviation can thus be interpreted as σ_X in this example. At the relocation point of 620m, the horizontal deviation exceeds the $50mm$ limit, and the surveyors need to undertake a full survey to fix the problem. After the full survey, the algorithm restarts at the location and treats it as if it is the first relocation. The engineers can easily predict when to introduce the time-consuming full survey and they can plan the shutdown during the design stage. For curved tunnels, the relocation distance must be adapted to the maximum straight visibility distance due to curvature, and the rest of the algorithm will work the same.

Chapter 6. CONCLUSION

This thesis illustrates a thorough framework for designing and optimizing the temporary facilities to support reliable and efficient tunnel boring machine guidance in the construction of tunnels with confined workspace and limited visibility. The foundation of the framework firmly rests on the state-of-the-art TBM guidance method, and the solid theory of survey errors. The framework can accurately calculate the positions where survey facilities can be set up, and to predict necessary full surveys. Moreover, the framework can keep collecting and observing the status of the construction, and providing instant and reasonable changes of plan when unpredicted conditions prevail. The framework guides the engineers in designing a proper plan for enabling the setup of guidance facilities based on mathematical models, in addition to the suggestions of the experienced surveyors.

For the important considerations of productivity, knowledge transfer, fast replication, and high quality, the framework explores all the important components for an automatic guidance system. The automatic system essentially differs from previous methodologies in that it can ensure the longest continuous construction process without unnecessary interruption and shutdown. However, there are many difficulties associated with building an automatic system that transfers more responsibilities to machine, and thus reduces the need for human intervention. This thesis develops solutions to build a competent automatic system.

The thesis first introduces an automatic guidance system for a tunnel-boring machine, and lays a solid foundation for tunnel research. Then chapter 4 introduces a “smart laser projector” solution for tunnel construction guidance, which complements the previously developed “three-point algorithm” based

VLTB method in order to cope with challenging spatial constraints in the tunnel construction field. The “smart laser projector” solution can provide continuous guidance in extremely tight visibility conditions, in which the VLTB that requires at least three observable points on TBM cannot work properly. The “smart laser projector” solution has been prototyped and lab tested in order to validate its effectiveness. The one-point algorithm is designed to overcome extreme application scenarios. The following three conclusions can be made: (1) the one-point algorithm behind the “smart laser projector” can provide less information for calculation when compared against the three-point algorithm underlying VLTB, (2) the one-point algorithm can provide the same level of accuracy as the three-point algorithm at the rear end, and (3) at the cutter-header, the one-point algorithm is prone to uncontrolled yaw angle. In such scenarios, TBM operators will have to apply additional methods to control the yaw angle manually. The test results shows that the smart laser projector can work properly as a complementary guidance method for VLTB in extreme visibility conditions. VLTB complemented by “smart laser projector” can potentially replace conventional laser systems. Moreover, time and cost calculation shows that the smart laser projector can save 78% comparing against the conventional laser tunnel guidance solution, thus potentially delivering both convenience and efficiency when applying newly developed tunnel guidance systems in the construction field. To control the errors in either the three-point algorithm or the one-point algorithm as described, this thesis also introduces and demonstrates a design algorithm for tunnel reference network design. This algorithm is introduced to find the optimum design of the reference network, which can help resisting the deformation caused by geotechnical conditions and TBM thrust. It can provide the optimum locations to set up reference locations for enabling guidance

systems as part of designing tunnel temporary facilities, and its ability is demonstrated using the VLTB three-point algorithm. The algorithm can handle deformations and update the design about when and where to introduce the least amount of full survey work. As such, construction engineers can make much more accurate predictions than they would if they used traditional experience-based estimation (Lu, Shen, and Mao 2014). These findings undoubtedly present construction engineers with a clear, effective plan during the construction design phase.

REFERENCES

Amiri-Simkooei, AliReza. 2004. “A New Method for Second Order Design of Geodetic Networks: Aiming at High Reliability.” *Survey Review* 37 (293): 552–60. doi:10.1179/sre.2004.37.293.552.

Amiri-Simkooei, A. R., J. Asgari, F. Zangeneh-Nejad, and S. Zaminpardaz. 2012. “Basic Concepts of Optimization and Design of Geodetic Networks.” *Journal of Surveying Engineering* 138 (4): 172–83. doi:10.1061/(ASCE)SU.1943-5428.0000081.

Anderson, J. M., and Edward M. Mikhail. 1998. *Surveying, Theory and Practice*. Boston : WCB/McGraw-Hill, c1998.

Baronti, Paolo, Prashant Pillai, Vince W. C. Chook, Stefano Chessa, Alberto Gotta, and Y. Fun Hu. 2007. “Wireless Sensor Networks: A Survey on the State of the Art and the 802.15.4 and ZigBee Standards.” *Computer Communications*, Wired/Wireless Internet Communications, 30 (7): 1655–95. doi:10.1016/j.comcom.2006.12.020.

Berberan, A., M. Machado, and S. Batista. 2007. “Automatic Multi Total Station Monitoring of a Tunnel.” *Survey Review* 39 (305): 203–11(9). doi:http://dx.doi.org/10.1179/003962607X165177.

Berné, J. L., and S. Baselga. 2004. “First-Order Design of Geodetic Networks Using the Simulated Annealing Method.” *Journal of Geodesy* 78 (1-2): 47–54. doi:10.1007/s00190-003-0365-y.

Bossler, John D. 1984. *Standards and Specifications for Geodetic Control Networks*. Rockville, Maryland: National Geodetic Information Branch. http://www.ngs.noaa.gov/FGCS/tech_pub/1984-stds-specs-geodetic-control-networks.htm.

Calvert, C. E. 1989. “Gps Observations and the Channel Tunnel.” *Survey Review* 30 (231): 3–14. doi:10.1179/sre.1989.30.231.3.

Caterpillar. 2014. “Caterpillar AccuGrade® GPS.” http://www.cat.com/en_US/support/operations/technology/earth-moving-solutions/accugrade-grade-control-system/gps.html.

Caterpillar Inc. 2012. “CATERPILLAR 777G Off-Highway Truck.” https://mining.cat.com/cda/files/3352106/7/AEHQ6553-00.pdf.

Chrzanowski, Adam. 1981. “Optimization of the Breakthrough Accuracy in Tunneling Surveys.” *The Canadian Surveyor* 35 (1): 5–16.

Cross, P. A., and K. Thapa. 1979. “The Optimal Design of Levelling Networks.” *Survey Review* 25 (192): 68–79. doi:10.1179/sre.1979.25.192.68.

D. Li, S. Mao, M. Lu, and X. Shen. 2015. “Analytical Tunnel-Boring Machine Pose Precision and Sensitivity Evaluation for Underground Tunnelling.” In *The Proceedings of 32nd International Symposium on Automation and Robotics in Construction and Mining*, 547–55. Oulu, Finland.

GEODATA group. 2014. “GEODATA - TAUROS for TBMs.” *TAUROS TBM*. http://www.geodata.at/en/sensors-systems-software/systems/TaurosTBM.php.

Goodenough, John B. 1975. “Exception Handling: Issues and a Proposed Notation.” *Communications of the ACM* 18 (12): 683–96. doi:10.1145/361227.361230.

Greening, W. J. Trevor. 1988. “GPS Surveys and Boston’s Central Artery/Third Harbor Tunnel Project.” *Journal of Surveying Engineering* 114 (4): 165–71. doi:10.1061/(ASCE)0733-9453(1988)114:4(165).

Greening, WJ Trevor, Gregory L Robinson, Jeffrey S Robbins, and Robert E Ruland. 1993. “Control Surveys for Underground Construction of the Superconducting Super Collider.” In , 267–74.

Herrenknecht AG. 2015. “Herrenknecht AG Navigation & Monitoring.” August 20. https://www.herrenknecht.com/en/products/additional-equipment/navigation-monitoring-systems/navigation-monitoring.html.

Jardón, A, S Martínez, JG Victores, and C Balaguer. 2014. “Extended Range Guidance System for the Teleoperation of Microtunnelling Machines.” In *The Proceedings of The 31st International Symposium on Automation and Robotics in Construction and Mining (ISARC 2014)*. Sydney, Australia.

Kontogianni, Villy A., and Stathis C. Stiros. 2005. “Induced Deformation during Tunnel Excavation: Evidence from Geodetic Monitoring.” *Engineering Geology*, Application of Gedetic Techniques in Engineering Geology Application of Gedetic Techniques in Engineering Geology, 79 (1–2): 115–26. doi:10.1016/j.enggeo.2004.10.012.

Kontogianni, Villy, Panos Psimoulis, and Stathis Stiros. 2006. “What Is the Contribution of Time-Dependent Deformation in Tunnel Convergence?” *Engineering Geology* 82 (4): 264–67. doi:10.1016/j.enggeo.2005.11.001.

Kuang, Shanlong. 1992. “A New Approach to the Optimal Second-Order Design of Geodetic Networks.” *Survey Review* 31 (243): 279–88. doi:10.1179/sre.1992.31.243.279.

———. 1993. “Second-Order Design: Shooting for Maximum Reliability.” *Journal of Surveying Engineering* 119 (3): 102–10. doi:10.1061/(ASCE)0733-9453(1993)119:3(102).

Leica Geosystem AG. 2010a. “Leica TPS1200+ User Manual v8.0.” LeicaGeosystemAG.

———. 2010b. “Surveying Tribrachs - White Paper Characteristics and Influces.” http://www.surveyequipment.com/PDFs/leica-white-paper-tribrachs.pdf.

Lu, Ming, Xuesong Shen, and Sheng Mao. 2014. “Estimating Potential Cost Savings from Implementing an Innovative TBM Guidance Automation System.” In *Computing in Civil and Building Engineering (2014)*, 1739–46. American Society of Civil Engineers. http://ascelibrary.org/doi/abs/10.1061/9780784413616.216.

Maidl, Bernhard, Martin Herrenknecht, Ulrich Maidl, and Gerhard Wehrmeyer. 2013. *Mechanised Shield Tunnelling*. John Wiley & Sons.

Mao, Sheng, Xuesong Shen, Ming Lu, and Xiaodong Wu. 2013. “Real-Time Tablet-Based Virtual Reality Implementation to Facilitate Tunnel Boring Machine Steering Control in Tunnel Construction.” In *Proceedings of 13th International Conference on Construction Applications of Virtual Reality*. London, United Kingdom.

Mao, S., X. Shen, and M. Lu. 2014. “Virtual Laser Target Board for Alignment Control and Machine Guidance in Tunnel-Boring Operations.” *Journal of Intelligent & Robotic Systems*, September, 1–16. doi:10.1007/s10846-014-0113-y.

Mikhail, Edward M., and Friedrich E. Ackermann. 1976. *Observations and Least Squares, with Contributions by F. Ackermann*. New York, IEP, c1976.

Pejić, Marko. 2013. “Design and Optimisation of Laser Scanning for Tunnels Geometry Inspection.” *Tunnelling and Underground Space Technology* 37 (August): 199–206. doi:10.1016/j.tust.2013.04.004.

PPS-GmbH. 2015. “Poltinger Precision Systems - A Maximum of Guidance on TBM.” http://www.pps-muc.com/index.php/en/tbm.

Schmitt, Günter. 1982. “Optimization of Geodetic Networks.” *Reviews of Geophysics* 20 (4): 877–84. doi:10.1029/RG020i004p00877.

Seemkooei, A. A. 2001. “Comparison of Reliability and Geometrical Strength Criteria in Geodetic Networks.” *Journal of Geodesy* 75 (4): 227–33. doi:10.1007/s001900100170.

Sheng Mao, Duanshun Li, and Ming Lu. 2015. “Analytical Comparison of Distance Based And Angle Based Kinematic Models for Positioning Backhoe Excavators.” In .

Shen, X., M. Lu, and W. Chen. 2011. “Computing Three-Axis Orientations of a Tunnel-Boring Machine through Surveying Observation Points.” *Journal of Computing in Civil Engineering* 25 (3): 232–41. doi:10.1061/(ASCE)CP.1943-5487.0000087.

Stiros, S., and V. Kontogianni. 2009. “Mean Deformation Tensor and Mean Deformation Ellipse of an Excavated Tunnel Section.” *International Journal of Rock Mechanics and Mining Sciences* 46 (8): 1306–14. doi:10.1016/j.ijrmms.2009.02.013.

Stiros, Stathis C. 2009. “Alignment and Breakthrough Errors in Tunneling.” *Tunnelling and Underground Space Technology* 24 (2): 236–44. doi:10.1016/j.tust.2008.07.002.

tacs GmbH. 2004. “tacs acs: Summary of the acs guidance system.” http://www.tacsgmbh.de/en/tacs_prod_acs_overview.htm.

Tao, Benzao, Weining Qiu, Jiana Huang, Haiyan Sun, and Yibin Yao. 2003. *Theory of Errors and Elementary Survey Adjustment*. Wuhan, China: Wuhan University Press.

The City of Edmonton. 2012. “The City of Edmonton - Design & Construction Standards - Volume 3: Drainage.” The City of Edmonton. http://www.edmonton.ca/city_government/documents/Volume_3_Drainage_.pdf.

Van Gosliga, Rinske, Roderik Lindenbergh, and Norbert Pfeifer. 2006. *Deformation Analysis of a Bored Tunnel by Means of Terrestrial Laser Scanning*. na.

VMT GmbH. 2003. “SLS-T APD Tunnel Guidance System.”

Wei, FQ, A Bergamo, P Furlan, J Grgic, and A Wrulich. 1993. “Survey and Alignment of the Synchrotron Light Source Elettra.” In .

Wei, FQ, K Dreyer, U Fehlmann, JL Pochon, and A Wrulich. 1999. “Survey and Alignment for the Swiss Light Source.” http://www.iaea.org/inis/collection/NCLCollectionStore/_Public/32/068/32068850.pdf.

Xiaodong Wu, Ming Lu, and Xuesong Shen. 2014. “Computational Approach to As-Built Tunnel Invert Survey Based on Processing Real-Time TBM Tracking Data.” *Journal of Computing in Civil Engineering* 0 (0): 05014012. doi:10.1061/(ASCE)CP.1943-5487.0000435.

ZED Tunnel Guidance Ltd. 2005. “Low-Cost PC Compatible Tunnel Guidance - The Minimised Basic System, ZED 20.” http://www.zed-tg.co.uk/uploads/brochures/MinimisedZed20.pdf.

Zhao, J., J. N. Shirlaw, and Krishnan R. 2000. *Tunnels and Underground Structures: Proceedings Tunnels & Underground Structures, Singapore 2000*. CRC Press.

Zheng-Lu Zhang, and Song-Lin Zhang. 2004. “Allowance of Lateral Breakthrough Error for Super Long Tunnels from 20km to 50km.” *Geo-Spatial Information Science / 地球空間信息科學學報*, no. 3: 198.

APPENDIX 1: ACCURACY AND ERROR IN CONSTRUCTION

Surveyors always start to establish a survey network from a few known variables. For example, surveyors will measure the water level by a sea, and record the levels for decades. Eventually they will be able to build a "datum" model, which is assigned the meaning of zero elevation. Later, surveyors will start from this zero elevation and establish an elevation control network for the whole country. However, surveyors need to walk through thousands kilometers of vast lands, and there are uncountable uncertainties during the network building. Surveyors need a standard to assess the final quality of the network, finally they choose errors.

Errors are not treated as something wrong, but as uncertainty. The errors are modelled as some stochastic variables, with normal distribution. This model enables the surveyors to describe the quality of their survey products in a statistic way. When a user is provided with a survey product, he/she gets two sets of properties on the results: one is position, and the other is uncertainty (error). User can know what the quality level of the results are, and what's more important, they can apply well-known statistical methods to deal with the survey results. A closer look at this topic is in later appendix, and here we only need to know that errors are important quality indicators in survey.

The accuracy in survey is measured by errors, and concept of errors in survey context is not equal to that in construction. In construction error means mistakes, and by nature is harmful, and they prefer the concept of quality to describe their work. For example, engineers demand that the grade deviation of the any tunnel section is less than $89m$, and this ensures that the tunnel will function correctly. They define quality as the as-built objects conform to the

design. In comparison, quality is a concept measured by accuracy (errors) in survey, handled completely by the surveyors internally. The TBM operators only care about the deviation from the as-designed path, and the foremen also are not aware of accuracy, and they only consider the surveyors when operators cry for loss of laser spot.

The reason for the detached definitions of quality is that survey's quality is not mathematically connected to cost and time of the projects, and thus is not conceptually part of the construction. In this paper, the author establishes a model to assess the time and cost of errors in tunnel guidance systems, and therefore embeds accuracy as an indicator of the tunnel construction.

In survey there are three categories of errors: blunders, biases, and random errors (random noise). Blunders are caused by wrong doings of surveyors, for example, read the number incorrectly; biases are related to internal error of the equipment or methods, for example, a measurement tape marks $1cm$, which is actually $1.2cm$; and random errors are caused by random noise in the equipment and methods. In survey, the first two error categories have the similar context as in construction, and luckily can be detected and eliminated; the random errors are the indicator for uncertainty in survey and they are unavoidable.

The errors incapacitate the certainty and trustworthiness of the steering guidance. Mathematically a random error (later called simply error) usually modelled as a normal distributed variable $N(0,\sigma)$, where σ is the standard deviation of the random variable, and therefore, the survey result is no long truly μ as measured, but a random variable of normal distribution $N(\mu,\sigma)$. This stochastic nature turns measurement of the given target as sampling over the random variable $N(\mu,\sigma)$. Take tunnel guidance for example, guidance system tells

operator that TBM deviates from alignment $45mm$, but the standard deviation of the random error is $15mm$. Then the true deviation can be sampled from the graph below:

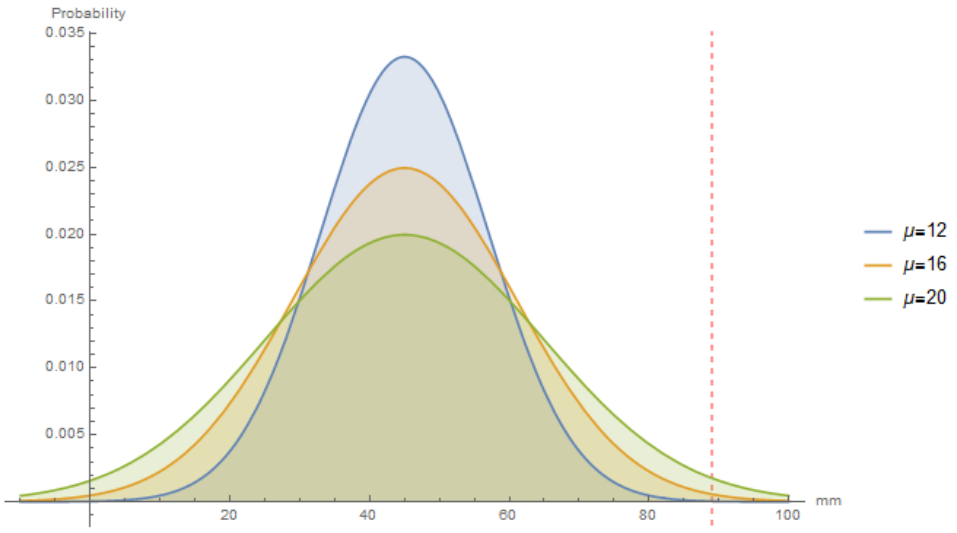

Figure 92. The sampling range of the true deviation of TBM. The red vertical dashed line is the $89mm$ maximum deviation according to construction standard (The City of Edmonton 2012).

Due to the random error, the true deviation may exceed the limit and later as-built survey will find out but too late. This risk forces the operators to think about the quality of the steering guidance, and when the accuracy is low, surveyors must be called in to lower the errors. To reduce the random error, there are two types of solutions: 1) introduce a survey method with lower random error (lower standard deviation σ), for example, use high-class survey procedure (better equipment, longer time, stricter rules); 2) set up more redundant benchmarks for guidance to perform self-correction. In this paper, we focus on the first type of solution. What's more, another reason to introduce a more accurate independent survey check is to rule out possible blunders and biases,

caused by damp conditions, e.g. settlement of the tunnel liners, where guidance system is mounted.

APPENDIX 2: DEFINITION OF CHAINAGE DISTANCE

There are many coordinate frameworks utilized in tunnel constructions, and although all of them are equivalent and interchangeable by applying coordinate transformation. But to express a formula or concept, some framework is way simpler and clearer than the others. One of the example is the polar framework in curved tunnel, which helps simplifying the one-point algorithm.

In reference network design algorithm, the most convenient coordinate system is chainage-distance framework. In chainage-distance framework, everything is first measured by its distance to the start point of the alignment. The convenience of the chainage distance will be shown later in prism setup section, and here in this section, formal definition of the chainage distance will be illustrated, as a solid mathematical foundation for later parts.

For a given tunnel, the basic known parameter is the coordinates of a series of connecting points $[P_0, P_1, \cdots, P_n]$. P_0 and P_n are called start point and end point, respectively; and the rest of the points are called turn points. The alignment is defined as connections between each two connecting points, and the tunnel/alignment is cut into n sections $[T_0, T_1, \cdots, T_{n-1}]$, and grades for each sections can be calculated. The connection between each two turn points can be either straight or curved. For each curved section, it has only one curvature parameter. The turn points can be either as-designed, for example, to separate straight and curved sections; or can be arbitrarily determined for calculation purposes.

The other parameters of the tunnel is the tunnel diameter ϕ, and tunnels can treated as a series tubes with the diameter of ϕ and the symmetric axis for each tube is $[T_0, T_1, \cdots, T_{n-1}]$. Each tube has a length, for straight tube, the tube's

length is the distance between start and end point; for curved tube, the length of tube is defined as the length of the arc of the alignment. Therefore, the lengths in the tunnel can be expressed as a sequence $\| T_0 \|, \| T_0 + T_1 \|, \cdots, \| T_0 + T_1 + \cdots + T_{n-1} \|$. The chainage distance is the distance between the start point and the any specific point Q in the tunnel, and section distance is defined as the distance between specific point on the alignment and the start point of the alignment. Then we can define function relationships between the chainage distance, section distance and section index:

$$L_s(i) = \begin{cases} \|T_0\| & i = 0 \\ \|T_1\| & i = 1 \\ \vdots & \\ \|T_{n-1}\| & i = n-1 \end{cases} \tag{9.63}$$

$$D_s(i) = \sum_{j=0}^{i} L_s(j) \tag{9.64}$$

$$idx(d_c) = \begin{cases} 1 & 0 \le d_c < D_s(0) \\ 2 & D_s(0) \le d_c < D_s(1) \\ \vdots & \\ n-1 & D_s(n-2) \le d_c \le D_s(n-1) \end{cases} \tag{9.65}$$

$$\begin{aligned} i &= idx(d_c) \\ d_s &= d_c - D_s(i) \end{aligned} \tag{9.66}$$

In (9.63), function $L_s(i)$ stands for length for each section, $D_s(i)$ is the accumulated length including all sections between start and current section. Function $idx(d_c)$ gives the corresponding section number of a given chainage distance. Eventually, a pair of section sequential number i and section distance d_s can be calculated from a given chainage distance.

APPENDIX 3: POSE CALCULATION IN ONE-POINT ALGORITHM

When the prism and the center of the rear ring are measured, the smart laser system can display either target center or the pose for the operator. By default, the smart laser displays target center. If the operator needs to know the pose, he/she can flip down the front board, and smart laser will emit the laser beam parallel to the alignment.

The most time consuming part of conventional laser is to adjust yaw and pitch angles, because the angles are not directly measurable, and surveyors need to depend on offsets on three strings to calculate the angle. With modern motor laser equipment, the angle measurement can be as accurate as 1", and the enhanced laser utilizes the precise motor to emit the parallel laser beam. The horizontal and vertical angles that laser should aim at is solely depending on the start/end points, and can be calculated as following:

$$\begin{aligned} u &\leftarrow P_e^l - P_s^l \\ \theta_{tc}^v &\leftarrow \frac{Z(u)}{\sqrt{X(u)^2 + Y(u)^2}} \\ \theta_{tc}^h &\leftarrow \tan^{-1} \frac{Y(u)}{X(u)} \end{aligned} \tag{67}$$

In curved sections, smart laser still emits laser beam, only consider the correction of the curve. However, the display on the target boards is a bit different. In straight tunnel, the position of the font and backboard should always be the same, as the two (2,4) points on the two boards in Figure 93.

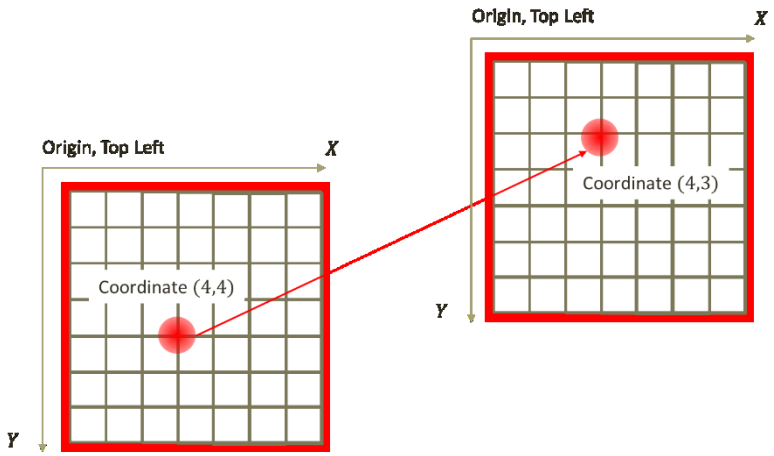

Figure 93. An example of the pose information, on front (left) and back (right) target board.

However, in curved tunnel, the operator should keep changing yaw angle at a given rate, to steer TBM along the alignment. TBM is driven and steered by the hydraulic pushes and the cylinders can either fully extend or not extend, thus operator does not always need to read the precise yaw angle and pitch angle. Although the more information the better, in a small diameter curved tunnel, it should allow some acceptable compromise. Therefore, the surveyors should translate the angles into positions of the laser spot. For example as in Figure 93, the *Y* coordinates of the two dots should be always the same, and this shows that the TBM is on the right pitch angle. But on *X* coordinates, the change rate is translated as two grids on the right. This is intuitive and operators can easily count on the board.

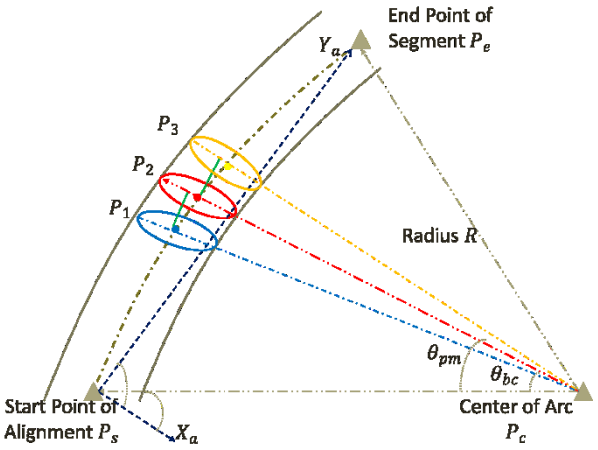

Figure 94. The TBM's positions in three consecutive time frames. The two green lines between blue-red and red-yellow are tangent lines, the first perpendicular to blue, and the second perpendicular to red.

The translation of the yaw angle change is an approximate solution and based on an assumption. As shown in Figure 94, as the TBM either full extends or does not extend a cylinder, the distance between two consecutive positions of TBM approximately equals the length of cylinders. The distance is shown in Figure 94 as green lines, which are tangent lines and perpendicular to blue and red radius. The grid offset can be computed approximately as:

$$\frac{L_{cylinder}}{R} = \frac{N \cdot L_{grid}}{D_{centers}} \approx \frac{N \cdot L_{grid}}{L_{cylinder}} \Longrightarrow N \approx \frac{L_{cylinder}^2}{R \cdot L_{grid}} \tag{68}$$

In equation (68), $L_{cylinder}$ is the length of cylinder, D_{center} is the distance between two centers of rear ring in consecutive positions and approximately, we assume these two are equal. L_{grid} is the length of the grid, and N is the number of grid offset. R is the radius of the curve. Thus, surveyors can calculate the grid offset and surveyor can use this as an indicator. If this assumption causes larger than expected error during the guidance, the deviation can be detected by the smart laser after move.

APPENDIX 4: LOCAL CARTESIAN FRAMEWORK

Surveyors need to deal with multiple coordinate systems during tunnel construction, including GPS coordinate system, geodesy coordinate system provided by the geodesy department of the government, and one or more local Cartesian coordinate systems defined by surveyors for survey/guidance purpose. At the beginning, the surveyors converts GPS/geodesy coordinate formed start/end points into local Cartesian coordinate system, and defined as P_S and P_E. For straight tunnel, the alignment is the segment between P_S and P_E, and for curved tunnel, the tunnel is divided into a series of turn points, and between each two turn points $P_1, P_2, \cdots, P_n$, the segment is straight or near straight. Every time when smart laser tries to guide a TBM, it will first determine the current segment the TBM stays, for example between (P_i, P_{i+1}), and then smart laser will temporarily define $P_s \leftarrow P_i, P_e \leftarrow P_{i+1}$.

The laser-based solutions work best with straight tunnels, as the laser naturally goes straight line. However, in reality there are many tunnels with curved sections, due to various reasons, such as geotechnical conditions or legal issues. However, as shown in Figure 51, when TBM passes through curved sections, laser may be blocked by obstacles like tunnel rings and gantry facilities. Therefore, laser solutions assume that the tunnel alignment it works with is locally straight, and as shown in Figure 95, it should be straight or near straight between P_s and P_e. For curved tunnels, laser will virtually divide the tunnel alignment into a series of near-straight sections, and apply the same solution. Generally, there are two rules for virtual divisions of curved tunnel: visibility and error, and a feasible solution should try to utilize the minimum number of sections that ensure the line-of-sight of laser beam and least errors. The line-of-

sight guarantees the laser beam can directly shoot on the target board without any interferences, and near-straight means the curvature doesn't block the line-of-sight, and can be treated as straight locally.

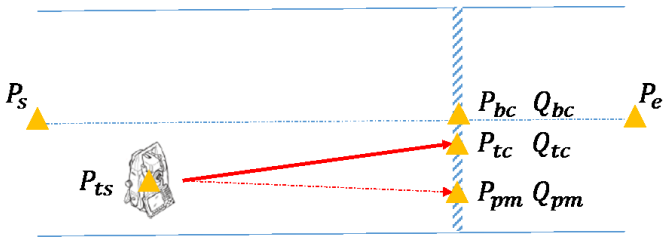

Figure 95. Inputs for smart laser.

Define the origin on the section start point, and $y-axix$ as the direction pointing from start to end point, represented as unit vector Y_a. Then define $x-axis$ as the direction of unit vector X_a (in which g is the unit vector on the direction of gravity). Last define $z-axis$ as the direction of unit vector Z_a:

$$\begin{aligned} X_a &\leftarrow Y_a \times (-g) \\ Z_a &\leftarrow X_a \times Y_a \end{aligned} \tag{69}$$

Then surveyors should measure the offset V_{pm} between prism P_{pm} and the center of the rear ring P_{bc} after installation of the TBM in the tunnel. This offset should be fixed and is a three-dimensional offset in the alignment framework. Surveyor should also measure the offset V_{tc} of the center of the target board P_{tc}. Due to the utilization of the alignment framework, all measurements can be done simply with measurement tapes.

$$\begin{aligned} V_{pm} &\leftarrow P^a_{pm} - P^a_{bc} \\ V_{tc} &\leftarrow P^a_{tc} - P^a_{bc} \end{aligned} \tag{70}$$

When in guidance mode, the smart laser first measures the as-built position of the prism in the local Cartesian framework as Q^l_{pm}, then converts it to the alignment framework $Q^a_{pm} \leftarrow M_{a \leftarrow l}(Q^l_{pm})$. The y value of Q^a_{pm} is the chainage

distance d of TBM since the section start point. Based on the chainage distance, the as-design center of the back ring can be computed as:

$$P_{bc}^{a} \leftarrow P_{s}^{a} + d \cdot Y_{a} \tag{71}$$

The as-designed center of the back ring stays exactly on the alignment, and smart laser computes the as-built center of back ring Q_{pm}^{a}:

$$Q_{bc}^{a} \leftarrow Q_{pm}^{a} - V_{tc}^{a} \tag{72}$$

Then smart laser can evaluate the as-built offset V_{bc}^{a} between as-designed center of rear P_{bc}^{a} and as-built counterpart Q_{bc}^{a}. Eventually, the as-built target board center can be computed, and converted back the local Cartesian framework:

$$\begin{aligned} Q_{tc}^{a} &\leftarrow Q_{bc}^{a} + V_{tc}^{a} \\ Q_{tc}^{l} &\leftarrow M_{l \leftarrow a}(Q_{tc}^{a}) \end{aligned} \tag{73}$$

In the alignment framework, the location and pose of the TBM is simplified, as if the TBM always follows a straight alignment on a flat ground. The definition of alignment framework defines a framework transformation $M_{a \leftarrow l}$, which converts any coordinate in local Cartesian framework to the corresponding coordinate in alignment framework; and the inverse transformation $M_{l \leftarrow a}$.

APPENDIX 5: SETUP AND RELOCATION OF TOTAL STATION AND PRISMS

The location for total station and prisms can be decided in two steps: the algorithm will first determine the chainage distance (which concrete ring to setup), and then some practical constraints and experience will determine where to set up prisms and total station.

There are two basic rules for prism and total station setup: (1) visibility; (2) safety. The prisms and total station must be placed at appropriate places to enable survey, and also considering the large size of the muck cars, the equipment cannot be put too low or too close to the passage of the cars. Thus the total station is always placed on the same side of the survey window of the TBM. For the prisms, the roof is always an ideal location.

The manufacturer of total station and prisms provides a general interface to adapt the equipment for different mounting scenarios. Basically, the survey equipment conceptually consists of three pieces: the main body, the tribrach, and the tripod. In a normal survey setup, the main body is hooked onto the tribrach, and the tribrach is screwed to the tripod. As shown in Figure 96, tribrach connects the equipment and tripod, and provides a flexible and reliable mounting interface.

Figure 96. Tribrach.

In the tunnel, there is no space for tripods, and the surveyors redesigned the mounting strategy. For total station, surveyors replace the tripod with mounting bracket. The mounting bracket has a curved face which will be fixed onto the tunnel liners with bolts, and the other end is a movable platform. The total station will be screwed to the platform, which shares the same design as the tripod's platform.

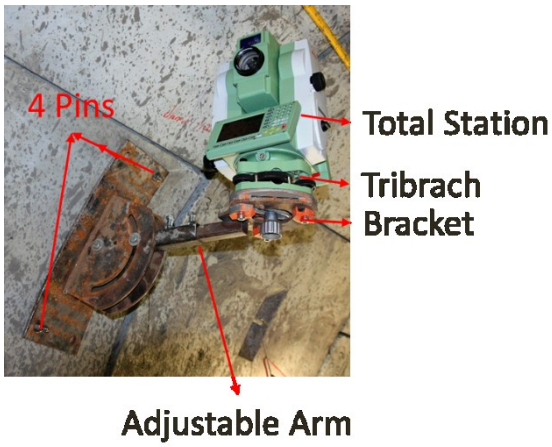

Figure 97. Mounting bracket for total station

For reference prisms, they are very large in size and placed at visible areas. Both tri-bracket and tripod of the reference prisms are replaced with mounting bolts. Surveyors will drill one end of the bolt into the tunnel liner, and the other

end utilizes the same design of the tri-bracket, and prisms can hook onto the bolts.

Figure 98. Mounting Bolt

For the target prisms on the rear end of TBM, the choice for mounting is magnetic hooks. These target prisms are always small prisms, and the diameters are no more than $10cm$. Moreover, it should be easily to switch the mounting point of the target prisms, even the operator can handle the switch without surveyors' help. Eventually a type a magnetic hook is chosen to provide a mounting base for target prisms. As shown in Figure 99, the center of the hook is drilled to fit the size of the screw of target prisms, and the operator can easily switch the target prisms by sticking them to new places, as shown in Figure 100.

Figure 99. Magnetic Hook (the image is at the courtesy of Princess Auto)

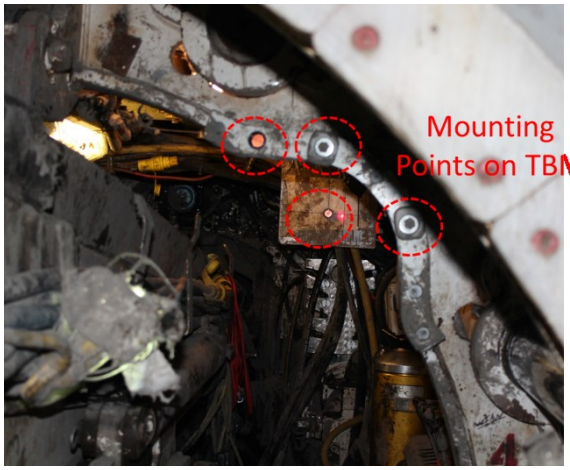

Figure 100. Mounting locations for target prisms.

After describing how the prisms and total station are mounted inside the tunnel, it is very easy to understand relocation process.

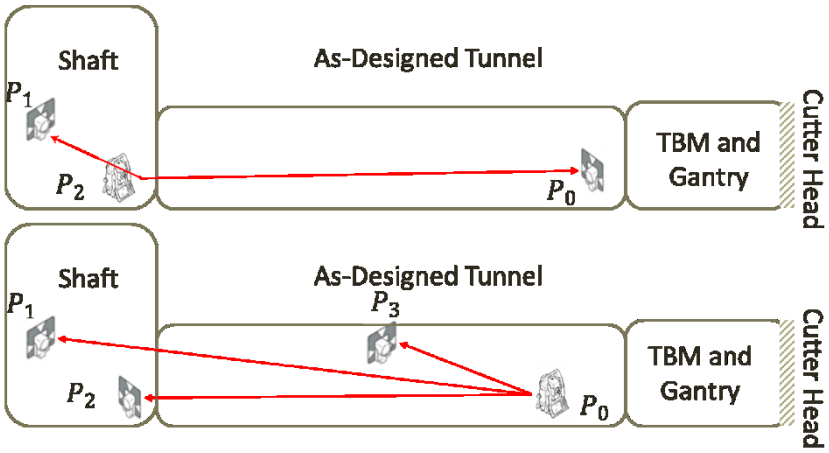

Figure 101. Relocation process

As shown in Figure 101, the redundant prism P_1 is already chosen and set up in the tail tunnel or beside the shaft. There is no special requirement for this position. The total station is placed in the hand-dug tunnel, just beside the entrance of concrete tunnel. This is to ensure the total station can guide the TBM as long as possible. The prism is mounted by the bolt, and the total station is mounted by the bracket.

After $160m$ of digging, the total station needs to be relocated. The first thing is to place a same type of bracket just behind the gantry. This is the next relocation place of total station. Before moving the total station to the new location, a reference prism will be placed at the new bracket, and total station will measure the position of the prism. Then surveyors will switch the equipment part of prism and total station, not the tribrach. The design of tribrach ensures that after switch, the two equipment have the same positions as the previous equipment. As shown in the lower figure in Figure 101, both positions of P_0 and P_2 are the same before and after switch. The last step is straightforward, the design algorithm will tell the surveyors where to drill the bolt for prism P_3, and prism P_3 will be fixed there and face the total station at P_2.

APPENDIX 6: ERRORS AND EXCEPTIONS

A well-designed system must meet the requirement of robustness, and a key feature is to properly handle not correct inputs. Similarly, the framework for TBM guidance design has its own “trouble shooting” design. The three fundamental parts of the framework, namely automatic system, one-point algorithm, and design algorithm, have to deal with the same enemy: unideal tunnel condition, however, this enemy is so overwhelming and a proper robust design should apply some divide-and-conquer technique.

Error handling and trouble-shooting are fundamental components of robust design of tunnel guidance system. The term "error" in this context is a more general concept, referring to things that are not correct rather than survey errors. The design framework is a concentration of expertise and experience, and it is supposed to handle most of the errors by itself. By design, the troubles are categorized as types: foreseeable errors and exceptions.

Foreseeable errors are those concluded by the system designer, and always concluded by tunnel survey experts. A typical example is the "robustness design" section of the automatic guidance system, it concludes all hardware related problems, including battery, wireless communication, dysfunction of total station, etc. One of the critical troubles is the deficit of visibility, which is popular in municipal service tunnels. This problem has been partially solved by the evolved one-point algorithm, which can work in adversary visibility environment. The "robustness design" section already proposes a general and thorough analysis of trouble-shooting process of system design. There is only one error specific to one-point algorithm is that if the only one prism is not visible, surveyors should

choose another candidate mounting point (as described in previous appendix), and inform the system which candidate prism location has been utilized.

For exceptions, which are not predefined by the designer, engineers, and experienced workers, the system has a complete mechanism to deal with the unexpected. The whole system relies on three core components: the computer to provide calculation, control and data display. The system records all states of the system, including control signals, survey data, and calculated data, into a local database. When the system is not working, the technician can easily find out which component fails to work. Exceptions are unavoidable, and the principal is to record all related states of the system, and leave the records with the designer. A previous exception may later be concluded as a new foreseeable error, and later the system can handle without human intervention.

The design algorithm is also required to be reliable and adaptive. There are three categories of troubles that may impair the design algorithm. They are survey errors, varying deformation parameters, and change of design. Survey errors are the least affecting factors, as the design algorithm is built upon stochastic mathematical model, and survey errors are purely part of the input parameters. For example, the "orientation error" in one-point algorithm is considered in the model of design, and is modeled as part of total station's resection error.

Varying deformation parameters and change of design can be treated similarly. Both of these problems can be seen as change of parameters during the construction. The design algorithm is able to be tuned for different scenarios. For example, the starting point can be set to any chainage distance, and design algorithm will be able to reset the prisms for new setups. Also engineers can adjust deformation parameters, position errors of any prism and total station.

The model will be able to uniformly redesign the setup of prisms based on the new setup.